Biogeochemistry of Mercury in Vermont and New Hampshire Lakes

An Assessment of Mercury in Waters, Sediments and Biota of Vermont and New Hampshire Lakes

Comprehensive Final Project Report
October 31, 2003

Project Funding Provided by
United States Environmental Protection Agency
Office of Research and Development

under the

Regional Environmental Monitoring and Assessment Program

Cooperative Agreement Number CR-82549501

Investigators:

Neil Kamman
Vermont Department of Environmental Conservation
103 S Main 10N
Waterbury VT 05671-0408

802 241-3795
neil.kamman@state.vt.us

Dr. Charles T. Driscoll
Syracuse University
Dep't Civil and
Environmental Engineering

Bob Estabrook
Biology Bureau
NH Department of
Environmental Services

Dr. David C. Evers
Biodiversity Research
Institute,
Falmouth ME

Dr. Eric. K. Miller
Ecosystems Research
Inc., Norwich, VT

Table of Contents

Table of Contents 2
List of Tables 4
List of Figures 5
Executive summary and recommendations 7
1.0 Introduction and acknowledgements 9
2.0 Project description, working hypotheses, and objectives 11
2.1 General overview and experimental design 11
3.0 Site selection and sampling procedures 14
3.1 Sampling site selection 14
3.2 Site description and timing of collection 14
3.3 Sampling procedures 14
3.4 Sample custody 18
3.5 Field protocols 19
4.0 Analytical procedures and calibration 23
5.0 Statistical approach to data analysis 25
6.0 Lakes sampled and data results 27
6.1 Study lakes 27
6.2 Water chemistry for core sampling lakes 32
6.3 Multiprobe profiles – core and paleolimnology lakes 33
6.4 Sediment chemistry – core lakes 34
6.5 Biological tissue chemistry 35
6.6 Paleolimnology of Hg in Vermont and New Hampshire lakes 36
7.0 Quality assurance and control results 40
7.1 Water chemistry parameters 40
7.2 Solid phase parameters 40
7.3 Laboratory intercomparison for HgT 41
7.4 Problems 42
8.0 Analysis of the project data 43
8.1 Calculation of age-adjusted yellow perch fillet means for each study lake 43
8.2 GIS analyses 44
8.3 Statistical evaluation of strata in the experimental design 46
8.4 Cumulative frequency distribution diagrams 46
8.5 Evaluation of inter-annual variability and replicate sampling 49

8.6 Evaluation of Hg variation in relation to trophic status **51**

8.7 Calculation of bioconcentration and bioaccumulation factors **53**

8.8 Relationships among variables – univariate correlations **53**

8.9 Principal components analysis - accounting for covariance among parameters **54**

8.10 The influence of land-use on Hg **57**

8.11 Development of candidate linear discriminant functions to predict tissue Hg levels in fillets given physicochemical data **59**

8.12 Summary of statistical analyses **61**

9.0 Estimation and mapping of atmospheric Hg deposition ***64***

9.1 Summary **64**

9.2 Concentrations of Hg species in the atmosphere **64**

9.3 Atmosphere-land surface transfers of Hg **68**

9.4 Tabulation of deposition results for the REMAP Lake-Watersheds **72**

9.5 Discussion **72**

9.6 Deposition maps **77**

9.7 Relationship of deposition to in-lake Hg measures **79**

10.0 Data Archive ***79***

11.0 References ***80***

Appendix A. Historical and present fluxes of mercury to Vermont and New Hampshire lakes inferred from ^{210}Pb dated sediment cores ***86***

Appendix B: Statistical Models of Atmospheric Hg Concentrations ***87***

Appendix C: Overview of the High Resolution Deposition Model ***89***

List of Tables

Table 2.1. Breakdown of number of lakes by strata and state. 12

Table 3.1. Referenced field sampling methods for water. 15

Table 4.1. Parameter table of referenced analytical procedures. 24

Table 5.0. Quality control sample frequency. 25

Table 6.1. Roster of 103 lakes sampled. 28

Table 6.2. Summary of water chemistry data. 32

Table 6.3. Summary of multiprobe profile metadata. 33

Table 6.4. Summary of sediment chemistry data. 34

Table 6.5 Summary of biological tissue data. 35

Table 6.7.1. Diagnostic ^{210}Pb dating values for 13 lakes. 37

Table 6.7.2. Modern, peak, and background Hg fluxes to the sediments of 13 lakes. 38

Table 7.1. Quality assurance and control indicators for aqueous-phase parameters. 40

Table 7.2. Quality assurance and control indicators for sediment-phase parameters. 41

Table 7.3. Results of 10 laboratory intercomparison aqueous HgT samples. 41

Table 8.3. Results of ANOVA and ANOVA on Ranks tests of the influence of four lake:watershed area classes on multiple Hg parameters measured from 92 REMAP study lakes. 46

Table 8.5. Results of MANOVA and follow-up ANOVA analyses of inter-annual variability and replicate sampling. 49

Table 8.7. Log bioconcentration and bioaccumulation factors for biological Hg parameters in relation to aqueous Hg parameters. 53

Table 8.8. Summary of significant ($p \leq 0.05$) Spearman correlation coefficients among water chemistry variables in relation to Hg parameters 54

Table 8.9.1. Results of principal components analyses for epilimnetic and hypolimnetic water chemistry datasets. 55

Table 8.9.2. Pearson correlation coefficients between principal components and measures of Hg in waters, sediments and biota. 56

Table 8.10. Spearman correlations between epilimnetic and sediment Hg parameters, and simplified land-use categories. 58

Table 9.2.1.1. Mercury monitoring stations used to interpolate regional atmospheric mercury concentration fields. 65

Table 9.2.1.2. Seasonal precipitation-weighted average concentrations for the Hg monitoring sites. Values for the UMAQL protocol sites were adjusted to an MDN basis (equation 3). Concentrations are reported in ng l^{-1} 66

Table 9.3.4. Characteristics of regional forest types used in the dry deposition and litter fall Hg accumulation models. Leaf biomass estimates are from the forest survey conducted by Miller et al. (in preparation). 72

Table 9.7. Spearman correlation matrix between atmospheric Hg deposition estimates, and in-lake Hg measures. 79

List of Figures

Figure 6.1. Geographic location of lakes sampled……..……..27

Figure 6.6 Mercury risk to breeding Common Loons (Gavia immer), based on adult and juvenile blood and egg Hg levels……36

Figure 6.7. ^{210}Pb-inferred Hg fluxes to the sediments of 13 VT and NH lakes…….……39

Figure 8.1. Relationship between age and length-adjusted yellow perch muscle-tissue least squared mean Hg concentrations……43

Figure 8.2. Mercury in sediment, waters, and yellow perch tissues……45

Figure 8.4.1. Cumulative frequency distributions for Hg parameters measured in VT and NH lakes……47

Figure 8.4.2. Cumulative frequency distributions for Hg parameters measured in VT and NH lakes……..…47

Figure 8.5.1. Tukey box-plots of epilimnetic HgT concentration by year and state, for samples collected during 1998, 1999, and 2000……...……..50

Figure 8.5.2. Mean concentrations of HgT in epilimnetic waters (and 95% confidence intervals) by year and State……..50

Figure 8.5.3. 1991-2001 mean June through September precipitation at Burlington, VT and Concord, N.H…….51

Figure 8.6. Back-transformed least-squares means and 95% confidence intervals for four mercury parameters in relation to four lake trophic states……52

Figure 8.9. Partial scatterplot matrix of several Hg parameters in relation to epilimnetic and hypolimnetic principal components of 11 water chemistry variables……57

Figure 8.11. Means and standard deviations for HgT in fillets of three species of freshwater fish from Maine lakes, in relation to the EPA 0.3 μg g^{-1} tissue Hg criterion……61

Figure 9.2. Estimated Hg concentration (ng l^{-1}) field for summer precipitation……..67

Figure 9.3.4. Growing season Hg accumulation in foliage…….. ……71

Figure 9.5.1. Ratio of modeled "throughfall" (see text) to modeled precipitation flux of Hg……73

Figure 9.5.2. Frequency distributions of modeled RGM flux (μg m^{-2} y^{-1})……73

Figure 9.5.3. Frequency distributions of modeled Hg fluxes (μg m^{-2} y^{-1}) via litterfall…….……73

Figure 9.5.4. Frequency distributions of the total and component Hg fluxes to the REMAP study watersheds..…74

Figure 9.5.5. Frequency distributions of precipitation Hg flux to the REMAP study watersheds by season…...…75

Figure 9.5.6. Frequency distributions of particulate-phase Hg flux to the REMAP study watersheds by season…75

Figure 9.5.7. Frequency distributions of RGM Hg flux……...…76

Figure 9.5.8. Frequency distributions of Hg_0 flux to the REMAP study watersheds by season……76

Figure 10.0. Data tables and structure for all information collected……..…….…79

The following document was prepared by the Vermont Department of Environmental Conservation, under a cooperative agreement with the United States Environmental Protection Agency, Office of Research and Development. This report is submitted in fulfillment of obligations under cooperative agreement CR 825495-01. The information and data expressed herein do not necessarily represent the views of the VT Department of Environmental Conservation, nor of the US Environmental Protection Agency. This document has not been subject to policy review by the US Environmental Protection Agency, and accordingly, the views expressed herein are neither statements of USEPA policy nor of USEPA policy intent.

The Vermont Department of Environmental Conservation is an equal opportunity agency and offers all persons the benefits of participating in each of its programs and competing in all areas of employment regardless of race, color, religion, sex, national origin, age, disability, sexual preference, or other non-merit factors.

This document is available upon request in large print, braille or audio cassette.

VT Relay Service for the Hearing Impaired
1-800-253-0191 TDD>Voice - 1-800-253-0195 Voice>TDD

Executive summary and recommendations

The present report summarizes findings of a three-year field study of mercury in freshwater lakes of Vermont and New Hampshire. The study was undertaken jointly by the Vermont Department of Environmental Conservation, New Hampshire Department of Environmental Services, and Syracuse University. Collaborating organizations included the Biodiversity Research Institute, Dartmouth College, the Ecosystems Research Group, the Science Museum of Minnesota, the United States Fish and Wildlife Service, and the Vermont Department of Fish and Wildlife. Project funding and guidance was provided by the United States Environmental Protection Agency, under a cooperative agreement with the EPA Office of Research and Development. The study was initiated in 1998, and field sampling was completed at the close of the 2000 field season. Data analysis and modeling exercises were executed during the period 2001-2002.

The study was designed specifically to determine the generalized level of mercury contamination in sediment, water, and biota of multiple trophic levels across the VT-NH region, using a geographically randomized approach. This type of approach ensures that results provide a statistically valid representation of regionwide conditions. In this summary, average mercury concentrations are provided for several types of measurements, along with the 95% confidence intervals. Results of data analyses are highlighted, and interpretations that carry significant management implications are discussed. These values are discussed in light of currently available guidelines or water quality criteria.

Mercury was detectable in waters of all lakes sampled. The average water-column total mercury (Hg) concentrations were 1.78 (± 0.1) parts-per-trillion (ppt) for shallow-water samples, and 11.52 (± 0.81) ppt in deep lake waters. The maximum concentrations were 9.44 and 33.41 ppt, for shallow and deep waters, respectively. Water methylmercury (meHg) showed a similar pattern of increase with depth. MeHg averaged 0.299 (± 0.018) ppt in shallow waters, and 0.829 (± 0.092) ppt in deep waters. The maximum concentrations were 3.12 and 4.45 ppt, for shallow and deep waters, respectively. The increased deepwater Hg and meHg concentrations suggest accumulation in bottom waters, either due to loss from upper waters by sedimentation, release from deepwater sediments, or a combination of both. The average Hg concentration in sediments was 0.240 (± 0.01) parts per million (ppm), and this agrees well with previous studies. Sediment methylmercury (meHg) averaged 1.7% (± 0.1%) of total sediment Hg. Sediment Hg concentrations were most elevated in lakes occupying the most remote and forested regions of VT and NH, and were lowest in lakes with the greatest levels of watershed development.

The historical deposition of Hg to the study region was reconstructed using paleolimnological techniques. Hg presently accumulates in lake sediments at a rate 3.7 times that of the period 1825 and before. In all lakes, a consistent increase in Hg accumulation was evident by the year 1850. The rate of sediment Hg accumulation is presently declining regionwide, and the onset of this decline is generally coincident with implementation of the 1990 Clean Air Act Amendments. The paleolimnological analysis indicated that net atmospheric deposition to lakes across VT and NH is 21 $\mu g\ m^{-2}\ yr^{-1}$, and this estimate is consistent with direct measurements made at the Underhill, VT Hg deposition monitoring site. The paleolimnological analysis suggested that a lag can be expected between reductions in emissions of Hg, and reductions in Hg accumulation to lake sediments, owing to Hg which is presently accumulated in watershed soils. The duration of this lag is unquantified at present, pending further study.

This study evaluated the accumulation of Hg in the tissues of lake fish and wildlife. Yellow perch (*Perca flavescens*) is a ubiquitous lake fish that is increasingly used to indicate of the strength of Hg bioaccumulation in lakes. In the present study, two size classes of perch were analyzed for Hg. Small perch were processed as composites of entire fish, to assess the level of contamination available to piscivorous wildlife. Larger perch were processed as fillets of individual fish, to assess the level of contamination relevant to human consumption. Methylmercury was analyzed in a subset of perch tissues, to determine the overall proportion of methylated Hg in the fish. Common loons (*Gavia immer*) are a threatened obligate fish-eating bird known to be sensitive to mercury contamination. Loon tissues were analyzed for Hg from those study lakes where loons were present, as an indicator of potential impact to this species. Fillets of yellow perch averaged 0.239 (± 0.007) ppm, and ranged from a low of 0.051 ppm

to a maximum of 1.3 ppm, which is quite elevated for yellow perch. Nearly 100% of the Hg in perch tissues was in the meHg form. Yellow perch fillets from NH lakes were significantly higher in Hg than were fish from Vermont lakes. Results of the loon tissue analyses suggest that across the region, 50% of Vermont lakes and 70% of NH lakes had loons with tissue Hg concentrations that placed those animals in a "moderate" or higher risk category. These perch and loon tissue data indicate that Hg contamination is readily bioaccumulated in most lakes across the VT-NH region. Further statistical analyses indicate that Hg and meHg derived from watersheds, and contributing to shallow lake waters, are more likely to be the main Hg source to fish and other biological tissues than are Hg and meHg derived from lake sediments.

The roles of watershed land-use and lake trophic state were evaluated in relation to perch tissue Hg burdens. Perch muscle tissue Hg levels were positively correlated with increases in forested land use, and negatively correlated with increases in developed watershed area. Importantly, while both eutrophic (e.g., high algal density) and dystrophic (e.g., light-limited due to tannic acid content) lakes had similarly elevated levels of water Hg and meHg relative to the remaining lakes, only the dystrophic lakes showed significant bioaccumulation in yellow perch. The eutrophic lakes displayed very low levels of tissue Hg contamination. This finding suggests that fish tissues of biologically-productive lakes may be far lower in Hg than is currently presumed by existing fish tissue advisories.

Various criteria exist for Hg to protect human health and aquatic life. The most conservative legal water quality criterion for mercury in VT waters is 12 ppt, to protect aquatic biota subject to chronic, low-level Hg exposure. The most conservative standard in NH is 51 ppt, to protect against bioaccumulation of Hg in gamefish. The National Oceanic and Atmospheric Administration has a long-standing sediment quality guideline for Hg of 0.15 ppm, above which a low or greater risk of impact to sediment-based biota is likely. The method employed by the VT Department of Health to set tissue advisories, based on 'normal' fish consumption patterns, yields a maximum tissue Hg concentration of approximately 0.2 ppm. Above this value, limited consumption is indicated for some portion of the population. EPA has recently promulgated a similarly-derived, tissue-based criterion of 0.3 ppm meHg as a safe maximum concentration. The present study provides an opportunity to evaluate these criteria and risk assessment concentration thresholds in light of VT and NH specific data.

In this study, no shallow lake waters violated the Vermont water column criterion, and only 16% of lakes across the region showed violations in the deep water portions of the lakes. No lakes exceeded the NH water column criterion. However, tissue contamination in excess of criteria limits was found in many lakes and most lake types. Thirty percent of lakes sampled had perch fillet means in excess of the USEPA criterion, and 60% of lakes had perch fillet tissues exceeding 0.2 ppm. Ninety percent of lakes displayed sediment Hg concentrations in excess of the National Oceanic and Atmospheric Administration sediment quality guideline. These findings clearly indicate that the existing numeric water column criteria within the VT and NH standards are not sufficiently conservative to limit accumulation of Hg to sediments, or to limit risks to humans due to fish consumption, and to limit risks to the wildlife.

A statistical model was developed to predict the likelihood that tissue meHg concentrations of yellow perch would exceed the USEPA meHg criterion, using data from the study lakes. This model uses simple measures of water chemistry (lake buffering capacity, conductance, acidity, organic content, flushing rate) and is applicable to VT and NH lakes 20 acres in size or larger. Based on the model results, 29% of all VT lakes and 62% of all NH lakes are likely to violate the USEPA criterion. This model can be used as a screening tool to identify lakes in need of additional fish tissue sampling.

One additional component of this study estimated Hg deposition to the VT-NH region based on a sophisticated, high-resolution and geographically-based deposition model. This analysis showed that dry deposition of Hg can equal or exceed that deposited in precipitation, and is enhanced in the higher elevations of the VT-NH region. Maps of deposition by type (e.g., precipitation, particulate, Hg vapor) indicate that dry deposition is most enhanced over higher-elevation, forested terrain. Wet Hg deposition showed regional patterns, with enhanced deposition in southern VT, southeastern NH, and along the mountain chains of both states. Overall deposition

estimates were in good agreement with those derived using paleolimnological techniques. The deposition estimates were assessed in relation to in-lake measures of Hg contamination. Both shallow-water meHg and prey-sized yellow perch Hg burdens were elevated in lakes where wet Hg deposition was greater. There were no significant relationships between estimates of dry Hg deposition and in-lake Hg measurements.

With respect to management recommendations, the following merit consideration:

1) Sufficient data are available within this project dataset to develop a TMDL for Hg for lakes in either VT or NH. USEPA Region 1 is presently deliberating on the applicability of individualized TMDLs for lakes, and is considering as an alternative a modeling analysis to support a New England-wide regional TMDL for Hg. While a regional TMDL is most applicable to the type of problem posed by Hg, should VT or NH be required to develop waterbody or state-specific TMDLs the integrated dataset presented herein will provide a sound basis for the analysis. The data from this project can also support a regional TMDL approach.

2) The existing water column criteria for Hg in Vermont and New Hampshire are not sufficiently conservative to protect human health and aquatic biota. These criteria should be revised during each states' water quality standards review. Consideration should be given to EPA criterion for meHg in fish tissue and also to ongoing research by the Biodiversity Research Institute to develop criterion values to protect piscivorous wildlife.

3) The findings regarding trophic status and pH mediation of bioaccumulation should be used to guide further fish tissue collection efforts for the refinement of consumption advisories. Specifically, additional eutrophic lakes should be sampled for tissue Hg, to identify waters where advisories may be relaxed. The statistical model derived for the study can also be used to identify previously untested lakes where tissues should be acquired.

4) The dataset generated by this study serves as a baseline assessment of Hg across the VT-NH region, for the period of 1998-2000. Several federal initiatives are presently under consideration for controlling Hg emissions, and numerous states have reduced both emission sources and the rate of disposal of Hg-bearing products. Accordingly, the level of Hg contamination of the northeastern landscape is expected to decline over the next decade or more. One or more components of this project, re-executed after a ten-year or longer time period has passed, would provide insight into the success of these initiatives.

1.0 Introduction and acknowledgements

Beginning in spring of 1998, the Vermont Department of Environmental Conservation (VTDEC), in cooperation with New Hampshire Department of Environmental Services, Syracuse University, USEPA, and several other collaborators, launched an effort to measure the level of mercury (Hg) contamination in lakes and lake biota across Vermont and New Hampshire. Over the course of the 1998 through 2000 field seasons, we conducted an intensive field measurement program on 103 lakes and ponds. On the vast majority of these lakes and reservoirs, water and sediment chemistry parameters including total mercury (HgT) and methylmercury (meHg) were collected. On a subset of the waterbodies, HgT (and in some cases meHg) was also measured in macrozooplankton, prey-sized and human consumption-sized yellow perch, and avian obligate piscivores such as common loons, mergansers, and belted kingfishers. On a smaller subset of lakes, the rate of historical Hg deposition of Hg to lake sediments was estimated using paleolimnological techniques. Estimates of atmospheric Hg deposition, derived by a project collaborator using data from the parallel "NESCAUM-EPA Region 1" companion REMAP project and other sources, were made for wet, dry, and particulate Hg deposition to the VT-NH region. These estimates were derived using a big-leaf modeling approach, and are reported herein.

The goal of this project was to determine which larger, publicly used Vermont and New Hampshire lakes are of the type that: 1) have excessive mercury in their sediments and waters; 2) possess the conditions linked to

processing this mercury into toxic meHg; and 3) have high mercury concentrations in plankton, fish, and fish-eating wildlife. The results of this study have already been used in part to refine fish tissue consumption advisories in Vermont and New Hampshire, and also to learn more about factors influencing bioaccumulation of mercury in freshwater biota. Our final results provide baseline chemical and biological indicators of Hg contamination, against which future reductions of atmospherically emitted mercury can be measured.

This study provides a large integrated dataset that compliments similar datasets in the State of Maine, and in the Adirondack region of New York. The present dataset is unique in the level of integration between measurements of Hg in multiple physical and trophic ecosystem compartments. Collaborators on the project included Drs. Celia Chen (Dartmouth College), Dr. Dan Engstrom (Science Museum of Minnesota), Dr. Dave Evers (Biodiversity Research Institute of Freeport, Maine), Dr. Peter Lorey (Syracuse University), Mr. Drew Major (US Fish and Wildlife Service New England Region), Mr. Bernie Pientka (Vermont Department of Fish and Wildlife), and Dr. Rob Taylor (Texas A&M). This report was written by Neil Kamman, and Section 9 and Appendices 1-3 were provided by Dr. Eric Miller.

We gratefully acknowledge project funding from USEPA-ORD under cooperative agreement CR-82549501. We also acknowledge the eager participation of the following individuals, without whom it would have been impossible to execute this project: Mr. Wing Goodale and Ms. Oksana Lane of the Biodiversity Research Institute, for their work capturing loons and kingfishers; Mr. Steve Couture, Mr. Steve Landry, and Ms. Elizabeth Roy of the NH Department of Environmental Services, for their countless hours of field work and logistical support in NH waters; Ms. Kelly Thommes of the Science Museum of MN, for her work dating sediment cores; Mr. Tim Gleason of the USFWS, for hours of patient fishing for yellow perch; Dr. Rochelle Araujo, Mr. Ray Thompson, and Mr. Alan VanArsdale of USEPA for their steadfast and long-term support of the project; and finally, Mr. Ed Glassford, who analyzed hundreds of sediment samples for the project. The team also wishes to acknowledge the major contribution to the project provided by Ms. Kate Peyerl of VTDEC, who coordinated all VT sampling events, processed countless sediment and fish tissue samples, entered hundreds of lines of data, and handled myriad logistical details.

2.0 Project description, working hypotheses, and objectives

2.1 General overview and experimental design

The purpose of this research was to characterize concentrations of HgT and meHg in waters and sediments of Vermont and New Hampshire lakes, and to relate these data to easily measured water column chemical parameters and watershed-level physical attributes. A primary research goal was to identify specific lake types in which elevated methylmercury is formed, and in which this toxic mercury is accumulated into middle and higher trophic-level organisms.

The general design of this comparative observational study follows. The project was conducted as a three-year, stratified, spatially randomized sampling employing the EPA Environmental Monitoring and Assessment Program (EMAP) Surface Waters experimental approach. In this approach, sampling units were selected by Geographic Information System, using the hexagon algorithm ensuring random identification of sampling units given the constraints of any stratification (blocking) imposed on the selection.

In this study, individual lakes were considered sampling units. This study evaluated two size-strata of lakes which are greater than 20 acres in size. These two size-strata were further grouped along their watershed to lake area ratios, since this index has been shown to influence total aqueous mercury in water (Mierle and Ingram, 1991). Individual selected lakes were assigned weights, proportional to the number of geographically proximal lakes represented by the selected lake within each heaxgon. Using these weights, it is possible to estimate the overall level of Hg contamination for the entire population of waters represented by the sample. A second group of lakes was sampled to estimate historic fluxes of Hg to lake sediments. The selection of lakes was as follows:

1) REMAP Core Sampling Lakes

1a) VT and NH lakes of 20 to <100 acres in size. These lakes were further grouped into two sub-strata, based upon their lake to watershed area ratio.

1b) VT and NH lakes, 100 or more acres in size. These lakes were further grouped into two sub-strata, based upon their lake to watershed area ratio.

- The EMAP spatially randomized selection protocol identified in excess of 90 lakes, representing approximately 11 percent of the total number of lakes of 20 acres in size or greater within the two States as candidates for sampling. Additional lakes were also selected, as 'overdraw' lakes. The number of lakes within each strata and by State, is listed in Table 2.1, and the final roster of lakes sampled is provided in Section 6.

2) Paleolimnology Lakes

-Thirteen such lakes were sampled. The selection process for these lakes was not random. Nine forested, so-called pristine lakes of a range of lake to watershed-area ratios were selected. Four additional lakes in developed or agricultural watersheds were also sampled.

For groups 1a and 1b, lakes were visited once, and surficial sediment samples for HgT and meHg acquired from a single, representive sampling station. Water samples for HgT and meHg were procured from the epi- and hypolimnion of the overlying water column, using strict mercury-clean collection protocols. Major solutes and parameters related to meHg formation were sampled from the overlying water column using standard limnological collection protocols and a multiparameter automated sonde. Details regarding sampling and analytical methods are given in sections 3.0 and 4.0 respectively.

For group two, sediment HgT and ^{210}Pb were measured. Fluxes of HgT to sediments were estimated as the product of sedimentation rate and HgT for each sediment core strata.

Field operations were conducted by the VTDEC - Water Quality Division, and NHDES - Biology Bureau. Chemical analyses of sediments, fish tissue, and most water samples were performed at the VTDEC LaRosa Environmental Laboratory. Dr. C.T. Driscoll (Syracuse University, Department of Civil, Environmental and Chemical Engineering) has overseen sediment meHg, and aqueous HgT and meHg analyses, and is participating in the analysis of the project data. Preyfish and piscivore Hg and meHg analyses were performed by Dr. Rob Taylor at Texas A&M University. A rigorous program of quality assurance and quality control was applied to both the field and laboratory phases of this project.

2.2 Project hypotheses and statement of project objectives

2.2.1 Hypotheses:

The concentrations of surficial sediment total mercury and aqueous total mercury in Vermont and New Hampshire lakes is related to physico-chemical lake and watershed characteristics.

> VTDEC and NHDES's respective lakes and ponds databases contain physical and chemical data on approximately 810 lakes of 20 acres in size or greater. The databases include such physical information as elevation, lake size and morphometry, watershed size, watershed area in wetlands as well as multiple parameters related to lake trophic state and land use. In addition, a new geographically based land-use data set is available for Vermont and NH. It is hypothesized that sediment total mercury concentrations co-vary with one or more of these measurements.

Concentrations of sediment and aqueous methylmercury in Vermont and New Hampshire lakes are related to sediment mercury concentrations, and are mediated by lake and watershed level physical and chemical parameters.

> It is hypothesized that sediment methylmercury, and water column total and methylmercury covary with sediment mercury concentrations, and with water quality parameters such as major solutes, hypolimnetic sulfide, measures of dissolved organic carbon (DOC), and degree of hypolimnetic anoxia.

Sediment-mercury fluxes evidenced in the stratigraphy of selected Vermont and New Hampshire lake sediment cores show detectable variation over the past 300 years.

> It is hypothesized that a rise above background sediment mercury concentrations and fluxes is detectable in ^{210}Pb-dated short cores, the time signature of which corresponds to the industrialization of the United States. It is further hypothesized that detectable declines in both concentrations and fluxes are apparent in recently deposed sediments.

Table 2.1. Breakdown of number of lakes by strata and state.

Lake strata	Number of eligible lakes	Number of selected NH lakes	Number of selected VT lakes
A: 20 - <100 acres Lake - Watershed ratio (%) <6.0[1]	518	12	16
B: 20 - <100 acres Lake - Watershed ratio (%) >6.0[1]		13	17

Lake strata	Number of eligible lakes	Number of selected NH lakes	Number of selected VT lakes
C: >100 acres Lake – Watershed ratio (%) <6.0[1]		13	5
D: >100 acres Lake – Watershed ratio (%) >6.0[1]		11	8
Paleolimnology lakes	24	6	7
Total number of lakes under evaluation		57	52

[1] Note: The watershed to lake area ratio breakpoint of six percent was determined as the median watershed-lake area ratio (%) for Vermont and New Hampshire lakes falling in the two size categories.

2.2.2 Project objectives

The following are statements of the specific project objectives.

1) Measure total and methylmercury concentrations in the water and surficial sediments of approximately 90 Vermont and New Hampshire lakes. Measure tissue total mercury concentrations of five large-bodied yellow perch, and one five-fish composite of small-bodied yellow perch, in 45 of these study lakes. Measure total mercury in aggregate large-bodied (>202 *u*) macrozooplankton on the 45 lakes from which fish tissue data are available.

2) Measure those water chemistry parameters which the scientific literature suggests accentuate methylation in the 90 study lake set.

3) Explore the relationship between sediment total/methylmercury concentrations, physical lake and watershed characteristics, and water chemistry conditions.

4) Explore the relationship between aqueous and sediment total/methylmercury concentrations, physical lake and watershed characteristics, and water chemistry conditions.

5) Explore the relationship between aqueous and total/methylmercury concentrations and fish-tissue mercury concentrations.

6) Statistically model the relationship between total sediment mercury and water column total/methylmercury.

7) Statistically model the relationship between water column total/methylmercury, zooplankton HgT and fish tissue HgT.

8) Investigate the historical deposition patterns of total mercury in dated cores collected from the sediments of 13 lakes. Compare stratigraphy of mercury fluxes to the sediments of Vermont and New Hampshire lakes with that determined by Adirondack, Maine, and Minnesota studies.

3.0 Site selection and sampling procedures

3.1 Sampling site selection

Individual study lakes were selected by the USEPA National Health and Environmental Effects Research Laboratory in Corvallis, OR, using the EMAP, stratified, spatially randomized lake selection process (USEPA 2002). In brief, this process employs a Geographic Information System (GIS) to overlay a hexagonal grid onto a base waterbody GIS datalayer. The mesh of the overlay grid is sized in proportion to the total number (population) of waterbodies from which the sample is drawn, and to the size of the geographic area under consideration. The computer system then assigns a series of randomly generated coordinates, which are scaled to fall within the coordinate-space of the overlay grid. The single lake waterbody nearest to each randomly-selected grid intersect is considered part of the sample. For this sample, lakes were selected from the USEPA Reachfile III waterbody base layer. Lakes were selected as described in Table 2.11. All Vermont and New Hampshire lakes of 20 acres in size or greater were considered 'eligible' for selection with the exception of the following:

1) Lakes Champlain, Memphremagog, Squam, and Winnipesaukee. The design of this monitoring effort is inadequate to characterize the very large and unique segments of these lakes.

2) Connecticut River Reservoirs. The configuration and hydrology of Connecticut River Reservoirs is such that they behave in a significantly different manner than other Vermont and New Hampshire lakes and reservoirs. While other reservoirs were eligible for selection as study lakes, the highly dynamic Connecticut River Reservoirs were excluded from the pool of potential study lakes.

3.2 Site description and timing of collection

The main sampling location for each lake was centrally-located over the lake's 'deep-hole.' Sediment and water column samples were collected from these stations.

Two critical water quality parameters which mediate methylation, hydrogen sulfide and dissolved oxygen, are strongly controlled by thermal stratification. The optimal timing for sampling such lakes is during mid- to late summer, when stratification is maximized. All dimictic (or mono/meromictic) lakes which were known to stratify during the summer months were sampled between late July and mid-August. The sampling of smaller polymictic lakes was relegated to the edges of this period. All lakes were sampled between June 28 and September 15 of each sampling season. To address interannual variability, as well as to address quality assurance concerns, several lakes were sampled in more than one season.

3.3 Sampling procedures

The sampling station was located in the field using GPS. On lakes on which gasoline powered craft were required for sampling, the engine was shut off downwind of the station, and rowed into place. When necessary, the boat was secured by anchor, and adequate scope let out to avoid contamination of the hypolimnetic zone of interest by the anchor or by sediment drift.

For all lakes, collection of parameters requiring clean handling preceded collection of other parameters in like matrices. The order of collection and handling was as follows:

Arrange sampling equipment - Don sampling attire and gloves - Surface grab for aqueous methylmercury and total mercury sample - Hypolimnetic teflon Kemmerer grab for aqueous methylmercury and total mercury sample - Remove clean attire and gloves - Collect then handle other water chemistry parameters using Kemmerer sampler - multiprobe profile and Secchi measurement - Dirty hands collects sediments - Clean hands' handles extruded sediment for methylmercury and total mercury.

3.3.1 Acquisition of water for Hg and meHg

A surface grab for aqueous mercury samples was collected at each study lake. In addition, for those lakes which stratify strongly, a sample was acquired from one meter above the sediment water interface, using an all-teflon Kemmerer sampler, cleaned to Method 1669 specifications (USEPA 1996a). The sampling depth was determined by on-board SONAR. Techniques for the collection of aqueous mercury samples conformed to EPA method 1669 'clean hands-dirty hands' techniques. Briefly, sampling staff wore clean and new Tyvek™ windsuits, and powder-free vinyl gloves. 'Clean hands' wore shoulder-length gloves, and, if necessary for the logistics of the collection, additional shorter gloves. Gloves were new from the box at the time they were put on. Aqueous mercury samples were stored in a separate, designated clean cooler. Samples were preserved in situ with 3.6*ml* concentrated trace-metals grade HNO_3 (Dr. C.T. Driscoll, pers. comm.), using a new pipette tip rinsed twice in mercury-clean 10% HCl, and once in trace metal grade HNO_3. A detailed field protocol can be found in section 3.5.

3.3.2 Other water chemistry parameters

Water column sampling procedures are referenced in Table 3.1. Water sample aliquots were decanted to appropriate laboratory sample containers in the field, and transported on ice to the Vermont Department of Environmental Conservation LaRosa Laboratory for analysis. Aliquots for dissolved parameters were filtered in the field using Gelman Sciences 0.45*u* filter membranes.

Table 3.1. Referenced field sampling methods for water.

Parameter	Collection Method	Method Reference[1]	Field Sample Container	Sample Preservation
Alkalinity	Kemmerer grab	2.2.3	250 ml HDPE	4°C,
Dissolved and Apparent Color			50 ml poly-carbonate tube.	4°C
Dissolved Organic Carbon			50 ml poly-carbonate tube.	4°C, filtered to 0.45*u*, acidified with H_2SO_4 to pH < 2
Sulfate Chloride			50 ml poly-carbonate tube.	4°C
NOx			250ml HDPE	4°C, H_2SO_4 to pH <2
Sulfide			250 ml glass	4°C, Zn Acetate, NaOH
Mercury	Surface grab and all-teflon Kemmerer grab (hypolimnion)	1669[2]	1000ml teflon 500ml teflon	4°C 3.6ml conc. HNO_3, double-bagged. Stored frozen after delivery to Syracuse
Temperature DO, field pH Conductivity	Multi-probe sonde (Hydrolab®), water column profile	Hydrolab Minisonde Surveyor IV Manual	in situ	N/A
Water Transparency	Secchi disk observation	1.2.1	in situ	N/A

[1)]Field Methods Manual, Vermont Department of Environmental Conservation, 1990.
[2)]USEPA 1996a.

Water column samples for all non-Hg parameters were collected in the epilimnion and hypolimnion of each lake which displayed thermal stratification, and in the epilimnion only for shallow, mixed lakes. For epilimnetic samples, a Kemmerer grab from one meter depth, and from one meter above the upper knee of the thermocline were composited. Hypolimnetic samples were collected from one meter above the sediment-water interface.

3.3.3 Acquisition of sediments for Hg analysis

In designing this part of the sampling protocol, we polled research professionals with experience in the collection of sediments for mercury analysis for their suggestions. The sediment collection methods presented below were designed accounting for these comments and observations, provided by the following. Dr. J. Becker; Dr. R. Bindler; Mr. P. Garrison; Dr. M. Ostrofsky; Dr. B. Simmers; Dr. E.B. Swain; and Dr. C.J. Watras.

Sediments were acquired using a Glew-design, modified KB corer with a 60 cm by 7 cm lexan core tube, or a KB corer with a 60 cm by 5cm lexan tube and a cellulose acetate butyrate liner (NH lakes in 1998 only). The use of core catchers with the KB corer was precluded due to their potential to contaminate surficial sediments during the coring operation. Prior to initiation of sampling, the core tubes were acid cleaned. The tubes were also rinsed copiously in lake water prior to use, and copiously re-rinsed in lake water after sediments were extruded. Core tubes were stored in doubled, plastic bags between acquisitions. These storage bags were replaced regularly, and core tubes were re-acidwashed not less than after every core collected. In most cases, tubes were acidwashed after every fifth sample. Core sectioning tools (scraper, lexan sectioning tray) were cleaned following the same schedule as core tubes, and were also stored in plastic. We adapted clean hands-dirty hands protocol when collecting and sectioning sediments, as described in detail in Section 3.5.

3.3.3.1 REMAP study lakes

Two cores were acquired from the sampling station, and the 'best' core reflecting the least disturbance was selected for analysis. The top five centimeters of sediment was extruded onto a copiously-rinsed, clean lexan sectioning tray (Gilmour et al., 1992; EPRI, 1996). The extruded sediments were moved into a new, clean ziplock bag using an acid-clean plastic scraper. Sediments were stored double-bagged, in a specially designated cooler. At no time were sediment samples placed into the same cooler as aqueous mercury samples. Samples were kept dark at 4°C, and returned to the laboratory for analysis of HgT by CVAA. Sediment aliquots for MeHg analysis by CVAFS were frozen upon receipt at the Syracuse laboratory. Detailed analytical procedures are provided in Section 4 below.

3.3.3.2 Paleolimnology lakes

Sediments were collected using either a KB™ (Wildlife Supply Corp., Buffalo, N.Y.) or Glew-design modified KB corer at the deep lake station. In the field, sediment subsamples (cookies) were extruded each centimeter to the bottom of each core. In general, sediment cores collected with these gravity corers were approximately 50cm in depth.

As described by the "Coring Procedure" (Section 3.5.3 below), two cores were acquired from the sampling station, and the core reflecting the least disturbance was selected for sectioning and analysis. One centimeter sediment 'cookies' were stored in lot-certified PETE 125 ml round bottles. HgT and percent carbon as loss on ignition (LOI) was subsequently analyzed from sediment aliquots on the following cookies: 0-1, 1-2, 2-3, 3-4, 4-5, 5-6, 7-8, 10-11, 12-13, 15-16, 17-18, 20-21, 25-26, 30-31, 35-36 (additional cookies were acquired from each fifth centimeter interval as needed, to the core bottom). All remaining sediments were analyzed for percent solid by gravimetric analysis, then ground by mortar and pestle for ^{210}Pb/^{226}Rn counting and dating.

3.3.4 Acquisition of fish tissue

Fish were collected using fike and experimental net sets, by electroshocking, or by angling. This element of the project was conducted in NH by NHDES staff with assistance from the USFWS. In Vermont, fish were collected by VTDFW. Fish were doubly bagged in new ziplock bags, and frozen for subsequent analysis at the LaRosa laboratory.

At least ten 10 yellow perch per lake were targeted from 45 lakes. Yellow perch were selected because the species has successfully been used in previous studies of fish-Hg uptake, and in the development of fish consumption advisories (Driscoll et al., 1994, VTDEC 1992 rev. 2001). In addition, yellow perch are ubiquitous in Vermont and New Hampshire (T. Hess, VT Department of Fish and Wildlife, Waterbury, Vermont, personal communication). Targeting this single fish species controls for problems associated with the differential abilities of varying fish species to assimilate and depurate Hg.

Fish were frozen until prepared for laboratory analyses as described in Section 4 below. These analyses were performed between December, 1999 and January, 2000. Each outer bag was accompanied by an identification label with the following information.

1. Identification number (lake_code - fish#). For example KENTP - 01
2. Date
3. Species
4. Length (cm)
5. Weight (grams)

3.3.5 Acquisition of zooplankton samples

Protocol for Acquiring Zooplankton for Mercury Analysis for the REMAP Assessment of Mercury in Vermont and New Hampshire Lakes Project

Bulk zooplankton in the ≥201 u size fraction were collected with specially designed nets fabricated of non-metal materials. The dimensions of these nets were 30 cm by 125 cm, ≥201 μ, equipped with a detachable 200ml 'Dolphin' reduction bucket (Wildlife Supply Company, Saginaw MI). All zooplankton collections were made between 7/18/2000 and 9/6/2000.

In summary, a minimum of 5 tows were collected from the immediate vicinity of the lakes' REMAP project sampling station, and the contents composited, reduced, and decanted to a pre-weighed, graduated 50ml sample vial, after which the total volume of the sample was constituted to 50ml. The length of each individual tow composited was recorded on the field sampling sheet. This sample was used to measure HgT in the plankton, as well as total planktonic biomass. The modified clean-hands dirty hands protocol used for this collection is described in detail in Section 3.5.

3.3.6 Tissues samples from piscivores

All sampling used nonlethal methods. Blood and feathers were collected from captured adult and juvenile loons. Loons were captured using nightlighting methods. The technique of using vocalizations and playback recordings to attract a loon is most effective for capturing parental adults. Once within reach, the loon is scooped with a large dip net into the boat. The captured bird is then measured, banded, and blood and feathers taken before release in its territory 20-40 minutes later. Eggs were opportunistically collected from abandoned nests. Second flight secondary feathers were used for Hg analysis, and were cut at a standardized location along the rachis and weighed on a digital scale. These procedures are described in detail by Evers et al. (2000).

For blood samples, blood was drawn from the metatarsal vein through a leur adapter directly into 5-10 cc vacutainers with sodium heparin (green tops). Vacutainers were opened once 10-14 hours later to add 10%

buffered formalin (1:20 formalin-blood ratio) from a sealed container with a new 1 cc syringe. The vacutainer with blood preserved by formalin was then refrigerated and not opened again until reaching the lab. Feathers were clipped at the calamus and placed in a polyethylene bag. Whole eggs were frozen in a polyethylene bag after field removal. Frozen eggs were later cracked and the contents (including the inner shell membrane) placed in lot-certified I-Chem jars and not opened until reaching the lab.

All piscivore samples were labeled in the field using a standard protocol which includes date, species, age, sex, band number, lake and territory name, and state, and all samples were double labeled. A catalog accompanied the samples when they were sent to the analytical lab.

3.4 Sample custody

3.4.1 Sample handling and transport protocols, and labeling and tracking

Since VTDEC and NHDES maintain their own small and efficient laboratory operations, chain-of-custody procedures typically required of regulatory samples were not employed in conjunction with field operations. Field personnel were personally responsible for the samples until they were logged into the LaRosa Environmental Laboratory. In the laboratory, samples were accessioned according to the LaRosa laboratories' standard protocol. All samples sent to other laboratories were delivered via tracked Federal Express shipments.

3.4.2 Field forms

A standard field form was filled out and accompanied all samples collected in conjunction with this study. The field forms identified the study lake, station location from GPS, date and time of sampling, and sampling crew. In order to trace potential contamination problems, serial numbers for sampling equipment were also included on the field form, and tracked using sample field identification numbers. This information was entered into the project database as samples were submitted.

3.4.3 Field data entry

In order to avoid potential transcription error and maximize efficiency, data entry was largely automated. Date, field data and other ancillary information was entered into the LaRosa Laboratory Management System at the time of sample log-in, and was available for automated download to the project database. The format of the Lab Management System log-in code for samples submitted follows:

Standard REMAP samples: FieldId_Time_QA_SampleDepth_SeccDepth_Apparatus#

Paleolimnological samples: FieldId_P_Time_CookieDepth_Apparatus#_Tube#

For example:

SILVL01_1200_A_16.5_03.4_VT-1 consisted of a regular sample from Silver Lake (Leicester, VT), collected at noon, using Kemmerer bottle VT-1, at 16.5 meters depth, with a corresponding Secchi transparency of 3.4 meters.

SILVL01_P_1353_08.0_GL_01 consisted of a sediment sample from Silver Lake (Leicester, VT) from 8 centimeters downcore, collected at 1353 using the Glew corer and core tube 1.

The following QA codes were valid for entry associated with field samples: A- regular sample; B-field blank; D-field duplicate.

Multiprobe data were ported from the datalogger directly into the project database on a weekly or more frequent basis.

3.5 Field protocols

Precise field protocols for sampling of waters and sediments for HgT and meHg, and zooplankton, fish tissue, and piscivore tissue for HgT, are provided below.

3.5.1 Water samples for HgT and meHg

Epilimnetic Grab Sampling

- Waterproof sample labels are prepared using waterproof ink.
- 'Dirty hands' opens the 'clean box,' gloves, and dons a tyvek suit.
- 'Dirty hands' removes shoulder gloves, and assists 'Clean hands' in donning shoulder-gloves and shorter gloves if necessary. From this point forward, 'Clean hands' handles nothing but the sample bottle, or the inner ziplock bag which contains the sample bottle.
- 'Dirty hands' opens the 'clean cooler,' and removes 1 1000ml double bagged bottle. 'Dirty hands' opens the outer bag.
- 'Clean hands' reaches into the outer bag, opens the inner bag, removes the bottle, and folds the inner bag over.
- 'Dirty hands' seals the outer bag, and replaces it into the 'clean cooler.'
- 'Dirty hands' removes the autopipet from the clean cooler, and affixes a new pipet tip.
- 'Dirty hands' rinses the pipet tip 2X in reagent-water dilute 10% HCl, and 1X in HNO3. Rinsates are evacuated into a waste-acid container.
- 'Clean hands' opens the sample bottle, evacuates the contents, and closes the bottle.
- 'Clean hands' submerses the bottle to a 0.5 meter minimum depth, opens the bottle, fills it 1/3rd full, and closes it. The bottle is then surfaced, shaken, opened, and the rinsate evacuated away from the immediate sampling point. The bottle is resealed. This is repeated 2X.
- 'Clean hands' re-submerses the bottle, and allows the bottle to fill entirely. The bottle is recapped underwater.
- 'Clean hands' surfaces the bottle, and opens the cap slightly.
- 'Dirty hands' draws 3.6 ml trace-metal grade HNO3, and pipets this into the sample bottle. 'Clean hands' then tightly caps the bottle.
- 'Dirty hands' opens the clean cooler, withdraws, then opens the outer bag.
- 'Clean hands' unfolds the inner bag, replaces the bottle, and seals the inner bag. 'Dirty hands' then seals the outer bag, affixes the label, and replaces the double-bagged sample in the clean cooler.

Hypolimnetic Kemmerer Sampling

- 'Dirty hands' un-bags the double-bagged teflon Kemmerer, affixes the line, and rinses the sampler 3x in lake water by submersing the sampler, forcefully retrieving it, and allowing it to drip off. The sampler is then lowered 2 meters below the boat, and tied off.
- 'Dirty hands' opens the 'clean cooler,' and removes a 500ml double bagged bottle. 'Dirty hands' opens the outer bag.
- 'Clean hands' reaches into the outer bag, opens the inner bag, removes the bottle, and folds the inner bag over.
- 'Dirty hands' seals the outer bag, and replaces it into the 'clean cooler.'
- 'Dirty hands' lowers the Kemmerer sampler to 1 meter from the sediment-water interface, and trips the closure mechanism with the non-metallic messenger. The sampler is retrieved.
- 'Clean hands' opens and evacuates the bottle. 'Dirty hands' directs the sample stream from the Kemmerer sampler to fill the bottle 1/3. 'Clean hands' caps the bottle, shakes vigorously, and evacuates the rinsate. This is repeated 2X.
- 'Dirty hands' directs the sample stream to fill the bottle entirely. 'Clean hands' caps the bottle, and 'Dirty hands' re-submerses and ties off the Kemmerer sampler at 2 meters of depth.
- 'Dirty hands' draws 1.8 ml trace-metal grade HNO_3 and pipets this into the sample bottle which was opened by 'Clean hands'. 'Clean hands' tightly caps the bottle.
- 'Dirty hands' opens the clean cooler, and withdraws then opens the outer bag.

- 'Clean hands' unfolds the inner bag, replaces the bottle, and seals the inner bag. 'Dirty hands' then seals the outer bottle, affixes the label, and replaces the bottle in the clean cooler.
- 'Dirty hands' bags the Kemmerer sampler with new bags, using "Clean hands" assistance.

3.5.2 Sediment samples

Surficial Sediment Sampling

- Sample bottles and associated ziplock bags are labeled using a waterproof label and ink.
- 'Clean hands' and 'dirty hands' are designated.
- 'Clean hands' gloves with regular-length non-powdered vinyl gloves.
- 'Clean hands' rinses the core tube 3X in lake water, and places it into the corer head.
- 'Dirty hands' is responsible for handling the corer head and line, and for collecting the core. The core descent is tracked using SONAR. The corer should be released to free-fall such that an adequate depth of sediment is acquired, without causing surficial sediments to extrude out the top of the corer. In many undisturbed and forested north-temperate lakes, a 1.5 meter free-fall is sufficient.
- 'Clean hands' caps the core bottom upon its arrival at the surface with a rubber stopper which has been 3x rinsed in lake water. The top of the core is also capped to maintain pressure on the sediments.
- The senior crew member examines the core, deciding to retain or reject it.
- 'Dirty hands' uses tools to remove the lexan tube from the core head, while 'clean hands' holds the core.
- 'Clean hands' maintains the core upright, while, 'Dirty hands' assembles extrusion equipment.
- 'Clean hands' places the core onto the extruder.
- 'Clean hands' affixes sectioning tray onto the core tube.
- 'Dirty hands' uses tools to tighten associated fasteners.
- 'Clean hands' removes sectioning tools from their bags.
- 'Dirty hands' extrudes the core at one-cm intervals.
- While 'dirty hands' controls extrusion from the core bottom, 'clean hands' sections the sediment into the sample bottle. The first five one-cm 'cookies' are sectioned into the sample bottle. 'Clean hands' closes the sample bottle and places it into the ziplock-style bag, which is held open by 'dirty hands.' The sample is subsequently placed into a cooler with ice packs. A dark environment should be maintained around the sample whenever possible.

Observations regarding sediment color, texture, degree of hydration, and odor will be noted. Sediment samples will be submitted as bulk (unsieved).

Cores will be rejected and the core re-collected if:

1) sediments contact metal portions of the corer head (overflow);
2) the sediment-water interface is disturbed;
3) the field coordinator judges that a contamination may have occurred; the core is of poor quality; or
4) gaseous ebullition caused by temperature differential causes the core to break apart before sectioning.

3.5.3 Sampling for macrozooplankton:

Collections of zooplankton within the $201 *u* size fraction are to be collected with specially designed project nets which are fabricated of non-metal materials. The dimensions of these nets are 30 cm by 125 cm, $201 *u*, equipped with a detachable 200ml 'Dolphin' reduction bucket (Wildlife Supply Company, Saginaw MI). Collections are to be performed during a constrained time period to control for seasonal variation in the zooplankton assemblage. In the present study, sampling will be performed during August.

Summary:

For the HgT sample, a minimum of 5 tows will be collected from the immediate vicinity of the lakes' REMAP project sampling station, and the contents composited, reduced, then decanted to a pre-weighed, graduated 50ml sample vial, after which the total volume of the sample will be constituted to 50ml. The length of each individual tow composited will be recorded on the field sampling sheet. This sample will be used to measure HgT in the plankton, as well as total planktonic biomass. A modified clean-hands dirty hands protocol will be used for this collection, which is described in the detailed steps below.

Two additional samples will be collected for the purpose of taxonomic analyses. The first sample, the $201 *u* size fraction, will be composited from two individual tows, which is then decanted to a 50ml sample vessel, narcotized with CO_2, and preserved with formalin solution. The second sample, the 45 - 200 *u* size fraction, will be composited from two individual tows, which is then decanted to another 50ml sample vessel, narcotized with CO_2, and preserved with formalin solution. The length of each composite contributing tow will be recorded on the field sampling sheet.

Zooplankton-HgT samples will be handled in the same method as sediment samples, and in accordance with the REMAP Quality Assurance Project Plan.

Equipment:
-201 u zooplankton net described above
-45 u zooplankton net
-200 ml lot-certified PETE 'compositing vessel'
-500ml acidcleaned squeeze bottle (this should be re-cleaned after every tenth sampling event).
-500ml squeeze bottle for CO_2 water (seltzer)
-CO_2 (seltzer) water
-1 pre-weighed, pre-coded, lot-certified 50ml polycarbonate sample vessel
-2 non-weighed 50ml polycarbonate vessels
-powder-free vinyl gloves
-protective plastic sheet 4'x 4' or larger
-field sampling sheet

Preparatory Steps:

- Prior to going out into the field, a pre-coded 50ml sample vessel is weighed to the nearest 0.001 g, and the weight and code recorded.

- In the field, after the vessel has arrived at station and has been securely anchored, 'clean hands' and 'dirty hands' are designated. 'Clean hands' and 'dirty hands' don regular-length powder-free vinyl gloves.

- A plastic sheet is draped over the gunwale of the sampling boat, such that the net will not have the opportunity to contact the boat.

- 'Dirty hands' removes and assembles the non-metallic net, and 'clean hands' and 'dirty hands' jointly backflush the net 3X in lake surface water. The dolphin bucket is similarly rinsed.

Tows for HgT and Biomass Determination:

- 'Dirty hands' lowers the net to within 1 meter of the lake bottom, and rests the net 30 seconds to allow the water column to recolonize.

- 'Dirty hands' records the depth of this tow on the field sampling sheet.

- 'Dirty hands' retrieves the net at a rate of < 1 m per second.

- When the net-hoop breaches the surface, 'dirty hands' lifts the net, and rinses the contents down along the net-sides using lake water and an acid cleaned squeeze bottle.

- Once the sample is condensed into the dolphin bucket, 'clean hands' removes the bucket, further reduces the sample, and decants it into the 100 ml 'compositing vessel.'

- This tow collection procedure is repeated until a minimum of 5 tows are collected. The field coordinator will determine if additional tows are necessary to obtain sufficient material for biomass and HgT analyses.

- The contents of the compositing vessel is decanted to the 201*u* dolphin bucket, and the contents reduced to < 50ml volume.

- 'Clean hands' opens the 50ml sample vessel, rinses it 3X with lake water, and decants the reduced composite plankton material into the vessel. The vessel is then filled to 50ml with lake water, and capped tightly[1].

- 'Dirty hands' opens a zip-bag, and 'clean hands' drops the filled 50ml vessel into the bag.

- 'Dirty hands' closes the bag and places it into the designated cooler for submission to the VTDEC LaRosa laboratory for analysis.

Tows for Taxonomic Analyses - $201 *u*:

- Two additional tows are composited, using the 201 *u* net, into the compositing vessel using the procedure outlined above.

- The contents of the compositing vessel is then covered with seltzer water, capped, and allowed to sit 60 seconds. At this time, the contents are returned to the dolphin bucket, reduced to the maximum extent possible, rinsed using the seltzer-squeeze bottle into a labeled 50 ml sample vessel, to approximately 25ml volume.

- The sample is capped and allowed to sit 5 minutes. The sample is then opened, and filled to 50 ml with formalin-solution.

Tows for Taxonomic Analyses - 45-200 *u*:

- Two tows are composited using the 45 *u* net, following the procedure outlined directly above.

- While the 201 *u* dolphin bucket is held above the assembled 45 *u* net, the contents of the 45 *u* composite is passed through the 201 *u* dolphin bucket, and allowed to run out into the 45 *u* net. This step removes plankton in the $201 *u* fraction from the 45 -200 *u* fraction.

- The 45*u* sample is then recondensed, and transferred back to the compositing vessel.

- The contents of the compositing vessel is then covered with seltzer water, capped, and allowed to sit 60 seconds. At this time, the contents are returned to the dolphin bucket, reduced to the maximum extent

---

[1]Available REMAP project data indicates that epilimnetic water HgT concentrations are > 2 orders of magnitude smaller than plankton concentrations which were determined during the planktonHgT method demonstration. Such concentrations are unlikely to contaminate the zooplankton samples. Thus, it is recommended that the plankton sample be kept in the lake water from it was obtained until the sample is dried for biomass determination and digestion in the laboratory.

possible, rinsed using the seltzer-squeeze bottle into a labeled 50 ml sample vessel, to approximately 25ml volume.

- The sample is capped and allowed to sit 5 minutes. The sample is then opened, and filled to 50 ml with formalin-solution.

- The taxonomy samples are submitted to Dartmouth University.

3.5.4 Sampling for yellow perch

Fish were collected by net sets, or by electroshocking. This element of the project was conducted by the Vermont Department of Fish and Wildlife for Vermont lakes, and by the NHDES in conjunction with US Fish and Wildlife Service for New Hampshire lakes.

A 2 to 4 inch portion (dorsal to ventral) section of fillet was taken from each individual beginning behind the head using a stainless steel knife, rinsed with distilled water between each fillet. These fillet sections were individually wrapped and labeled as described below. Filleting of the fish was performed in the field, to avoid potential mercury contamination from the lab or office setting. Offal were retained from the filleted fish for the purpose of reconstructing whole-body Hg burdens.

All fish items were individually wrapped in plastic wrap, labeled, and secured in an air-free zip lock bag. The bag, along with the offal, was placed in a second bag.

A new pair of plastic gloves was used for each fish that 1) had scales removed for aging and 2) had a fillet collected. This minimized cross contamination of mercury on the mucus. Collected samples were immediately stored on ice in a cooler, and then transferred to a freezer upon return to the office. Fish were frozen until laboratory analyses. Each outer bag was accompanied by an identification label with the following information.

1. Identification number (lake_code - fish#). For example KENTP - 01
2. Date
3. Species
4. Length (cm)
5. Weight (grams)

3.5.5 Sampling for piscivores

Complete details regarding field methods are provided by Biodiversity Research Institute, and are posted for public access at their world wide web site. These procedures, updated in 2003, are available at http://www.briloon.org/methods.htm.

4.0 Analytical procedures and calibration

Analytical procedures for water and sediment sample analyses are summarized and referenced in Table 4.1. With the exception of cold vapor atomic fluorescence and radiometric sediment dating, the methods presented in Table 4 are standard for limnological analyses, and are not discussed in text. Analytical methods for piscivore tissue samples available from the Biodiversity Research Institute site, at http://www.briloon.org/methods.htm.

Table 4.1. Parameter table of referenced analytical procedures.

Parameter	Units	PQL/ Hold Time	Target QA Precision(RPD) / Accuracy(% recovery)	S.O.P. Number[a]	Number of Samples	Method Reference	Lab
Dissolved Organic Carbon	mg/l	0.10/ 30d	<5 *mg/l* 10/90-110[7] >5*mg/l* 5/90-110	n/a	108	415.1[1]	Syracuse University
Dissolved and Total Color	Pt-Co units	0.00	5/NA[8]	n/a	108	Black and Christman, 1963.	LaRosa
Alkalinity	mg/l as $CaCO_3$	<0.0/ 7d	1/NA	5.1.2	216	2320B[2]	LaRosa
Sulfide, iodometric	mg/l	0.20/ 7d	NA	5.15	108	4500-S[2]-E[2]	LaRosa
Sulfate, Chloride, by IC	mg/l	0.20/28d 0.02/28d	3/90-110 4/90-120	1.1	216	300.1[1]	LaRosa
NOx, by AutoAnalyzer	mg/l	0.02/28d	2/80-116	1.5	216	353.2	LaRosa
Total Mercury in Solids	*µ*g/g	0.10/ 28d	6/70-111	2.3.5/ 2.5.7	260	245.5[3]	LaRosa
Total Mercury in Fish, Offal, Plankton, Piscovires	*µg*/g	0.05/ 28d	4/70-114	2.4.1/ 2.5.8	46	245.5	LaRosa / Texas A&M
Total and Methylmercury in Waters, Methylmercury in Solids	ng/g, ng/l	0.002[5] 0.02[5] / 6 mo.[8]	24/75-125[7]	n/a	108	1631[4]	Syracuse University
Percent Solids	percent	0.0 / 6mo.[9]	1/NA	2.3.1	99	2540B[2]	LaRosa
Loss on Ignition	percent	0.0 / 28d	NA	n/a	99	See QAPP [10]	LaRosa

a) VTDEC, (1992 revised 2001)
1) EPA 1979 and revisions
2) APHA 1995
3) USEPA 1994
4) USEPA 1996a
5) Liang, 1996.
6) Minimum acceptance criteria listed for Method 1631 (USEPA 1996b).
7) Morrison, 1991.
8) Provided that samples are preserved with HCl within 48 hours of collection.
9) Provided that subsample is double bagged and maintained frozen.
10) VTDEC 1992 rev. 2001

A brief method overview for Hg is as follows. HgT was oxidized from sample aliquots using BrCl, and reduced using $SnCl_2$. The reduced Hg was purged to a gold trap, thermally desorbed as Hg(O) into He gas, and measured

by cold vapor atomic fluorescence spectroscopy. Methylmercury in water was measured by aqueous-phase ethylation, cryogenic gas chromatograph separation, and detection by CVAFS. These techniques are described by Lorey (2002) and are presented in detail in USEPA Method 1631 (USEPA 1996b). A detailed description of the chemical procedures involved in the execution of Method 1631 is outside the scope of this document. Practical quantitation limits for HgT and MeHg in waters were 0.02 and 0.005 ng/l respectively. The practical quantitation limit for sediment meHg was 0.005 ng/g d.w. It is implicit in this method that even in clean blank (D.I.) water, some level of Hg will be quantifiable.

Dating of sediment cores was accomplished by determination of ^{210}Pb emission, and corroborated by ^{226}Ra emission, as described by Oldfield and Appleby (1984). These analyses were performed at Dr. D.R. Engstrom's laboratory at the St. Croix Watershed Research Station of the Science Museum of Minnesota.

5.0 Statistical approach to data analysis

As stated in the objectives section, a major goal of this study was to ascertain the physico-chemical identity(ies) of lakes which produce and deliver meHg into the food chain. For the purpose of meeting those objectives, a variety of statistical tools were useful. For this project, a validation phase, inquiry and hypothesis testing phase, and statistical model development phase were used to meet project goals.

Validation of the project data involved identifying datapoints where field or laboratory errors may have compromised reported values. In this study, a robust quality assurance program was implicitly joined to the sampling and analytical phases. Details regarding quality assurance goals and the quality assurance program applied to this study are provided in the Quality Assurance Project Plan (VTDEC 1998 rev. 2000), which was approved by analytical chemists at both the USEPA Region 1 Environmental Effects Laboratory in Lexington, Mass, and at the USEPA Office of Research and Developments' Ecosystem Effects Laboratory in Athens, Ga. A summary of quality assurance measures taken for this study is shown in Table 5.0.

Table 5.0. Quality control sample frequency.

Quality Control Sample Type	**Frequency (n per n samples)**
Equipment Blank (aqueous mercury only)	After cleaning of teflon Kemmerer
Field Blank	1 in 10
Field Duplicate	1 in 10
Matrix Spike / Matrix Spike Duplicate	1 in 10
Analytical Duplicate	1 in 10 (every sample for Hg parameters)
Standard reference material -CVAFS -Other	As required by method 1631 (USEPA 1996b), or as required by the LaRosa Laboratory QA Plan (VTDEC 1992 rev. 2001)

In order to validate the project data, available quality assurance indicators were reviewed and compared to target values. Quality control samples were applied to the set of 'normal' samples which preceded, such that QC results outside of target ranges were cause for the entire set of preceding measurements results to be examined. In many cases, the cause of a poor QC sample result was traced to sampling or measurement error, and resulted in re-sampling or reanalysis. In this study, a common identified cause for poor duplicate results has been the sampling of hypolimnetic waters overly close to the microzone, where aqueous Hg results can be compromised by minute

quantities of resuspended sediment in the sample. Results of the quality control and assurance program are reported in Section 7.0.

6.0 Lakes sampled and data results

6.1 Study lakes

Lakes sampled and data results are summarized in a series of tables within Section 6. Sampling for this project took place between June, 1998 and August, 2000. Project lakes were selected for initial sampling in either 1998 or 1999. In total, 93 lakes were sampled between 1998 and 1999, evenly split between years. A subset of 1998 lakes was resampled during 1999 and/or 2000, to verify out-of-control results, and to assess interannual variability. In addition, 13 lakes were sampled under the paleolimnology project, and 10 of lakes these were outside of the spatially randomized lake set. Table 6.1 provides a roster of the 103 unique study lakes, their geographic locations, initial sampling years, design blocks and weights, and matrices measured. The locations of these lakes are shown in Figure 6.1.

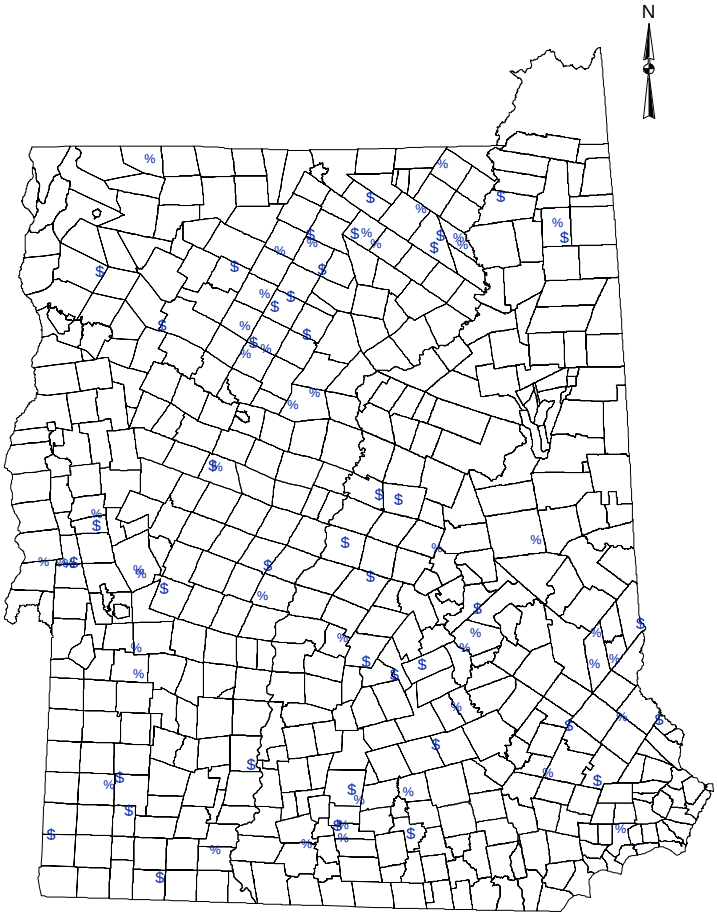

Figure 6.1. Geographic location of lakes sampled in conjunction with the Assessment of Hg in Sediment, Water, and Biota of VT and NH Lakes Project. Initial sampling year also shown (▲- 1998; ■- 1999).

Table 6.1. Roster of 103 lakes sampled.

Lake Name	Town	State	Initial sampling year	Stratification block (see table 2.1)	Sample weight	Lat ddmmss	Lon ddmmss	Core parameters collected	Fish collected	Piscovire collected	Paleo core collected
ADDER POND	ANDOVER	NH	1998	B	11.00	432645	714830	YES	NO	NO	NO
ARMINGTON LAKE	PIERMONT	NH	1998	D	10.00	435725	715815	YES	YES	NO	NO
BAKER (BARTON)	BARTON	VT	1998	A	4.18	444445	721407	YES	NO	NO	NO
BAKER POND- UPPER	ORFORD	NH	1999	C	5.94	435330	715934	YES	YES	NO	NO
BEARCAMP POND	SANDWICH	NH	1999	C	5.94	434755	712228	YES	YES	YES	NO
BEAVER	DERRY	NH	1999	PALEO		424530	711830	NO	NO	NO	YES
BRANCH	SUNDERLAND	VT	1999	B	4.52	430456	730110	YES	NO	NO	YES
BRUCE	SHEFFIELD	VT	1998	B	4.52	443822	721118	YES	NO	NO	NO
CARMI	FRANKLIN	VT	1999	PALEO		445820	725235	NO	NO	NO	YES
CAWLEY POND	SANBORNTON	NH	1999	A	12.00	433215	713620	YES	NO	YES	NO
CHASE POND	WILMOT	NH	1998	A	12.00	432500	715500	YES	NO	NO	NO
CHILDS BOG	HARRISVILLE	NH	1999	D	10.00	425652	720649	YES	YES	YES	NO
CHITTENDEN	CHITTENDEN	VT	1999	D	4.60	434340	725318	YES	YES	NO	NO
CLUB POND	NEW DURHAM	NH	1999	A	12.00	432600	710900	YES	NO	NO	NO
CRANBERRY MEADOW	WOODBURY	VT	1998	A	4.18	442516	722727	YES	YES	NO	NO
CURTIS	CALAIS	VT	1999	B	4.52	442317	722938	YES	YES	NO	NO
DENNIS	BRUNSWICK	VT	1999	C	6.67	444344	713930	YES	NO	NO	NO
DUDLEY	DEERING	NH	1999	PALEO		430730	715030	NO	NO	NO	YES
DUNMORE	SALISBURY	VT	1999	D	4.60	435444	730435	YES	YES	NO	NO
DUTCHMAN POND	SPRINGFIELD	NH	1998	B	11.00	432615	720046	YES	NO	NO	NO
EASTMAN POND	GRANTHAM	NH	1999	D	10.00	433037	720611	YES	NO	YES	NO
ECHO (CHARTN)	CHARLESTON	VT	1998	C	6.67	445136	715934	YES	YES	NO	NO
ECHO (HUBDTN)	HUBBARDTON	VT	1999	B	4.52	434451	731058	YES	YES	NO	NO
ELM BROOK POOL	HOPKINTON	NH	1999	C	5.94	431100	714345	YES	YES	NO	NO
FERN	LEICESTER	VT	1998	B	4.52	435146	730414	YES	YES	NO	NO
FISH POND	COLUMBIA	NH	1998	A	12.00	444952	712931	YES	NO	NO	NO

Lake Name	Town	State	Initial sampling year	Stratification block (see table 2.1)	Sample weight	Lat ddmmss	Lon ddmmss	Core parameters collected	Fish collected	Piscovire collected	Paleo core collected
FREESES POND-UPPER	DEERFIELD	NH	1998	A	12.00	430930	711400	YES	NO	NO	NO
GILES POND	SANBORNTON	NH	1999	A	12.00	432846	713851	YES	YES	NO	NO
GILMAN	ALTON	NH	1999	PALEO		433030	711200	NO	NO	NO	YES
GREAT HOSMER	CRAFTSBURY	VT	1999	D	4.60	444109	722152	YES	YES	NO	NO
GREENWOOD POND	KINGSTON	NH	1999	B	11.00	425612	710343	YES	YES	YES	NO
HALL POND- UPPER	SANDWICH	NH	1998	B	11.00	435054	713303	YES	NO	NO	NO
HARDWICK	HARDWICK	VT	1998	C	6.67	443118	722228	YES	NO	YES	NO
HARDWOOD	ELMORE	VT	1999	B	4.52	442804	723002	YES	YES	YES	NO
HIGH (SUDBRY)	SUDBURY	VT	1998	B	4.52	434510	730914	YES	NO	NO	YES
HILDRETH DAM POND	WARREN	NH	1998	A	12.00	435630	715325	YES	NO	NO	NO
HORN POND	WAKEFIELD	NH	1998	C	5.94	433342	705731	YES	YES	YES	NO
HORTONIA	HUBBARDTON	VT	1999	D	4.60	434519	731208	YES	YES	YES	NO
HOWE RESERVOIR	DUBLIN	NH	1999	C	5.94	425410	720634	YES	YES	NO	NO
INTERVALE	SANDWICH	NH	1999	PALEO		434730	713130	NO	NO	NO	YES
ISLAND POND	STODDARD	NH	1998	C	5.94	430400	720456	YES	YES	NO	NO
IVANHOE- LAKE	WAKEFIELD	NH	1998	D	10.00	433605	705925	YES	NO	YES	NO
JACKSONVILLE	WHITINGHAM	VT	1998	A	4.18	424803	724900	YES	YES	YES	NO
JENNESS POND	NORTHWOOD	NH	1998	D	10.00	431525	711500	YES	YES	YES	NO
KENT	SHERBURNE	VT	1998	A	4.18	434032	724609	YES	NO	NO	NO
LARY POND	CANAAN	NH	1998	A	12.00	434230	720010	YES	NO	NO	NO
LEFFERTS	CHITTENDEN	VT	1999	A	4.18	434255	725411	YES	YES	NO	NO
LEVI	GROTON	VT	1999	B	4.52	441558	721341	YES	NO	NO	NO
LILY POND	SOMERSWORTH	NH	1998	B	11.00	431518	705460	YES	NO	NO	NO
LITTLE AVERILL	AVERILL	VT	1999	D	4.60	445702	714256	YES	NO	YES	NO
LONG (WESTMR)	WESTMORE	VT	1999	B	4.52	444506	720103	YES	NO	YES	NO
LOON LAKE	PLYMOUTH	NH	1999	C	5.94	434637	714509	YES	YES	NO	NO
LOVELL LAKE- STN 1	WAKEFIELD	NH	1999	D	10.00	433144	710118	YES	YES	YES	NO

Lake Name	Town	State	Initial sampling year	Stratification block (see table 2.1)	Sample weight	Lat ddmmss	Lon ddmmss	Core parameters collected	Fish collected	Piscovire collected	Paleo core collected
LYFORD	WALDEN	VT	1998	B	4.52	442623	721504	YES	YES	NO	NO
MANSFIELD	STOWE	VT	1998	A	4.18	442823	724843	YES	NO	NO	NO
MCCONNELL	BRIGHTON	VT	1999	A	4.18	444904	714806	YES	NO	YES	YES
MILLSFIELD POND	MILLSFIELD	NH	1999	C	5.94	444439	711703	YES	NO	NO	NO
MILTON	MILTON	VT	1998	B	4.52	443804	730350	YES	YES	NO	NO
MINARDS	ROCKINGHAM	VT	1998	B	4.52	430840	722810	YES	NO	NO	NO
MITCHELL	SHARON	VT	1998	A	4.18	434448	722415	YES	NO	NO	NO
MOOSE POND	MILLSFIELD	NH	1998	A	12.00	444344	711348	YES	NO	YES	NO
MOUNTAIN LAKE-UPPER	HAVERHILL	NH	1999	A	12.00	440705	715725	YES	NO	NO	NO
NEWARK	NEWARK	VT	1999	D	4.60	444303	715856	YES	YES	YES	NO
NORTH (BRKFLD)	BROOKFIELD	VT	1998	A	4.18	440253	723708	YES	YES	NO	NO
NOTCH	FERDINAND	VT	1998	A	4.18	444424	714306	YES	NO	NO	NO
NOYES	GROTON	VT	1999	A	4.18	441339	721822	YES	NO	NO	NO
PARAN	BENNINGTON	VT	1998	A	4.18	425558	731407	YES	YES	NO	NO
PARKER	GLOVER	VT	1999	C	6.67	444312	721402	YES	YES	NO	NO
PAUGUS BAY- STN 1	LACONIA	NH	1998	C	5.94	433358	712800	YES	NO	NO	NO
PAWTUCKAWAY LAKE	NOTTINGHAM	NH	1998	D	10.00	430500	710900	YES	YES	NO	NO
PEMIGEWASSET LAKE	MEREDITH	NH	1998	D	10.00	433654	713541	YES	YES	YES	NO
PERCH (BENSON)	BENSON	VT	1999	B	4.52	434501	731651	YES	YES	NO	NO
PLEASANT VALLEY	BRATTLEBORO	VT	1999	A	4.18	425304	723641	YES	NO	NO	NO
POUT POND	LYME	NH	1998	B	11.00	434853	720609	YES	NO	YES	NO
POWWOW POND	KINGSTON	NH	1998	C	5.94	425410	710241	YES	YES	NO	NO
ROBB RESERVOIR	STODDARD	NH	1999	C	5.94	430114	720317	YES	YES	NO	NO
ROLF POND	HOPKINTON	NH	1998	B	11.00	431139	714516	YES	NO	NO	NO
ROUND POND	BARRINGTON	NH	1999	D	10.00	431637	710252	YES	YES	NO	NO
SABIN	CALAIS	VT	1999	C	6.67	442411	722507	YES	YES	NO	NO

Lake Name	Town	State	Initial sampling year	Stratification block (see table 2.1)	Sample weight	Lat ddmmss	Lon ddmmss	Core parameters collected	Fish collected	Piscovire collected	Paleo core collected
SESSIONS	DUMMER	NH	1999	PALEO		444220	711150	NO	NO	NO	YES
SHAWS POND	NEW DURHAM	NH	1999	A	12.00	433060	710906	YES	NO	NO	NO
SILVER LAKE	HARRISVILLE	NH	1998	D	10.00	425730	720825	YES	YES	NO	NO
SOMERSET	SOMERSET	VT	1998	D	4.60	425832	725652	YES	YES	YES	NO
SOUTH AMERICA	FERDINAND	VT	1998	A	4.18	444218	714442	YES	NO	NO	NO
SPRING (SHRWBY)	SHREWSBURY	VT	1999	PALEO		432942	725512	NO	NO	NO	YES
SPRUCE POND	DEERFIELD	NH	1999	B	11.00	430609	712047	YES	NO	NO	NO
STRATTON	STRATTON	VT	1998	B	4.52	430617	725810	YES	NO	NO	NO
SUNCOOK POND-UPPER	BARNSTEAD	NH	1998	C	5.94	432319	711710	YES	YES	YES	NO
SUNRISE LAKE	MIDDLETON	NH	1999	D	10.00	432715	710430	YES	YES	YES	NO
SUNSET (BRKFLD)	BROOKFIELD	VT	1999	A	4.18	440237	723614	YES	YES	NO	NO
TRIO PONDS- ONE AND TWO	ODELL	NH	1998	B	11.00	444240	712200	YES	NO	NO	NO
TUTTLE (HARDWK)	HARDWICK	VT	1998	B	4.52	443330	721836	YES	NO	NO	NO
UNNAMED POND	DEERING	NH	1999	B	11.00	430320	715220	YES	NO	NO	NO
WALKER POND	BOSCAWEN	NH	1999	C	5.94	431804	714059	YES	YES	YES	NO
WALLINGFORD	WALLINGFORD	VT	1999	PALEO		432341	725432	NO	NO	NO	YES
WHEELER (BRUNWK)	BRUNSWICK	VT	1999	PALEO		444230	713829	NO	NO	NO	YES
WILLARD	ANTRIM	NH	1999	PALEO		430130	720130	NO	NO	NO	YES
WILLEY POND- BIG	STRAFFORD	NH	1999	A	12.00	431646	711107	YES	NO	NO	NO
WILLEY POND-LITTLE	STRAFFORD	NH	1999	B	11.00	431735	711040	YES	NO	NO	NO
WILLOUGHBY	WESTMORE	VT	1998	D	4.60	444506	720344	YES	YES	YES	NO
WILSON POND	SWANZEY	NH	1999	B	11.00	425402	721544	YES	YES	NO	NO
WOLCOTT	WOLCOTT	VT	1999	B	4.52	443355	722516	YES	YES	YES	NO
ZEPHYR LAKE	GREENFIELD	NH	1998	B	11.00	425603	715123	YES	YES	YES	NO

6.2 Water chemistry for core sampling lakes

Water chemistry results are summarized by lake zone (epilimnion and hypolimnion), and are calculated from both raw and geographically weighted data. Incorporation of geographic sample weights (Table 6.1) accounts for the density of lakes in geographic proximity to the target sampling lake. Thus, statistics based on raw data summarize only the current dataset, while statistics based on weighted datapoints provide geographically unbiased estimates for all lakes in Vermont and New Hampshire. Water chemistry results for aqueous parameters are presented in Table 6.2.

Table 6.2. Summary of water chemistry data.

Summary statistics based on raw data										
Parameter	Strata	Count	Min.	Mean	Median	Max.	Range	St. error	95% lower C.L.	95% upper C. L.
Acid Neut. Capacity	EPI	127	-1.10	26.03	8.10	198.00	199.10	3.28	19.54	32.52
Acid Neut. Capacity	HYP	75	0.23	30.62	11.60	151.00	150.77	4.21	22.23	39.00
CL^-_mg/l	EPI	129	0.10	7.44	3.28	45.70	45.60	0.84	5.77	9.11
CL^-_mg/l	HYP	80	0.21	7.54	2.57	52.20	51.99	1.24	5.06	10.01
Diss. Color PtCo units	EPI	90	0.20	29.61	17.45	216.00	215.80	3.68	22.29	36.93
Diss. Color PtCo units	HYP	55	3.90	45.00	24.00	210.00	206.10	6.64	31.68	58.32
DOC mg/l	EPI	130	0.35	4.26	3.59	13.30	12.95	0.18	3.90	4.62
DOC mg/l	HYP	80	1.29	3.83	3.19	11.30	10.01	0.22	3.39	4.27
HgT_ng/l	EPI	129	0.22	1.74	1.23	9.66	9.44	0.13	1.47	2.00
HgT_ng/l	HYP	68	1.13	10.40	7.07	34.54	33.41	1.12	8.17	12.62
MeHg_ng/l	EPI	129	0.038	0.291	0.239	3.120	3.082	0.027	0.238	0.345
MeHg_ng/l	HYP	68	0.051	0.814	0.409	4.454	4.403	0.121	0.573	1.054
NOx_mg/l	EPI	128	0.02	0.03	0.02	0.33	0.31	0.00	0.03	0.04
NOx_mg/l	HYP	80	0.02	0.04	0.02	0.24	0.22	0.00	0.03	0.05
SO4_mg/l	EPI	129	1.95	4.20	3.92	10.00	8.05	0.13	3.94	4.45
SO4_mg/l	HYP	80	0.90	4.09	3.68	12.80	11.90	0.21	3.67	4.51
Sulfide_mg/l	EPI	44	0.02	0.10	0.02	1.40	1.38	0.03	0.04	0.17
Sulfide_mg/l	HYP	72	0.02	0.14	0.03	1.30	1.28	0.03	0.08	0.19
Total Color PtCo units	EPI	127	5.00	43.46	32.70	227.00	222.00	3.36	36.81	50.11
Total Color PtCo units	HYP	78	4.70	72.37	52.00	272.00	267.30	6.74	58.96	85.79
Summary statistics based on individual lake weights										
Acid Neut. Capacity	EPI	127	-1.1	19.1	6.4	198.0	199.1	1.0	17.1	21.1
Acid Neut. Capacity	HYP	75	0.2	24.1	10.3	151.0	150.8	1.5	21.2	27.0
CL^-_mg/l	EPI	129	0.10	8.09	4.18	45.70	45.60	0.32	7.46	8.72
CL^-_mg/l	HYP	80	0.21	7.84	3.02	52.20	51.99	0.47	6.93	8.76
Diss. Color PtCo units	EPI	90	0.20	27.10	17.00	216.00	215.80	1.35	24.46	29.74
Diss. Color PtCo units	HYP	55	3.90	41.24	22.40	210.00	206.10	2.61	36.11	46.38
DOC mg/l	EPI	130	0.35	4.31	3.70	13.30	12.95	0.07	4.18	4.44
DOC mg/l	HYP	80	1.29	3.91	3.60	11.30	10.01	0.08	3.75	4.07
HgT_ng/l	EPI	129	0.22	1.78	1.31	9.66	9.44	0.05	1.68	1.88
HgT_ng/l	HYP	68	1.13	11.52	7.70	34.54	33.41	0.46	10.62	12.41
MeHg_ng/l	EPI	129	0.038	0.299	0.259	3.120	3.082	0.009	0.281	0.318
MeHg_ng/l	HYP	68	0.051	0.829	0.402	4.454	4.403	0.047	0.738	0.921
NOx_mg/l	EPI	128	0.02	0.03	0.02	0.33	0.31	0.00	0.03	0.04

NO_X_mg/l	HYP	80	0.02	0.04	0.02	0.24	0.22	0.00	0.04	0.04
SO4_mg/l	EPI	129	1.95	4.11	3.92	10.00	8.05	0.04	4.03	4.19
SO4_mg/l	HYP	80	0.90	3.96	3.66	12.80	11.90	0.07	3.82	4.10
Sulfide_mg/l	EPI	44	0.02	0.12	0.02	1.40	1.38	0.01	0.09	0.14
Sulfide_mg/l	HYP	72	0.02	0.13	0.03	1.30	1.28	0.01	0.12	0.15
Total Color PtCo units	EPI	127	5.00	39.75	30.00	227.00	222.00	1.15	37.48	42.01
Total Color PtCo units	HYP	78	4.70	65.94	48.00	272.00	267.30	2.44	61.15	70.73

6.3 Multiprobe profiles – core and paleolimnology lakes

There exist 1,218 data records generated using the Hydrolab® multiprobe instruments employed by the project. Parameters include temperature, dissolved oxygen (and percent saturation), conductivity, salinity, and pH. The total number of individual records, summarized by lake and date, is presented in Table 6.3.

Table 6.3. Summary of multiprobe profile metadata.

Lake name	Date	# Indiv. measures	Lake name	Date	# Indiv. Measures	Lake name	Date	# Indiv. measures
Adder Pond	07/30/98	11	High (Sudbry)	08/31/00	12	Parker	08/02/00	12
Adder Pond	08/03/00	6	Hildreth Dam	08/24/98	9	Paugus Bay	07/24/98	23
Armington Lake	06/24/98	9	Horn Pond	07/12/98	10	Pawtuckaway Lake	08/11/98	16
Armington Lake	08/09/00	9	Horn Pond	08/16/00	10	Pawtuckaway Lake	08/17/99	14
Baker (Barton)	09/02/98	10	Hortonia	07/20/99	18	Pemigewasset Lake	08/20/98	9
Baker Pond- Upper	06/08/99	5	Hortonia	09/06/00	14	Pemigewasset Lake	08/21/00	10
Baker Pond- Upper	06/23/99	6	Howe Reservoir	08/24/99	6	Perch (Benson)	08/02/99	13
Bearcamp Pond	08/05/99	11	Island Pond	06/29/98	9	Perch (Benson)	08/23/00	12
Branch	08/19/99	10	Island Pond	08/25/00	12	Pleasant Valley	07/14/99	9
Bruce	07/02/98	3	Ivanhoe- Lake	07/15/98	7	Pout Pond	07/14/98	4
Cawley Pond	08/23/99	4	Jacksonville	07/14/98	1	Powwow Pond	07/01/98	7
Chase Pond	07/13/98	6	Jacksonville	08/09/00	1	Powwow Pond	08/07/00	6
Chase Pond	08/02/00	6	Jenness Pond	07/08/98	9	Robb Reservoir	07/12/99	4
Childs Bog	07/07/99	8	Jenness Pond	08/14/00	9	Round Pond	07/27/99	7
Chittenden	07/26/99	1	Kent	07/07/98	5	Sabin	07/22/99	15
Chittenden	07/19/00	8	Lary Pond	07/06/98	6	Shaws Pond	08/27/99	5
Club Pond	08/27/99	5	Lefferts	07/26/99	1	Silver Lake	07/20/98	14
Cranberry Meadow	06/30/98	8	Levi	07/06/99	7	Silver Lake	07/28/99	25
Cranberry Meadow	09/01/99	8	Lily Pond	06/30/98	3	Somerset	08/10/98	14
Curtis	07/22/99	11	Little Averill	08/17/99	16	Somerset	08/09/00	23
Curtis	07/20/00	9	Long (Westmr)	07/21/99	20	South America	08/05/98	1
Dennis	08/12/99	1	Loon Lake	07/29/99	9	Spruce Pond	08/13/99	6
Dunmore	07/29/99	23	Lovell Lake	08/04/99	12	Stratton	07/15/98	5
Dunmore	08/22/00	19	Lyford	07/08/98	7	Suncook Pond-Upper	08/17/98	14
Dutchman Pond	07/31/98	5	Lyford	09/03/99	6	Suncook Pond-Upper	08/14/00	13
Eastman Pond	08/30/99	11	Lyford	08/30/00	5	Sunrise Lake	07/15/99	7
Echo (Chartn)	08/26/98	16	Mansfield	06/23/98	7	Sunset (Brkfld)	08/11/99	11
Echo (Chartn)	08/15/00	23	Mcconnell	07/15/99	6	Sunset (Brkfld)	08/03/00	10
Echo (Hubdtn)	07/20/99	11	Millsfield Pond	08/09/99	5	Trio Ponds	08/03/98	10
Echo (Hubdtn)	08/23/00	13	Milton	07/22/98	5	Trio Ponds	08/23/00	10

Lake name	Date	# Indiv. measures	Lake name	Date	# Indiv. Measures	Lake name	Date	# Indiv. measures
Elm Brook Pool	08/19/99	6	Milton	08/24/00	4	Tuttle (Hardwk)	07/01/98	1
Fern	07/23/98	13	Minards	07/29/98	14	Unnamed Pond	07/14/99	3
Fern	07/29/99	13	Minards	09/01/00	15	Walker Pond	08/16/99	13
Fern	08/22/00	13	Mitchell	09/09/98	4	Willey Pond- Big	07/22/99	8
Fish Pond	08/04/98	5	Moose Pond	08/05/98	5	Willey Pond- Little	07/22/99	5
Freeses Pond-Upper	07/08/98	5	Mountain Lake	08/09/99	6	Willoughby	08/14/98	19
Giles Pond	08/23/99	6	Newark	07/21/99	9	Willoughby	08/08/00	32
Great Hosmer	07/27/99	13	North (Brkfld)	07/20/98	5	Wilson Pond	08/03/99	5
Great Hosmer	08/30/00	14	North (Brkfld)	08/03/00	4	Wolcott	08/24/99	7
Greenwood Pond	07/19/99	8	Notch	08/05/98	9	Wolcott	08/02/00	7
Hall Pond- Upper	08/19/98	14	Notch	08/16/00	8	Zephyr Lake	07/27/98	11
Hardwick	07/28/98	4	Noyes	07/07/99	3	Zephyr Lake	08/24/99	6
Hardwood	07/01/99	4	Paran	07/14/98	5			
Hardwood	08/02/00	5	Paran	08/09/00	5			
High (Sudbry)	07/30/98	17	Parker	07/27/99	13			

6.4 Sediment chemistry – core lakes

Sediment chemistry summary statistics were calculated from both raw and geographically weighted data, for percent solids and loss on ignition, HgT, meHg, and percent of total as meHg. These statistics are presented in Table 6.4. study region is shown in Figure 6.4.

Table 6.4. Summary of sediment chemistry data.

Summary statistics based on raw data									
Parameter	Count	Min.	Mean	Median	Max.	Range	St. error	95% lower C.L.	95% upper C. L.
Sediment HgT - ug/g	129	0.07	0.24	0.22	0.62	0.55	0.01	0.22	0.26
Sediment meHG - ug/g	78	0.0004	0.004	0.003	0.021	0.021	0.0001	0.004	0.005
Sediment meHG, % of HgT	78	0.240	1.842	1.462	7.840	7.600	0.156	1.530	2.154
Solid content %	129	1.56	8.01	6.50	43.90	42.34	0.48	7.07	8.95
Loss on ignition %	129	9.20	32.56	30.60	69.20	60.00	1.11	30.36	34.75
Summary statistics based on individual lake weights									
Sediment HgT - ug/g	129	0.07	0.24	0.21	0.62	0.55	0.00	0.23	0.25
Sediment meHG - ug/g †	78	0.0004	0.004	0.003	0.021	0.021	0.0001	0.004	0.004
Sediment meHG, % of HgT †	78	0.240	1.713	1.430	7.840	7.600	0.054	1.607	1.818
Solid content %	129	1.56	8.35	7.00	43.90	42.34	0.19	7.97	8.72
Loss on ignition %	129	9.20	32.17	30.50	69.20	60.00	0.39	31.40	32.95

†) please refer to section 7.4 for a discussion regarding the quality of the sediment meHg data results.

6.5 Biological tissue chemistry

Summary statistics were calculated for: HgT in yellow perch fillets, residual perch offal, bulk macrozooplankton (≥ 201 μ) and avian piscivore blood, feathers, and eggs; HgT and meHg in prey-sized (≤15cm) yellow perch composites; and, physical characteristics of tissue samples. Summary statistics, calculated using both raw and geographically weighted data, are provided in Table 6.5. Based on paired analyses of composited prey-sized perch, meHg was equivalent to HgT ($r^2 = 0.94$, $p<0.001$).

Table 6.5 Summary of biological tissue data.

Summary statistics based on raw data									
Parameter	Count	Min.	Mean	Median	Max.	Range	St. error	95% lower C.L.	95% upper C. L.
Filet Length_cm	278	14	20.7	20.0	36.3	22.3	0.3	20.2	21.2
Filet Weight_g	278	29.30	117.59	89.05	568.00	538.70	5.63	106.49	128.68
FishAge	232	1.0	4.9	4.0	28.0	27.0	0.2	4.5	5.3
Yellow Perch Fillet HgT_ug/g ww	278	0.014	0.238	0.190	1.300	1.286	0.010	0.218	0.258
Yellow Perch Offal HgT	80	0.045	0.223	0.203	0.976	0.931	0.016	0.191	0.256
Yellow Perch Prey weight_ g	45	3.06	85.64	83.89	159.14	156.08	6.41	72.72	98.57
Yellow Perch Prey HgT ug/g w.w.	45	0.030	0.095	0.089	0.320	0.290	0.008	0.079	0.111
Yellow Perch Prey meHg ug/g w.w.	30	0.0290	0.0917	0.0803	0.2570	0.2280	0.0097	0.0719	0.1114
Zooplankton % Solid	41	0.01	0.26	0.21	0.65	0.64	0.03	0.21	0.32
Zooplankton HgT ug/g d.w.	38	0.100	0.379	0.291	1.710	1.610	0.051	0.276	0.481
Zooplankton HgT ug/g w.w.	38	0.015	0.093	0.077	0.336	0.319	0.012	0.068	0.177
Loon blood HgT ppm w.w.	19	0.012	1.373	1.270	3.430	3.418	0.251	0.845	1.901
Loon egg HgT ppm w.w.	15	0.271	0.743	0.589	1.590	1.319	0.095	0.539	0.948
Kingfisher blood HgT ppm w.w.	10	0.115	0.647	0.532	1.435	1.320	0.170	0.263	1.031
Summary statistics based on individual lake weights									
Filet Length_cm	278	14	20.6	20.0	36.3	22.3	0.1	20.4	20.8
Filet Weight_g	278	29.3	114.59	90.10	568.00	538.70	1.99	110.69	118.49
FishAge	232	1	4.6	4.0	28.0	27.0	0.1	4.5	4.7
Yellow Perch Fillet HgT_ug/g ww	278	0.014	0.239	0.197	1.300	1.286	0.004	0.232	0.246
Yellow Perch Offal HgT	80	0.045	0.209	0.177	0.976	0.931	0.005	0.199	0.219
Yellow Perch Prey weight_ g	45	3.06	80.99	80.85	159.14	156.08	2.35	76.35	85.62
Yellow Perch Prey HgT ug/g w.w.	45	0.030	0.098	0.094	0.320	0.290	0.003	0.092	0.103
Yellow Perch Prey meHg ug/g w.w.	30	0.0290	0.0914	0.0806	0.2570	0.2280	0.0035	0.0846	0.0983
Zooplankton % Solid	41	0.01	0.24	0.19	0.65	0.64	0.01	0.22	0.26
Zooplankton HgT ug/g d.w.	38	0.100	0.432	0.350	1.710	1.610	0.023	0.387	0.478
Zooplankton HgT ug/g w.w.	38	0.016	0.091	0.074	0.336	0.321	0.005	0.082	0.101
Loon blood HgT ppm w.w.	18	0.012	1.356	1.400	3.430	3.418	0.087	1.184	1.528
Loon egg HgT ppm w.w.	15	0.271	0.762	0.589	1.590	1.319	0.032	0.699	0.825
Kingfisher blood HgT ppm w.w.	10	0.115	0.759	0.554	1.435	1.320	0.068	0.623	0.895

note: Zooplankton HgT values are given as both dry and wet weight to facilitate comparison to other biological matrices.

6.6. Risk characterizations to common loons

Tissue samples acquired from common loons permit assessment of the overall risk to loons posed by Hg bioaccumulation. Risk characterizations were derived using either adult or juvenile blood, or abandoned eggs. The type of sample acquired was determined in the field based on availability and opportunity. Risk attributions followed the protocols of Evers et al. (2000). Based on these characterizations, samples collected from lake in this study were evaluated by state, and in relation to loon tissues acquired from the Maine REMAP study lakes (MEDEP, 1995). Results are provided in Figure 6.6.

Fifty percent of loons from Vermont study lakes, and 70% of loons from NH study lakes, have sufficient Hg in their tissues so as to pose a moderate or greater risk to the animals themselves. In Maine, the proportion is 78%. The total percentages of birds at high or extra high risk increases from 20% in VT, to 27% in Maine. A geographic gradient is apparent in these data, with a clear increase from west to east. This is consistent with the findings of Evers et al. (1998).

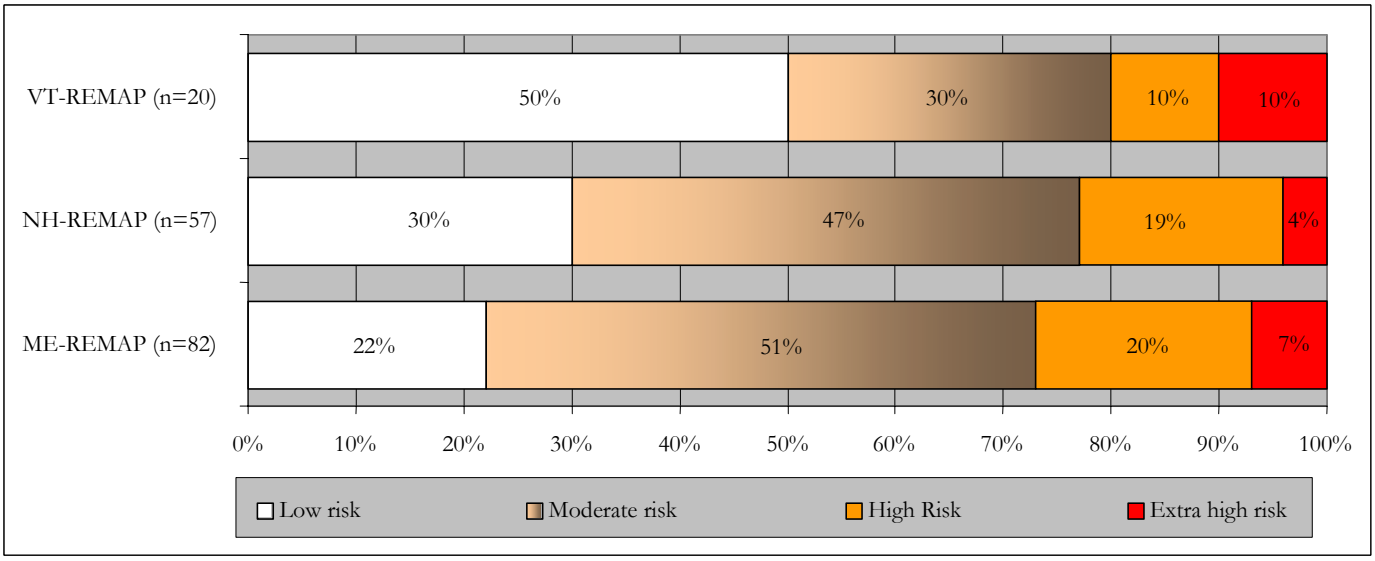

Figure 6.6. Mercury risk to breeding Common Loons (*Gavia immer*), based on adult and juvenile blood and egg Hg levels.

Evers (e.g., 2003 in prep.) further indicates that these proportions are sufficient so as to threaten entire loon populations. The present hypothesis regarding population-level impacts to loons is that chronic Hg exposure impacts to loons is reducing the ability of loon pair to successfully produce chicks, owing to impacts to individual birds within the parent pair (Evers, pers. comm.). Individual-level impacts include reduced ability to acquire food for chicks, and reduced ability to defend nesting territories from predators and other loons. However, in the field, observations regarding loon nesting habits from citizen monitoring groups show continuing increases in overall numbers of nesting loon pair. While these two phenomena seem at odds, they are in fact consistent, when the effect of the male loon "buffer population" is accounted for. The "buffer population" is that group of male birds (typically juvenile or subadult, lone birds) which are available to fill in for a nesting male bird, if that bird is unable to successfully defend it's territory, or is lost due to disease or other factors. It is the decline in the "buffer population" which is cause for concern. Declines in actual nesting loon pair and reared chicks is expected to accompany further reductions in the buffer population.

6.7 Paleolimnology of Hg in Vermont and New Hampshire lakes

Results of the paleolimnology component are presented in the form of total ^{210}Pb counts, Hg fluxes for current and pre-1850 time periods, and Hg flux profiles with time, in Tables 6.7.1, 6.7.2, and Figure 6.7.1, respectively. Overall, the results of the paleolimnological analysis underscore that Hg fluxes to lake sediments: exhibited a temporally coincident initial increase ~1850; are presently decreasing; and, fluxes vary by individual lake. Lakes that incur watershed disturbance are likely to have enhanced Hg sedimentation relative to less disturbed lakes. As an example, baseline fluxes for the disturbed Beaver Lake in New Hampshire exceed peak fluxes for the small undisturbed Willard Pond (Table 6.7.2). Detailed analysis of data provided by the paleolimnological component for the ten least disturbed lakes in the study set are reported in the primary literature by Kamman and Engstrom (2002). This paper is provided in entirety in Appendix A. Results of that analysis are summarized by the abstract from that article:

> "Lakes across the northern hemisphere have experienced enhanced atmospheric deposition of anthropogenically-derived Hg for over 100 years. In the present study, we quantified Hg fluxes to the sediments of ten small drainage lakes across Vermont and New Hampshire, USA, for the period ~1800 to present. Dates were established by ^{210}Pb. Total Hg (HgT) fluxes to sediments ranged from 5 to 17 $\mu g \cdot m^{-2} \cdot yr^{-1}$ during pre-industrial times, and from 21 to 83 $\mu g \cdot m^{-2} \cdot yr^{-1}$ presently. Present-day HgT fluxes are between 2.1 to 6.9 times greater than pre-1850 fluxes. Current-day direct atmospheric Hg deposition to the study region was estimated at 21 $\mu g \cdot m^{-2} \cdot yr^{-1}$, which agrees well with measured HgT deposition, when re-evasion of Hg is accounted for. Our data suggest that Hg fluxes to lake sediments have declined in recent decades, owing to reductions in atmospheric Hg deposition to the lake surface. Watershed export of atmospherically deposited Hg remains elevated relative to present-day deposition rates, which contributes to the impression that Hg retention by watershed soils has declined."
>
> © Elsevier Science Inc.

Table 6.7.1. Diagnostic ^{210}Pb dating values for 13 lakes.

	Supported ^{210}Pb, pCi g^{-1} (s.e.)	N supported samples	Cumulative un-supported ^{210}Pb, (pCi cm^{-2})	Unsupported ^{210}Pb flux, (pCi cm^{-2} yr^{-1})
BEAVER	2.35 (.05)	3	18.44	0.60
BRANCH	1.14 (.02)	2	12.78	0.41
CARMI	1.42 (.03)	3	18.08	0.58
DUDLEY	0.28 (.07)	3	11.08	0.36
GILMAN	0.75 (.01)	2	6.77	0.22
HIGH	1.88 (.06)	5	14.73	0.47
INTERVALE	1.74 (.06)	6	12.49	0.40
MCCONNELL	1.68 (.06)	1	11.32	0.36
SESSIONS	1.09 (.06)	5	10.63	0.35
SPRING	2.50 (.05)	4	22.02	0.71
WALLINGFORD	0.64 (.02)	2	12.34	0.40
WHEELER	0.64 (.05)	4	10.54	0.34
WILLARD	0.85 (.02)	4	12.60	0.41

Table 6.7.2. Modern, peak, and background Hg fluxes to the sediments of 13 lakes.

	Modern (1998) Hg flux $\mu g\ m^{-2}\ yr^{-1}$	Peak flux (year of occurrence) $\mu g\ m^{-2}\ yr^{-1}$	Baseline flux (years used to estimate) $\mu g\ m^{-2}\ yr^{-1}$	Ratio of modern to baseline
BEAVER	133	203 (1970)	57 (1892)	3.6
BRANCH	73	102 (1960)	28 (1825-1854)	3.6
CARMI	54	72 (1984)	13 (1785-1828)	5.5
DUDLEY	46	68 (1992)	10 (1777-1860)	4.6
GILMAN	26	26 (1998)	11 (1863)	2.4
HIGH	23	39 (1979)	5 (1693-1813)	4.6
INTERVALE	48	55 (1995)	7 (1626-1834)	6.9
MCCONNELL	83	106 (1992)	13 (1777-1834)	6.4
SESSIONS	30	48 (1985)	14 (1766-1848)	2.1
SPRING	25	41 (1963)	11(1755-1808)	2.3
WALLINGFORD	45	66 (1987)	17 (1731-1787)	2.6
WHEELER	78	92 (1990)	16 (1715-1819)	4.9
WILLARD	21	50 (1968)	10 (1704-1844)	2.1
Average	52.7	74.5	16.3	4.0

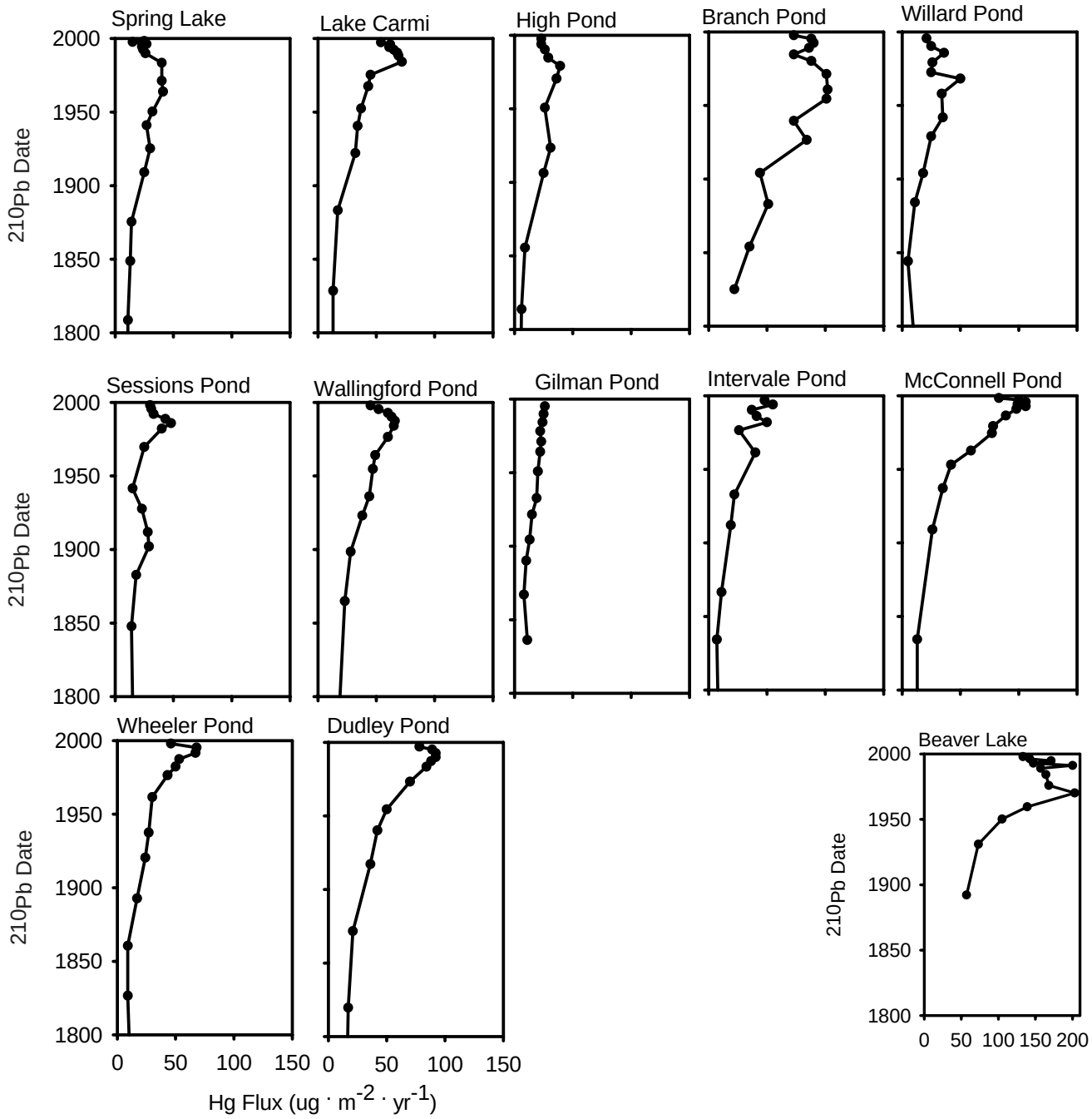

Figure 6.7. ^{210}Pb-inferred Hg fluxes to the sediments of 13 VT and NH lakes. X-axis scaling for Wheeler and Dudley Ponds applies to all unlabelled axes.

7.0 Quality assurance and control results

7.1 Water chemistry parameters

Quality assurance metrics for aqueous phase parameters are presented in Table 7.1. Relative differences and standard deviations are expressed as percentages, along with the number of quality assurance samples acquired, for field and laboratory duplicates. These metrics provide information on sampling and analytical accuracy. Mean blank concentrations are presented for pooled field and equipment blanks, and provide information related to sampling and analytical contamination. Mean recoveries are expressed as percentages, and provide an estimate of precision. There is good agreement between the QC indicators measured for this study, and target limits published in the LaRosa Laboratory's Quality Assurance Plan (see Table 4.1).

Table 7.1. Quality assurance and control indicators for aqueous-phase parameters.

Parameter	ANC	CL^-	NO_X	SO_4	Sulfide	DOC	TC	meHg	HgT
Mean RPD[1] for all F.D.[2]	8.0%	12.1%	10.9%	2.2%	11.7%	6.7%	9.0%	28.8%	36.6%
# Duplicates	19	25	25	25	14	25	21	22	22
Mean RPD for Epilimnetic F.D.	4.3%	4.7%	7.8%	2.0%	6.1%	5.5%	6.5%	32.6%	26.5%
# Epilimnetic Duplicates	10	11	11	11	3	11	10	10	10
Mean RPD for Hypolimnetic F.D.	12.2%	16.2%	15.6%	2.6%	13.2%	8.1%	12.3%	28.0%	45.9%
# Hypolimnetic Duplicates	9	12	12	12	11	12	10	10	10
Mean Blank Concentration[3]	0.7	0.16	0.03	0.2	<0.02	0.82	2.65	0.0547	1.35
# Blanks	16	16	16	16	6	16	16	15	15
Mean RPD for L.D.[4]		1.6%	13.7%	0.9%	1.2%	--	--	16.5%	10.4%
# Duplicates	--	--	19	3	13	--	--	20	56
Mean recovery for M.S.[5]	--	--	113.9%	96.0%	98.09%	--	--	--	--
# M.S.	--	--	4	2	14	--	--	--	--
RSD[6]	--	--	--	--	--	--	--	--	19.9%
# Analytical Sets	--	--	--	--	--	--	--	--	18

1) Relative percent difference
2) Field duplicates
3) Units are defined Table 6.2
4) Lab duplicates
5) Matrix spikes
6) Relative standard deviation

7.2 Solid phase parameters

Quality assurance metrics for solid phase parameters are presented in Table 7.2. Relative percent differences and recoveries are expressed as percentages, along with the number of quality assurance samples acquired, for field and laboratory duplicates, matrix spikes, and standard reference material. These metrics provide information on sampling and analytical accuracy. Mean blank concentrations are not provided for solid-phase parameters. Mean recoveries are expressed as percentages, and provide an estimate of precision. There is good agreement between the QC indicators measured for this study, and target limits published in the LaRosa Laboratory's Quality Assurance Plan.

Table 7.2. Quality assurance and control indicators for sediment-phase parameters.

Parameter	Sed. HgT (s.d.[1])	Sed. meHg	% meHg	Perch HgT	% Solid	% LOI
Mean RPD for F.D.	3.2%	32.5%	34.8%	--	8.0%	1.7%
# Duplicates	13	8	8	--	13	13
Mean RPD for L.D.	3.2%	--	--	5.7%	1.1%	--
# Duplicates	328	--	--	265	19	--
Mean recovery for M.S.	97.0%	--	--	92.9%	--	--
# M.S.	64	--	--	37	--	--
SRM[2] – Certified 0.72 ppm	0.730 (0.029)	--	--	--	--	--
# SRM	14	--	--	--	--	--
SRM Certified 1.12 ppm	1.20 (0.19)	--	--	--	--	--
# SRM	17	--	--	--	--	--

1) Standard deviation
2) Standard reference material

7.3 Laboratory intercomparison for HgT

Given the sensitive nature of aqueous Hg at ambient concentrations, several samples were split between Syracuse University and an independent laboratory specializing in trace-level mercury analyses. Frontier Geosciences in Seattle, WA was chosen for this purpose. Table 7.3 provides results of this intercomparison.

Table 7.3. Results of 10 laboratory intercomparison aqueous HgT samples.

Strata	Lake abbr.	Date collected	HgT ng/l Frontier GeoSci.	HgT ng/l Syracuse Univ.	Relative percent difference
Epilimnion	BRANC	19-Aug-99	1.96	1.776	10%
	CURTI	22-Jul-99	0.71	0.63	12%
	FERNL	29-Jul-99	0.60	0.43	33%
	LAVER	17-Aug-99	0.56	0.501	11%
Hypolimnion	BRANC	19-Aug-99	13.40	25.843	63%
	CURTI	22-Jul-99	1.55	2.808	58%
	FERNL	29-Jul-99	2.43	7.699	104%
	LAVER	17-Aug-99	3.52	6.678	62%
	WOLCO A	24-Aug-99	27.30	2.894	162%
	WOLCO D	24-Aug-99	9.53	11.24	16%

These data show a strong difference in the magnitude of relative percent differences between epilimnetic and hypolimnetic samples. Table 7.1 clearly shows that field variability is greater for hypolimnetic samples collected with the Teflon Kemmerer sampler, than for epilimnetic grab samples. The reason for the very strong hypolimnetic differences at both the Fern and Wolcott locations is unclear. The Syracuse samples were re-run with similar results, while bench sheets and internal QC indicators were examined from Frontier Geosciences, providing no reason to question results. Due to required sample volumes, it was impractical to split samples directly from a single Kemmerer grab, and therefore these 'splits' are in reality field duplicates, which therefore

incorporate field variability. With specific regards to the Wolcott samples, it is possible that the hypolimnetic bottles samples were inadvertently switched (e.g. mislabeled).

7.4 Problems

Individual quality assurance problems (e.g. bad blanks, duplicates, or unanticipated results) were addressed throughout the course of the project, in accordance with this project's quality assurance project plan. Details on individual problems were discussed in the quarterly progress reports submitted throughout the course of the project, and included items such as switched labels, poor blank values for standard parameters, and contamination of one of the laboratory acid baths. Three larger-scale problems were encountered, which merit mention here.

The first involves high blank results for aqueous HgT collected using the Teflon Kemmerer sampler: This is discussed in some detail in the quarterly progress reports. In summary, it was a common occurrence for ambient Kemmerer bottle samples to run lower than blanks collected using the Kemmerer sampler. We attribute this to the volume of available Hg-clean blank/rinse water, which was insufficient to completely clean the sampler prior to processing the actual sample. This is owing to a limited availability of clean Teflon sampling bottles, and not to water itself. Carryover contamination from ambient samples to Kemmerer blanks may not have been completely cleaned given the limited (~200ml) quantity of blank water used to pre-rinse the sampler. This problem would not extend to actual ambient samples, owing to the large volume of available rinse water (e.g., the lake itself) during acquisition of the hypolimnetic samples. Thus, despite these blanks, the project team feels that the results for hypolimnetic samples are valid, and they have been retained in the database.

The second problem involved poor sediment meHg results for samples collected in 1998. The meHg analyses for the entire set of sediment samples collected during 1998 were compromised owing to what remain unknown factors. During that year, sediment samples were stored in zip-style bags from collection to analysis at Syracuse. We believe that methylation continued or was enhanced by the anaerobic environment within the zip-bags, for, when analyzed, numerous meHg values ran far above published values, and even in one or two instances, in excess of HgT. This of course did not make sense. The project team verified these poor results at independent laboratories (Dr. Robert Mason, University of MD), and the samples were re-run numerous times at Syracuse University with no improvement. We feel that the results for the 1998 meHg analyses were in gross error, and these results have not been incorporated into the project database. Accordingly, the unweighted and weighted means and confidence intervals reported in Table 6.4 do not represent the entire sample of VT and NH lakes

This final problem involved analysis of HgT in zooplankton. One of several zooplankton analytical batches yielded quality control measurements which were well out of limits for the LaRosa laboratory. Specifically, blank aliquots included in the run produced very high results (~0.2 ug/g), suggesting contamination within the reagents or DI water. Simultaneously, the spikes accompanying those samples yielded very low recoveries (41%); a finding at odds with the high blank results. The chemists, despite a relatively exhaustive investigation, were unable to uncover the root of the problem, which was not subsequently replicated. The source of the error was tracked to the digestion procedure, but the exact cause remains unknown. Owing to extremely limited quantities of sample, the analyses were not able to be re-run, and that single run of seven samples was lost.

8.0 Analysis of the project data

Numerous data analyses have been performed using these project data. These include: statistical age-adjustment of mean perch fillet Hg concentrations for each study lake; estimation of cumulative frequency distributions for all Hg parameters measures by the study; plotting of various Hg measurements using GIS to identify the existence of geographic patterns; formal statistical evaluation of project design factors; evaluation of inter-annual data variability; investigation of the effect of trophic status on Hg in waters and sediments; calculation of bioconcentration and bioaccumulation factors; examination of univariate correlations between physicochemical and Hg variables; estimation of principal components of physicochemical factors, and correlations of these factors to Hg variables; evaluation of the role of land-use on Hg in fish tissue; and, development of candidate linear discriminant functions to predict tissue Hg levels in fillets given physico-chemical data.

8.1 Calculation of age-adjusted yellow perch fillet means for each study lake

Yellow perch tissue HgT is known to vary both with fish size and fish age (Driscoll et al., 1994; Gilmour and Reidel, 2000; Carter et al., 2001). Both the length and age adjustment models were highly significant, with length and age explaining 31.6% and 19.1% of the total variance in inverse-root tissue HgT across lakes, respectively (length: $F = 57.44$, $p<0.001$, d.f.=214, 17; age: $F=7.29$, $p<0.001$, d.f.=109, 122). A clean 1:1 relationship in age vs. length adjusted HgT tissue concentrations existed for most lakes, although several outliers are apparent (Figure 8.1). Of these outliers, lakes falling well above the 1:1 relationship (Hardwood, Somerset, Suncook, and Wolcott) are all highly colored and acidic, while those falling below (Sunset-Brookfield and Sabin) are well buffered and pH circumneutral. Lakes of low pH and higher DOC are commonly those with more elevated fish-tissue Hg concentrations (Mierle and Ingram, 1991; Driscoll et al., 1994; Carter et al., 2001). Therefore, although the length-adjustment accounted for more overall variance than age, the age-adjusted concentrations were interpreted in this instance to more accurately estimate individual lake mean tissue concentrations. Mean muscle tissue HgT concentrations (inverse-root transformed), adjusted to the average age 4.6 year fish (the overall mean age, accounting for variance across study lakes) were retained for further analysis. These values were back-transformed to units of $\mu g\ g^{-1}$ for discussion and plotting purposes only.

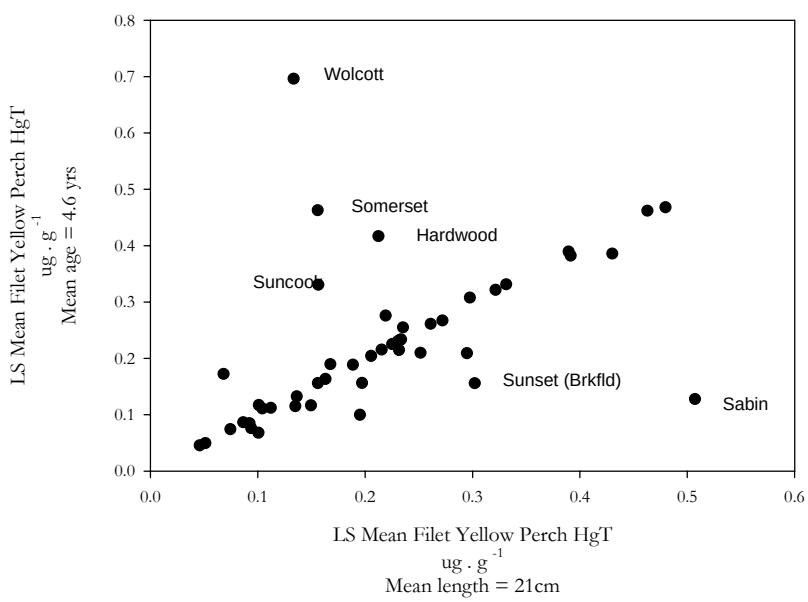

Figure 8.1. Relationship between age and length-adjusted yellow perch muscle-tissue least squared mean Hg concentrations.

8.2 GIS analyses

Several water and sediment Hg parameters were plotted using Arcview GIS (ESRI Inc, v 3.1, 2000), to visually evaluate whether patterns exist in several Hg parameters across the Vermont-New Hampshire landscape. Mean values of all sampling events, excluding blank samples, were used to generate these plots. Individual sample-lake values are displayed as their deviation from the grand mean for each parameter. Figure 8.2 displays the maps, which yield the following parameter-specific observations:

- Epilimnetic HgT: No discernable patterns in deviations from the mean are apparent.
- Epilimnetic meHg: A greater proportion of lakes displaying elevated meHg concentrations occur in New Hampshire. There is also a cluster of lakes showing elevated meHg in northeastern VT.
- Hypolimnetic HgT: New Hampshire lakes display greater hypolimnetic HgT concentrations overall. The highest hypolimnetic concentrations occur in the southern-most reaches of the study region.
- Hypolimnetic meHg: Hypolimnetic meHg is elevated in south central and southeastern New Hampshire.
- Sediment HgT: No discernable pattern is apparent.
- Sediment MeHg: No discernable pattern is apparent, save that a cluster of lakes showing elevated sediment MeHg exists in south-central New Hampshire.
- Yellow perch, whole-fish composites, < 15cm: No pattern is apparent in the geographic distribution of prey-sized yellow perch composite whole-body HgT or meHg. However, most southeastern New Hampshire lakes do appear to have elevated HgT and MeHg in prey-sized yellow perch
- Yellow Perch, fillet age-adjusted mean HgT: Two patterns are apparent. First, tissue HgT means are most variable in north-eastern Vermont. Second, there exists a cluster of lakes with elevated tissue Hg concentrations in southern New Hampshire. This 'hotspot' coincides with that noted for sediment meHg.
- Yellow perch fillets, exceedences of the 0.3 $\mu g\ g^{-1}$ meHg standard: Tissue criterion exceedences are apparent in the southern New Hampshire hotspot, in three central New Hampshire lakes, in one southern Vermont lake, and in two northern Vermont lakes.

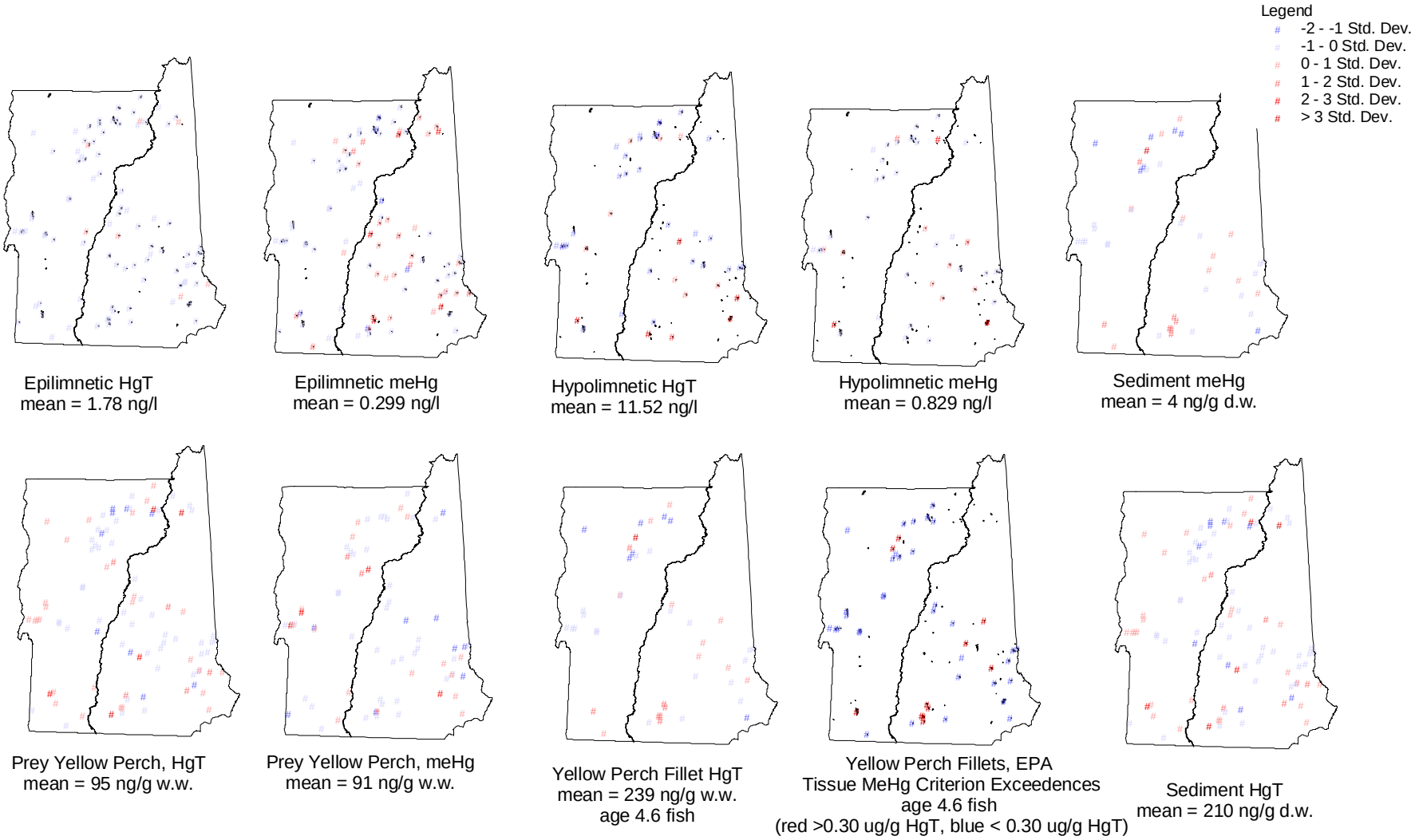

Figure 8.2. Mercury in sediment, waters, and yellow perch tissues of lakes sampled in conjunction with this project. Values are expressed as standard deviations from the mean. Weighted mean concentrations for each parameter are shown.

8.3 Statistical evaluation of strata in the experimental design

In initially designing this study, we imposed four watershed:lake area strata, or blocks, upon the random lake selection, under the premise that Hg in waters and sediments is influenced by the size of the watershed surrounding any given study lake (see Table 2.1). The sample draw was approximately balanced around these four blocks, and weights were assigned to individual study lakes to account for bias attributable to the stratification. Influence exerted on HgT and meHg in waters and sediments, and on age-corrected HgT in yellow perch fillets by the four strata was assessed using ANOVA. Data transforms were applied as necessary to satisfy statistical assumptions of normality and homoscedascicity. It is accepted that ANOVA modeling is robust to minor departures from normality so long as equality of variances is achieved (Kuehl, 2000). In some of these ANOVA's, normality was difficult to achieve, even while assumptions of equal variance, assessed using Levene's median test, were met. Thus, while the results of the parametric ANOVA's are valid, for completeness, they were re-run as non-parametric ANOVA on ranks. In no cases was significant variation in mean Hg values attributable to strata (Table 8.3), although variation in both sediment HgT and age-corrected tissue Hg was marginally significant for both tests. Based on these analyses, the stratification imposed upon the initial project design did not contribute to explaining variation in any of the Hg parameters at a significance level of 95%, and the strata were therefore not included as blocks in subsequent statistical analyses. Individual lake weights were incorporated in subsequent analyses to correct for the bias interjected by the stratification.

Table 8.3. Results of ANOVA and ANOVA on Ranks tests of the influence of four lake:watershed area classes on multiple Hg parameters measured from 92 REMAP study lakes.

Parameter	Epilimnetic HgT n=92	Epilimnetic meHg n=92	Hypolimnetic HgT n=53	Hypolimnetic meHg n=53	Sediment HgT n=92	Sediment meHg n=92	Mean yellow perch fillet HgT, adjusted to age 4.6 yr fish
P-value for ANOVA	0.154	0.570	0.790	0.534	0.063	0.131	0.072
P-value for ANOVA on Ranks	0.209	0.289	0.587	0.709	0.079	0.135	NA

8.4 Cumulative frequency distribution diagrams

A significant benefit to our project design has been the ability to produce unbiased estimates of overall levels of Hg contamination across the VT-NH region, as well as by state. Cumulative frequencies, accounting for individual study-lake weighting factors, were plotted for several Hg parameters, and are presented in Figures 8.4.1 and 8.4.2. Figure 8.4.1 shows that approximately 25% of lakes across Vermont and New Hampshire have yellow perch fillet concentrations that are in violation of the USEPA fish tissue meHg criterion of 0.3 $\mu g\ g^{-1}$ w.w (EPA 2001), when normalized to an age 4.6 year fish. In this study, meHg averaged 85% ± 4% of HgT (SAS Proc REG, $r^2 = 0.94$, n=30, $p<0.001$), based on paired total and meHg analyses for prey-sized whole yellow perch. There are clear differences in biological tissue Hg concentrations between states, which is apparent in Figure 8.4.2.

In 1993 and 1994, the State of Maine carried out a program designed to estimate average HgT levels in fish tissues statewide, using a stratified, randomized sampling design similar to that employed in the present study (MEDEP, 1995). While collection methods and data presentation approaches varied, there is a reasonable consistency between the data collected from the Maine study and that from the present REMAP study. Where data were available, Hg measurements from this Maine REMAP study were also plotted in Figure 8.4.2, to place the current results in a geographic context. Design weights were not available for the Maine study results, and thus the comparison of the Maine cumulative distributions to this study's results must be treated cautiously.

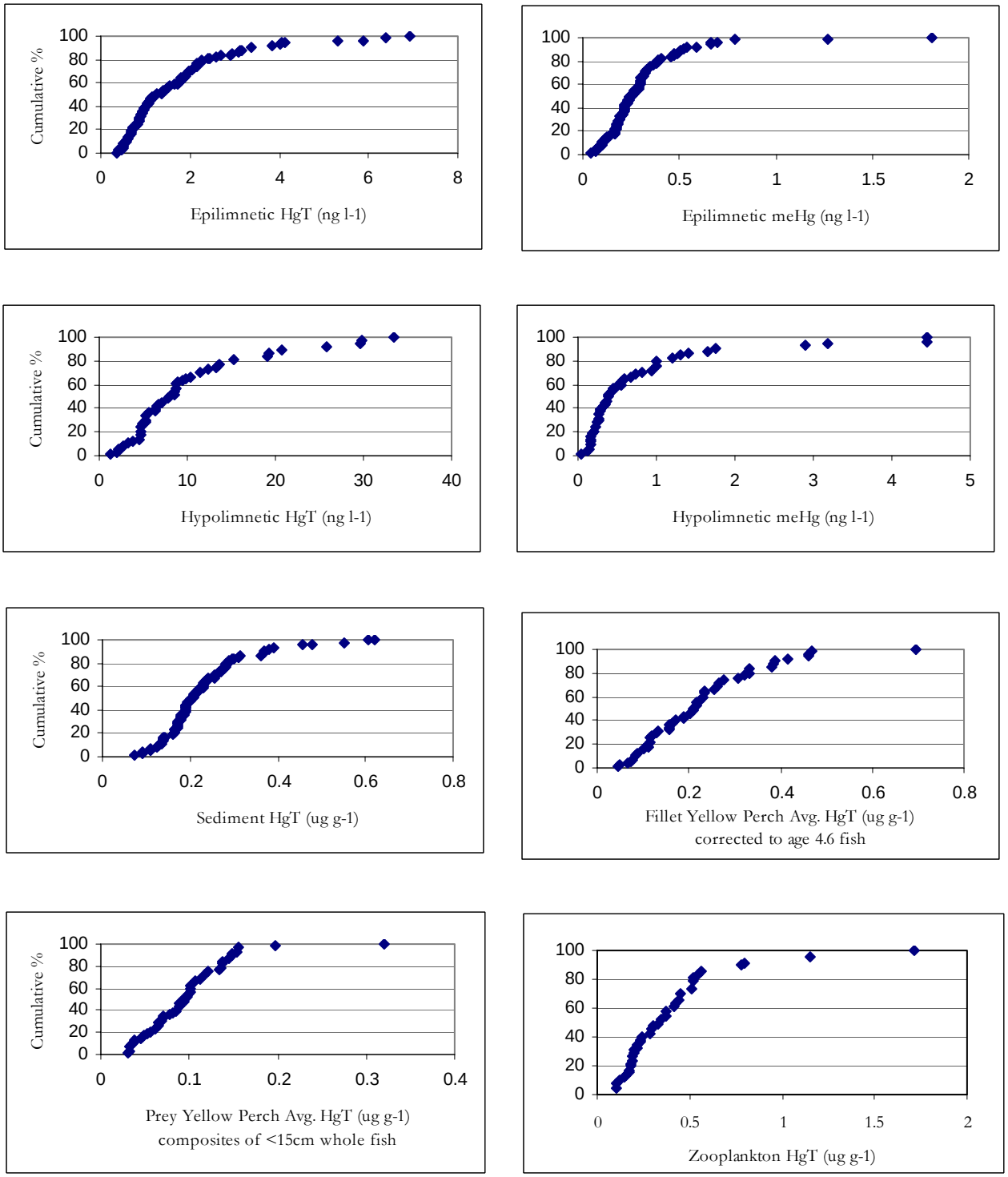

Figure 8.4.1. Cumulative frequency distributions for Hg parameters measured in VT and NH lakes.

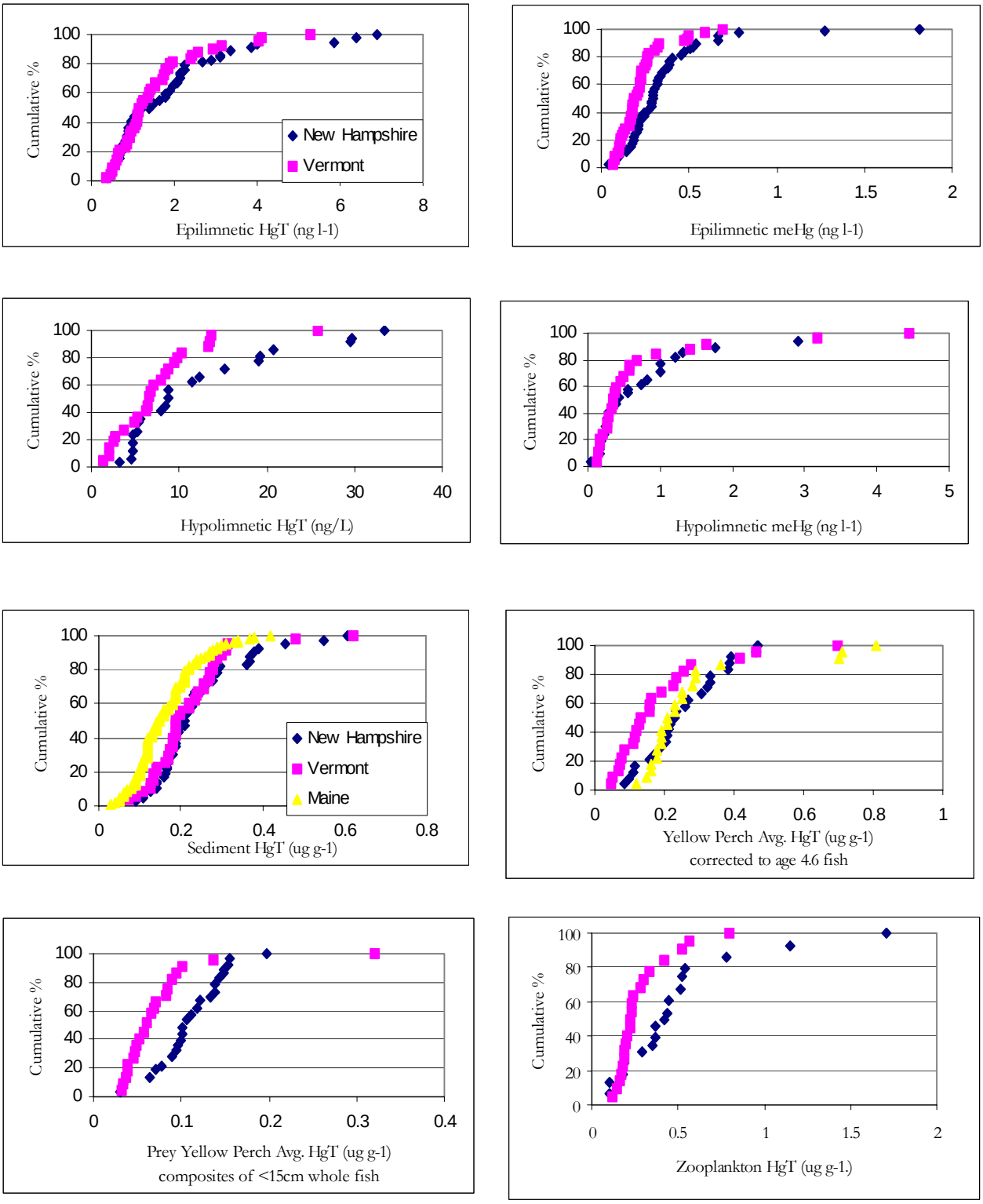

Figure 8.4.2. Cumulative frequency distributions for Hg parameters, by State.

8.5 Evaluation of inter-annual variability and replicate sampling

Since the sampling effort for this study spanned 1998 to 2000, an assessment of inter-annual variability was performed to determine whether significant variation in water and sediment chemistry could be attributed either to the years in which the samples were collected (1998 vs. 1999), or to sample replication. This analysis was conducted using multivariate analysis of variance (MANOVA), to account for simultaneous covariance among the numerous parameters measured. For both analyses, separate MANOVA were performed on epilimnetic and hypolimnetic water chemistry, and on sediment chemistry. Where MANOVA indicated a significant difference attributable to year, follow-up univariate ANOVA was used to determine which parameters influenced this variation. The 1998 vs. 1999 statistical model evaluated the null hypothesis that no linear combination existed which could produce a significant difference in the mean multivariate water or sediment chemistry observation, between years. For the replication analysis, the statistical model evaluated the null hypothesis that no linear combination existed that could produce a significant difference in the mean multivariate water or sediment chemistry observation, while accounting for the expected variation due to individual lakes.

For epilimnetic samples, a statistically significant difference in water chemistry was evident between years (Table 8.5). Follow-up ANOVA indicated that log-HgT was the only parameter which varied significantly between 1998 and 1999. For hypolimnetic water chemistry and sediment chemistry, no significant differences between years were noted. The analysis of replicates (collected in 2000) yielded identical results (Table 8.5); differences in replicates were apparently confounded with differences attributable to year. For hypolimnetic water chemistry and sediment chemistry, no significant differences between sampling events were noted.

Table 8.5. Results of MANOVA and follow-up ANOVA analyses of inter-annual variability and replicate sampling. P-values are provided only where there is significant variation across years or between replicates (ns: not significant at the 95% probability level).

	Epilimnetic water	Hypolimnetic water	Sediment	Epilimnetic water	Hypolimnetic water	Sediment
	Comparison 1998 to 1999			Comparison replicate measurements, 1998 to 2000		
Wilks' Λ, F statistic *p*-value	0.520, 10.26, **<0.001**	0.860, 0.97, ns	0.970, 0.99, ns	0.326, 4.39, **0.005**	0.444, 2.00, ns	0.809, 1.80, ns
	Follow-up univariate ANOVA *p*-values for transformed variables					
Secchi transparency	ns			ns		
ANC	ns			ns		
Chlorides	ns			ns		
SO4	ns			ns		
DOC	ns			ns		
Total color	ns			ns		
meHg	ns			ns		
HgT	**<0.001**			**0.002**		
Sediment HgT	--			--		
Loss on Ignition	--			--		
Solid %	--			--		

In order to test that observed differences in HgT between replicate samples was indeed confounded with that variation attributable to year, data from each year of sampling (1998, 1999, and 2000) were plotted as separate groups (Figure 8.5.1). Although no statistical comparisons are possible because the lakes visited in 2000 were not randomly selected, it is clear from this plot that any differences are between the mean HgT concentrations from 1998 through 2000 are obscured by the large variance exhibited in 1998.

Two-way ANOVA indicates that epilimnetic HgT varied with year and with state (F = 30.37, $p<0.001$, d.f.=3, 94). Year was highly significant ($p<0.001$), but a significant interaction existed between year and state ($p=0.028$), in that New Hampshire lakes appeared to display higher concentrations than did Vermont lakes in 1998 (Figure 8.5.2). However, no statistical difference in the mean HgT concentrations between the states existed, once the effect of year was accounted for. In 1998, mean epilimnetic HgT was elevated by 1.46 ng l^{-1} over the 1999 mean.

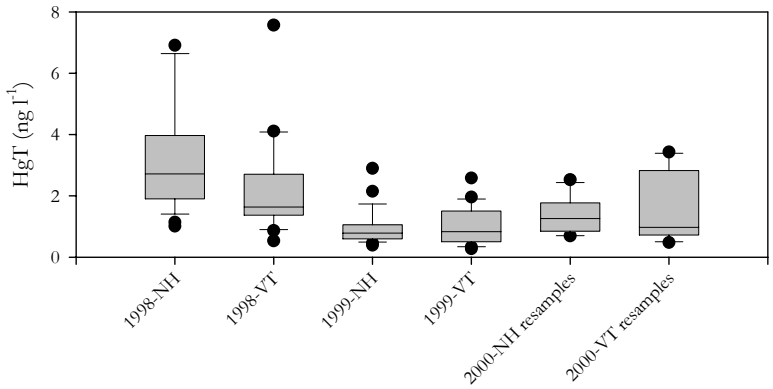

Figure 8.5.1. Tukey box-plots of epilimnetic HgT concentration by year and state, for samples collected during 1998, 1999, and 2000.

There are several potential reasons for the observed differences in HgT means across the two main sampling years. Chief among these are laboratory error, sampling error, and real differences driven by natural factors such as weather. Lorey (2002) discusses the ramifications of a change in laboratory location at Syracuse University which occurred between 1998 and 1999. The only quantifiable change in analytical results was a reduction in mean blank concentrations. Sampling for this project was performed by two separate teams, one from VT, and the other from New Hampshire. If a sampling problem were to blame for the observed differences in HgT across years, it would be expected that the 1998 results from one state would be significantly elevated over the other. The analysis presented above only marginally supports this inference for 1998, and not at all for 1999 (difference between mean 1998 VT and NH samples = 0.33 ± 0.37 ng l^{-1}, p = 0.079). Moreover, no significant differences were detected in any other parameters, including hypolimnetic HgT and meHg, and sediment HgT.

The most likely explanation for the differences in epilimnetic HgT concentrations was observed between 1998 and 1999 is related to rainfall. Mean monthly rainfall totals from Burlington, VT (annual mean ~36 inches) and Concord, NH (annual mean ~50 inches) in relation to long-term averages for the period 1991 to 2001 show very different patterns (Figure 8.5.3). In 1998, rainfall for June through September, measured at Burlington, VT was 232% of the long-term average; at Concord, N.H., it was 117 % of the long-term average (National Weather Service, 2002). In 1999 and 2000, rainfall averages were at or below long-term means. A very significant proportion of annual wet Hg deposition can result from a very few storms of high intensity, with peak deposition in the spring or summer period (Burke et al., 1995; Hoyer et al., 1995; Shanley et al., 1999). The degree to which this may translate to increased observed concentrations in lake waters is unclear. Nonetheless, the summer of 1998 produced four record single-day rainfall events recorded at the Burlington, VT weather station between May 31 and August 30. Two record storms passed over Boston in 1998, including one

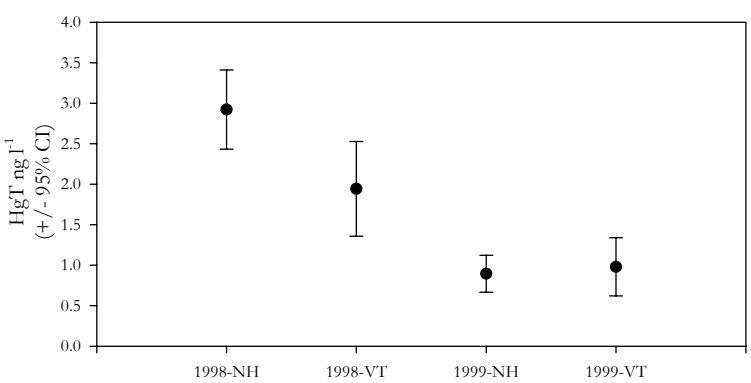

Figure 8.5.2. Mean concentrations of HgT in epilimnetic waters(and 95% confidence intervals) by year and State. Plotted values are back-transformed least-squares estimates.

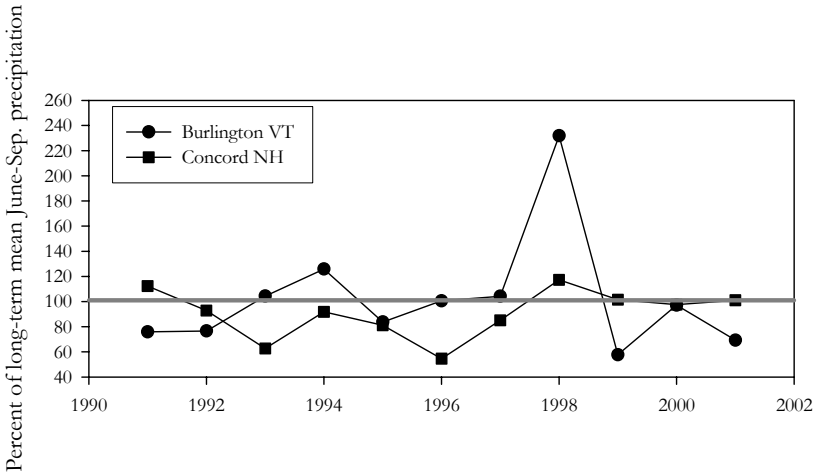

Figure 8.5.3. 1991-2001 mean June through September precipitation at Burlington, VT and Concord, N.H., expressed as percent of the long-term June-September mean. Period of record: Burlington, 119 years; Concord, 82 years.

5.67 inch, 24 hour deluge. Obviously, actual precipitation conditions in close proximity to the study lakes will directly affect in-lake HgT concentrations, and such precipitation data are unavailable as of this writing. It seems clear, however, that 1998 was a particularly wet year, and abnormally so in Vermont. This may partially explain the elevated HgT observations in our study lakes in 1998.

8.6 Evaluation of Hg variation in relation to trophic status

Understanding the degree to which Hg varies in lakes in response to trophic gradients can be useful in determining where trophic transfer of Hg may be enhanced or dampened. Dystrophic lakes are well understood to display elevated tissue Hg concentrations. Lakes of increased trophic status are those which may be expected to have experience enhanced watershed disturbance, and thus receive greater Hg loadings from the watershed (Shanley et al., 1999; Mason and Sullivan, 1998), which would yield increased in-lake and sediment Hg burdens. Moreover, Pickhardt et. al. (2002) convincingly demonstrated that Hg is biodiluted in waters where phytoplankton densities are elevated. This so-named 'bloom dilution' results from algal density-dependant incorporation of the bioavailable Hg pool into the phytoplankton. When algal densities are higher, Hg per unit of algal density will be lower, the result being that the available Hg pool is spread across a larger primary aquatic production base. Pickhardt et al. show that biodilution of Hg by high densities of phytoplankton results in reduced HgT in *Ceriodaphnia sp.*, suggesting that bioaccumulation at higher trophic levels will be muted, a phenomenon noted by Chen et al. (2000). The present dataset provides a good means to independently evaluate the hypothesis that mean fish tissue Hg concentrations will be reduced in lakes of elevated trophic status.

To investigate variation in Hg measures with trophic state, lakes were allocated into one of four groups, based on total phosphorus concentrations and on DOC and color data, as described by VTDEC (1996). Trophic data were acquired from the VTDEC and NHDES respective Lake Inventory Databases, and were based on each State's long-term monitoring and assessment programs. The four trophic classes were oligotrophic (<8 $\mu g\ l^{-1}$ total phosphorus), mesotrophic (8-16 $\mu g\ l^{-1}$ total phosphorus), eutrophic (>16 $\mu g\ l^{-1}$ total phosphorus), and dystrophic (TC >50 PtCo units and/or DOC > 4 mg l^{-1}). A series of ANOVA analyses was employed to evaluate the hypotheses that lake trophic status display influences aqueous, sediment, and tissue Hg concentrations. Sample weights were incorporated into the analyses, and post-test pairwise comparisons were adjusted to an overall experiment-wise error rate of 5% using the method of Scheffe (SAS Institute, 2002).

ANOVA showed that epilimnetic HgT and meHg, and hypolimnetic meHg varied significantly with trophic state, while hypolimnetic HgT did not. Neither sediment HgT nor meHg showed significant differences, but HgT in perch tissue was highly significantly different between trophic states. Scheffé contrasts showed that epilimnetic HgT (Figure 8.6A) was elevated in dystrophic lakes relative to mesotrophic and oligotrophic lakes (p=0.017 and 0.047 respectively), and in eutrophic lakes relative to mesotrophic lakes (p = 0.021). Epilimnetic meHg (Figure 8.6B) in dystrophic and eutrophic lakes was marginally elevated relative only to oligotrophic lakes (p = 0.097 and 0.089 respectively). Hypolimnetic meHg (Figure 8.6C) in eutrophic lakes was marginally elevated relative to

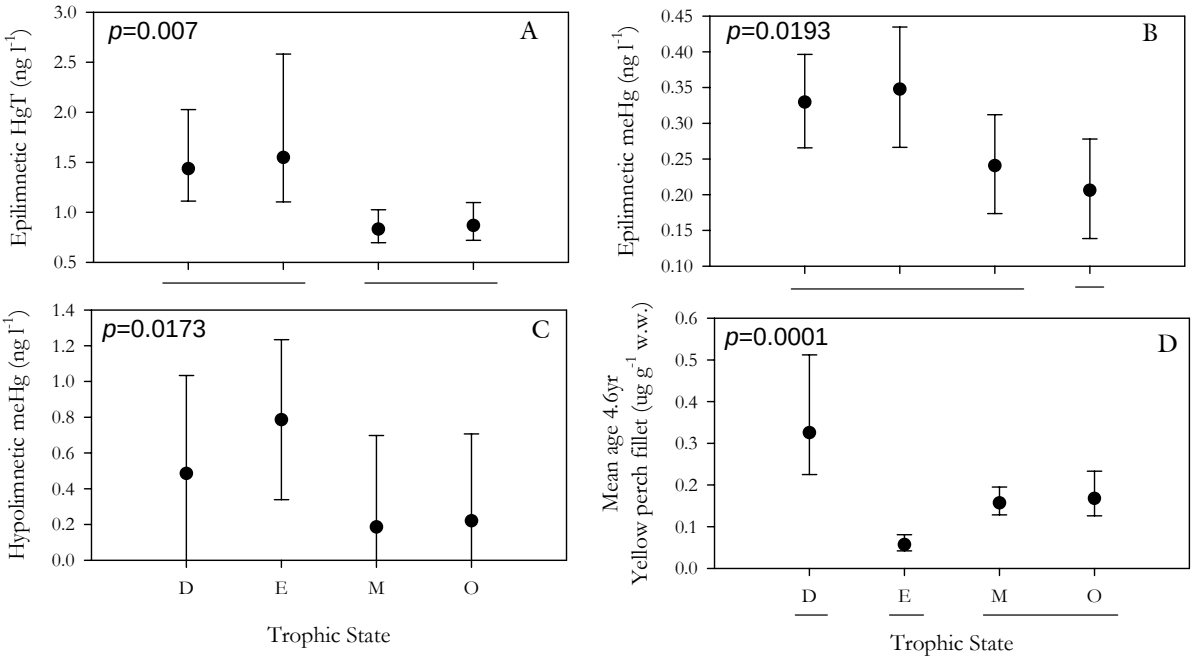

Figure 8.6. Back-transformed least-squares means and 95% confidence intervals for four mercury parameters in relation to four lake trophic states. D: dystrophic; E: eutrophic; M: mesotrophic; O: oligotrophic. P-values from ANOVA. Underlined means were not significantly different based on Scheffé contrasts.

mesotrophic lakes (p=0.063). Age-adjusted yellow perch Hg tissue (Figure 8.6D) was significantly elevated in dystrophic lakes relative mesotrophic lakes (p=0.012), and significantly lower in eutrophic lakes relative to all other lake types (p<0.005). These data also indicate that, on average, age 4.6 year perch from dystrophic lakes have tissue levels that were elevated by 0.218 μg g1 over the mean for all other lake types (p <0.001).

These findings are noteworthy in relation to currently available literature. Elevated HgT in dystrophic waters is not surprising, and is well documented (e.g., Mierle and Ingram, 1991; Driscoll et al., 1994; Ullrich et al., 2001). Equally unsurprising and well documented (e.g., Driscoll et al., 1994; USEPA 1997; Carter et al., 2001) is the fact that yellow perch from dystrophic lakes also show elevated mercury. Somewhat more interesting is the elevated HgT observable in epilimnetic waters of eutrophic lakes relative to lakes of lower trophic status, a finding which partially supports the hypothesis that lakes with disturbed watersheds incur greater HgT loading. Of greatest interest in this analysis is the finding that tissue HgT was quite low in eutrophic lakes (mean = 0.056 μg g^{-1}). Although this finding must be treated cautiously owing to a small sample size (n=3 for eutrophic lakes with tissue HgT data in this dataset), the finding directly supports the hypothesis of algal biodilution, and is consistent with other studies showing low tissue HgT in fishes from eutrophic lakes (Pickhardt et al. 2002). Further evaluation of tissue Hg data in relation to lake trophic status could be accomplished using myriad state fish tissue contamination databases, and presents a fruitful avenue for additional inquiry.

8.7 Bioaccumulation and biomagnification factors

Bioaccumulation and biomagnification factors (BAF's and BMF's) were calculated for biological Hg parameters, in relation to aqueous Hg parameters, in order to characterize the degree to which Hg is enhanced in increasing trophic levels, and to provide a baseline of comparison with other studies. Calculation methods followed standard risk assessment protocols (USEPA 1998). A summary of values is provided in Table 8.7, along with simple descriptive statistics.

Table 8.7. Log bioconcentration and bioaccumulation factors for biological Hg parameters in relation to aqueous Hg parameters.

Comparison	Mean logBAF	Mean logBMF	Minimum	Maximum	Count of values	Key to abbreviations
Zoop: EpiHgT	4.85	--	3.87	5.59	34	Epi: epilimnetic
Zoop: EpiMeHg	5.56	--	4.69	6.68	34	
Zoop: HypHgT	4.07	--	2.91	5.04	24	Hyp: hypolimnetic
Zoop: HypMeHg	5.29	--	4.44	6.22	24	
PreyYP: EpiHgT	4.89	--	4.40	5.36	45	
PreyYP: EpiMeHg	5.59	--	4.91	6.44	45	YP_age: HgT in yellow perch fillets, adjusted to age 4.9 year fish
PreyYP: HypHgT	4.00	--	3.19	4.83	28	
PreyYP:HypMeHg	5.26	--	4.36	6.29	28	
YP _age: EpiHgT	5.25	--	4.72	6.01	47	
YP _age: EpiMeHg	5.94	--	5.23	6.85	47	Loon: HgT in loon blood
YP _age: HypHgT	4.37	--	3.58	5.12	29	
YP _age: HypMeHg	5.64	--	4.83	6.45	29	
Loon: EpiHgT	6.07	--	5.43	6.50	8	Prey YP: HgT in five-fish composites of whole body yellow perch, < 15 cm
Loon: EpiMeHg	6.94	--	6.27	7.37	8	
Loon: HypHgT	5.07	--	4.36	5.53	6	
Loon: HypMeHg	6.36	--	5.72	7.12	6	
PreyFish: ZoopHg	--	0.03	-0.62	0.78	34	ZoopHg: HgT in ≥201*u* macrozooplankton
YP_age: ZoopHg	--	0.39	-0.42	1.27	34	
YP_age: PreyFish	--	0.35	-0.24	0.89	45	

Log-BAF's in general are highest for epilimnetic-based comparisons, owing to the low HgT and meHg concentrations found in these lake zones. Conversely, log-BAF's are lowest for hypolimnetic-based comparisons. The largest log-BCF's are those calculated using loon blood in relation to epilimnetic meHg. Log BAF's for yellow perch fillet HgT with respect to epilimnetic HgT range from 4.72 to 6.01, which is in excellent agreement with other published studies (e.g. Driscoll et al., 1994).

8.8 Relationships among variables – univariate correlations

The strength of interrelations between parameters in this dataset can be assessed by reviewing correlations among water chemistry and Hg parameters. To perform this assessment, a pairwise non-parametric Spearman correlation matrix (SPSS Science Inc, 2000) was developed using all aqueous and sediment parameters. This large matrix (33 parameter-specific intercomparisons) is summarized by Table 8.8.

A common thread observable within Table 8.8 is the preponderance of significant ($p<0.05$) and strong (e.g. $R>0.4$) correlations between Hg and parameters related to lake acidification status (ANC, pH, conductivity), or to organic content (DOC, color). The strongest correlations to prey and fillet yellow perch tissue are with ANC, and with pH. These findings are not unexpected, and are well supported by available literature (e.g., Carter et al., 2001, Driscoll et al., 1994). Certain lake physical characteristics (depth, volume, flushing rate) correlate to several

Hg parameters, indicating that hydrology exerts influence over epilimnetic and hypolimnetic HgT concentrations, on methylation, and on sediment HgT sequestration. Flushing rate also has a minor influence over perch HgT concentrations.

Table 8.8. Summary of significant (p≤0.05) Spearman correlation coefficients among water chemistry variables in relation to Hg parameters. Parameter names in ***bold*** *indicate Spearman R values of >0.4, names in* **italic bold** *indicate values >0.7, names in* ~~*strikeout*~~ *are expected mathematical artifacts.*

	EpiMe	HypMe	EpiHgT	HypHgT	SHgT	SmeHg	ZoopHg	PreyYP	YP_age	EpiMe%	HypMe%	SedMe%
Parameters with significant Spearman R's.	EpiANC EpiSO4 **EpiDOC** HypDOC EpiTC HypTC MinTemp Mean pH **Mean Z** **Vol_m³** FlushRate	HypNOx HypSO4 **EpiDOC** **HypDOC** EpiTC **HypTC** Mean Z TP EpiMe	EpiANC HypANC EpiSO4 HypSO4 **EpiDOC** HypDOC **EpiTC** $HypH_2S$ Mean pH Mean cond WA:LA Mean Z Vol_m³ FlushRate TP **EpiMe** HypMe	EpiANC HypANC **EpiNOx** **HypNOx** HypDOC Mean pH **HypMe**	EpiANC HypANC EpiCl⁻ Mean pH MeanCond WA:LA FlushRate	**SHgT**	MeanCond	***EpiANC*** **HypANC** EpiSO4 **EpiDOC** **HypDOC** Min Temp ***Mean pH*** **MeanCond** FlushRate EpiMe EpiHgT	**EpiANC** ***HypANC*** EpiSO4 HypSO4 EpiDOC HypDOC ***Mean pH*** **MeanCond** FlushRate EpiMe EpiHgT ***PreyYP***	EpiCl⁻ HypCl⁻ EpiTC ~~EpiMe~~ ~~EpiHgT~~	HypTC Min DO TP ~~HypMe~~ ~~HypHgT~~ SHgT SmeHg	**HypANC** HypHgT ~~SmeHg~~ PreyYP
	Abbreviations: **Epi**: epilimnetic; **Hyp**: hypolimnetic; **S**: sediment; **Me**: meHg; **ZoopHg**: HgT in zooplankton; **PreyYP**: HgT in whole body-composites of <15 cm yellow perch; **YP_age**: age-adjusted yellow perch fillet (average age 4.9 years) HgT means; **Me%**: % of HgT as meHg; **ANC**: acid neutralizing capacity; **DOC**: dissolved organic carbon; **TC**: total color; **TP**: total phosphorus; **DO**: dissolved oxygen; **Cond**: conductivity; **WA:LA**: ratio of watershed:lake area, **Z**: depth.											

8.9 Principal components analysis - accounting for covariance among parameters

While a univariate correlation matrix is useful to look at individual relationships between parameters, it is clear from Table 8.8 that numerous parameters are simultaneously influencing Hg fate in the study lakes. Moreover, a 33 parameter correlation matrix is sufficiently large so as to yield spurious correlations. Accordingly, principal components analysis was used to reduce the dataset, to account for simultaneous covariance among parameters which jointly influence concentrations of HgT, meHg, sediment HgT, and tissue Hg, and to control for the occurrence of spurious correlations.

All non-Hg water chemistry variables were thus entered into two separate datasets describing mean epilimnetic and hypolimnetic water chemistry for each lake, accounting for all available sampling events. For each dataset, principal components were extracted and reported from the correlation matrix of untransformed variables (Rencher, 1995), using SAS Proc Princomp (SAS Institute, 2002). It was decided a-priori that the first three components would be retained. Component loadings for the first three axes from each dataset were calculated using SAS Proc Corr (SAS Institute 2002). Extraction of principal components requires a complete dataset. To avoid excessive data loss, missing values for several individual cell values were estimated by one of the following methods:

1) mean of the remaining parameter values (one SO_4 and one Cl^- datapoint for Childs Bog, NH);
2) relationship between total color and DOC ($p<0.001$, $r^2 = 0.560$, one total color datapoint for Noyes Pond, VT)
3) pH and conductivity: available data from NHDES Lake Inventory Database (15 datapoints)

The resultant epilimnetic dataset was comprised of 91 records, containing 11 water chemistry variables, and no missing values. The first three principal components captured 66.5 percent of the total dataset variation. The

hypolimnetic dataset was comprised of 40 records, containing 11 variables (no missing values), and the first three components captured 68.7 percent of the total dataset variation. Component loadings were examined to determine to which component each individual parameter was most highly correlated. To capture the essential dataset variance being explained by each component, individual loading values of <0.4 were not considered in interpreting the component.

The variance explained and component loadings for the epilimnetic and hypolimnetic water chemistry datasets is shown in Table 8.9. The first epilimnetic component (named EPI_1) assumes increasingly large values as ANC, sulfate, pH, and conductivity increase. Thus, EPI_1 describes an an acidity gradient. The second component (named EPI_2) increases as Secchi transparency declines, and as DOC, total color, and chlorides increase. Lakes which have high EPI_2 scores have elevated DOC and total color, resulting from autochthonous primary production, not acidity. EPI_3 increases for lakes with increasing minimum temperatures and dissolved oxygen concentrations. Low EPI_3 scores describe lakes with cold, oxygen-rich hypolimnia (oligotrophic lakes), and higher EPI_3 scores are indicate shallower lakes with hypolimnetic oxygen loss during the warmwater season. These latter lakes may be either eutrophic or dystrophic.

Table 8.9.1. Results of principal components analyses for epilimnetic and hypolimnetic water chemistry datasets. Component loadings are given for each variable used in the analysis. Shaded values indicate the strongest loadings, which were used to interpret the individual components.

Epilimnetic Water Chemistry												
Component label	Variance explained (%) by component	SD	ANC	CLI	NO_X	SO_4	DOC	TC	MinTemp	MinDO	Mean_pH	MeanCond
EPI_1	32.7	0.497	0.778	0.381	0.099	0.780	-0.532	-0.473	-0.435	-0.315	0.733	0.809
EPI_2	20.3	-0.744	0.405	0.435	-0.149	0.089	0.663	0.667	0.275	-0.156	0.201	0.525
EPI_3	13.5	-0.152	-0.021	0.315	0.130	0.071	-0.318	-0.292	0.759	0.747	0.069	0.137
Cumulative	66.5											
Hypolimnetic Water Chemistry												
Component label	Variance explained (%) by component	ANC	CLI	NO_X	SO_4	H_2S	DOC	TC	MinTemp	MinDO	Mean_pH	MeanCond
HYP_1	33.2	0.901	0.564	-0.080	0.842	0.299	-0.425	-0.062	-0.154	-0.226	0.759	0.941
HYP_2	21.2	0.091	0.391	-0.673	-0.160	0.115	0.722	0.665	0.237	-0.715	-0.312	0.217
HYP_3	14.3	-0.237	0.529	-0.219	0.095	-0.297	0.032	-0.498	0.849	0.313	-0.054	0.141
Cumulative	68.7											

For hypolimnetic water chemistry, the first component (HYP_1) increases when ANC, SO_4, pH, and conductivity increase. Like EPI_1, HYP_1 represents an axis of acidity, and lakes of higher HYP_1 scores have hypolimnia that are less acidic. HYP_2 increases in response to increasing DOC and color, and reduced dissolved oxygen and NO_x. This describes a trophic gradient ranging from oxic, DOC-poor hypolimnia (e.g., oligotrophic), to anoxic, organic acid dominated hypolimnia (e.g., eutrophic) influenced by autochthonous decomposition. Values of HYP_3 increase when minimum temperature is elevated.

There are interesting relationships between various mercury measurements and the principal component scores. These relationships can be visualized using the partial scatter plot matrix of Hg parameters which are significantly correlated with the principal components (Table 8.9.2, Figure 8.9). In the epilimnion, significant (p<0.05) negative correlations exist between EPI_1 and aqueous HgT (R= -0.455), aqueous meHg (R = -0.477) and age-corrected yellow perch tissue HgT concentrations (R = -0.572). These parameters are elevated where conditions are acidic. Significant positive correlations exist between EPI_2 and aqueous HgT (R=0.292), aqueous meHg (R=0.314),

and sediment HgT (R=-0.22), indicating that aqueous HgT and aqueous meHg increase, while sediment HgT decreases, as lakes increase in trophic status (this is shown independently in Figure 8.6). Tissue HgT does not increase with increasing EPI_2 values, suggesting that bloom dilution may damp Hg bioaccumulation to perch muscle tissues in lakes of elevated trophic status.

Table 8.9.2. Pearson correlation coefficients between principal components and measures of Hg in waters, sediments and biota.

Component	Statistic	Epilimnetic HgT	Epilimnetic meHg	Sediment HgT	Sediment meHg	HgT-Zooplankton	HgT-prey yellow perch	HgT-yellow perch fillets - adjusted to 4.6 year fish
EPI_1	R	-0.455	-0.477	-0.129	-0.12	-0.293	-0.637	-0.572
	p-value	0	0	0.222	0.317	0.0825	0	0
	n	91	91	91	71	36	45	47
EPI_2	R	0.292	0.314	-0.22	0.107	-0.0903	0.00923	-0.0548
	p-value	0.00509	0.00256	0.036	0.374	0.598	0.952	0.713
	n	91	91	91	71	36	45	47
EPI_3	R	-0.11	0.0898	-0.185	-0.137	0.135	0.197	-0.0469
	p-value	0.297	0.397	0.0792	0.254	0.43	0.192	0.753
	n	91	91	91	71	36	45	47
Component	Statistic	Hypolimnetic HgT	Hypolimnetic meHg	Sediment HgT	Sediment meHg	HgT-Zooplankton	HgT-prey yellow perch	HgT-yellow perch fillets - adjusted to 4.6 year fish
HYP_1	R	-0.315	-0.237	-0.337	0.014	-0.332	-0.565	-0.763
	p-value	0.0479	0.14	0.0334	0.935	0.12	0.00336	0
	n	40	40	40	36	23	25	26
HYP_2	R	0.297	0.572	0.11	0.294	0.109	0.248	0.0913
	p-value	0.063	0	0.499	0.0814	0.614	0.228	0.654
	n	40	40	40	36	23	25	26
HYP_3	R	-0.0298	-0.308	-0.00929	-0.183	-0.0213	0.191	0.169
	p-value	0.854	0.0529	0.954	0.284	0.919	0.355	0.407
	n	40	40	40	36	23	25	26

For the hypolimnion, findings are similar. Aqueous HgT (R=-0.315), sediment HgT (R=-0.337), and age-corrected yellow perch tissue HgT (R=-0.763) show significant negative correlations to HYP_1. Hypolimnetic aqueous meHg is relatively strongly correlated to HYP_2 (R = 0.572). This means that that hypolimnetic aqueous HgT, sediment HgT, and tissue Hg all increase in lakes with greater deepwater acidity, and that hypolimnetic aqueous meHg becomes enhanced in the anoxic hypolimnia of eutrophic lakes. In these lakes, the increase in meHg can be attributed to the accumulation of DOC as residual internally-derived algal production.

In summary, the principal components analyses indicate that water column HgT and meHg becomes elevated in lakes of low ANC, and high productivity. Although there was no statistically significant difference in mean sediment HgT levels between lakes of different trophic status ($F_{3,83}$=1.74, p=0.165), sediment HgT concentrations trend slightly higher with decreasing lake ANC, and decrease with increasing in-lake productivity. Finally, despite the increased concentration of HgT and meHg in productive systems, tissue Hg concentrations increase only in response to increased lake acidity. The availability of Hg to yellow perch in systems of higher trophic status may become reduced due to bloom dilution.

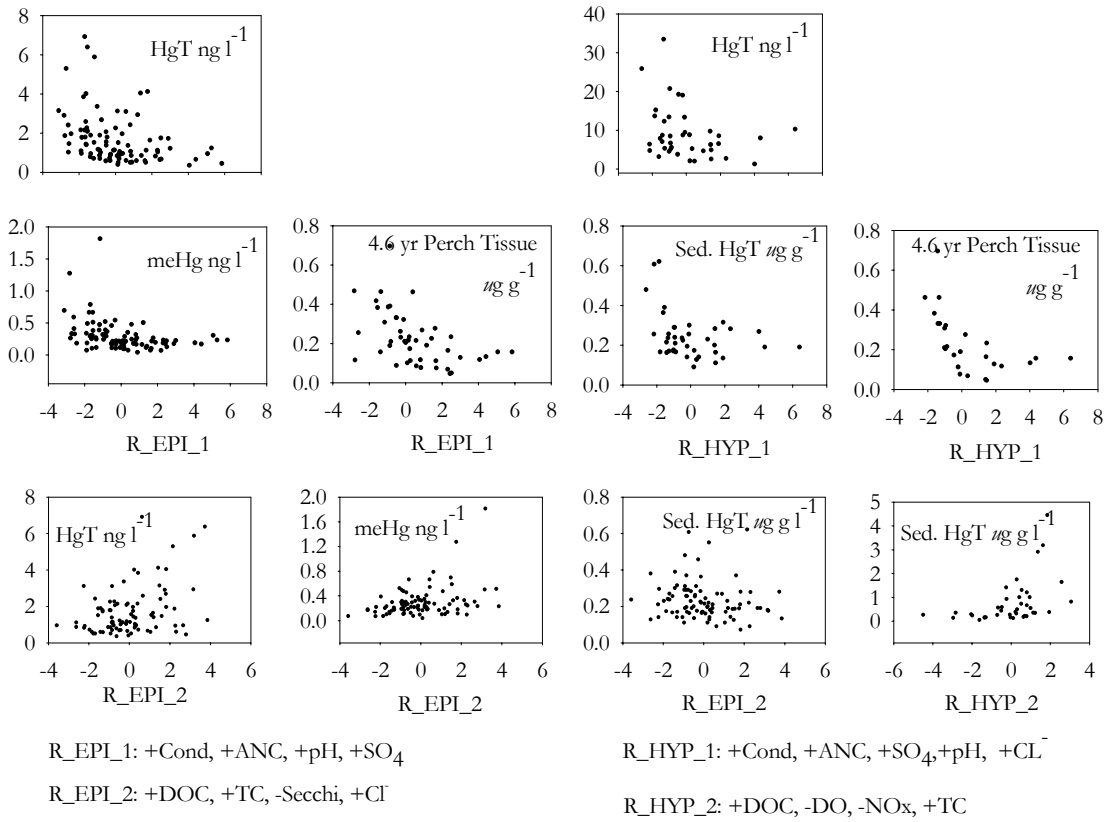

Figure 8.9. Partial scatterplot matrix of several Hg parameters in relation to epilimnetic and hypolimnetic principal components of 11 water chemistry variables. Interpretation of principal components provided below plots, with the direction of individual parameter change (+ or -) provided in relation to increased x-axis values. R_EPI-1: first principal component, epilimnetic water chemistry. R_HYP_2: second principal component, hypolimnetic water chemistry. Cond: conductivity; ANC: acid neutralizing capacity; SO_4: sulfates; Cl-: chlorides; TC: total color; DOC: dissolved organic carbon; DO: dissolved oxygen. Age-adjusted perch muscle tissue concentrations are plotted as back-transformed values.

8.10 The influence of land-use on Hg

The random nature of the present dataset provides opportunities to evaluate the relationship between land use and a variety of Hg parameters, using Spearman correlations. Land-use data for this purpose were acquired from two sources. In Vermont, the 1996 Vermont Center for Geographic data Land Use and Cover Dataset (VCGI, 1996) provides the highest-resolution (30-meter) land cover data for the State, with a known accuracy of > 80%. The Multi-Resolution Land Characteristics dataset (USGS 1992) provides land cover for New Hampshire at a similar scale. Both land use and cover datasets were developed from Thematic Mapper satellite imaging data acquired in 1992 (MRLC) and 1993 (VCGI). Land cover categories are highly analogous between the two datasets, and for the purpose of this analysis, were considered sufficiently consistent so as to be pooled for a regionwide analysis. Land uses were summarized by immediate lake watershed (e.g. the watershed surrounding an individual study lake, not including the watersheds of upstream lakes in multi-lake drainage networks). 'Immediate watersheds' were favored to avoid the confounding effects of Hg attenuation in lakes upstream of the target study lake.

Epilimnetic HgT and meHg, sediment HgT and meHg, zooplankton Hg, prey perch HgT, and age-corrected fillet perch HgT were correlated to five pooled categories of land use. These were forested (sum of deciduous, forested, and mixed forest), agriculture (hayfield, rowcrop, pasture, orchards), wetland and openwater (forested and non-forested wetland, openwater), developed (urban, low and hi-density residential), and for Vermont only, "E911." The State of Vermont recently released an enhanced emergency response geographic database providing locations of virtually every addressed dwelling in the state. In addition to the intended use as an emergency property location system, the so-called E911 dataset permits geographic analysis of development levels and settlement patterns across the Vermont landscape. While E911 is under development in New Hampshire, no such geographic dataset has yet been released for public use. For the purpose of determining the influence of watershed development on Hg parameters, counts of E911 sites were summarized by immediate study lake watershed, and included as a land-use characteristic for Vermont lakes only.

Spearman correlations between Hg parameters and land use categories are shown in Table 8.10. Epilimnetic meHg and tissue Hg were positively correlated with increased forested areas, and tissue Hg was significantly negatively correlated with total developed area. Surprisingly, there was no significant correlation between perch tissue Hg and wetland area, as would be expected given the results of Driscoll et al. (1994) and Carter et al. (2001), and understanding that meHg is produced in wetlands (e.g., Branfirun et al., 1996). Strong negative correlations were observed between sediment HgT and both agricultural land and E911 count.

The elevated epilimnetic meHg and tissue Hg concentrations observed in relation to increases in forested areas are unsurprising and are well described in the literature, beginning with Lee and Iverfeldt (1991) and corroborated by numerous others since. That perch muscle tissue Hg did not vary with wetland area likely reflects the large degree of heterogeneity in the dataset, where numerous factors in concert with land-use are simultaneously influencing Hg bioaccumulation. The reductions in sediment HgT concentrations in lakes occupying agricultural watersheds and watersheds with larger "E911" building counts is likely the result of enhanced transport of inorganic sediment particles due to land disturbance. These factors act to reduce in-lake sediment HgT concentrations in two complimentary ways: first, HgT is effectively diluted simply as a result of enhanced sediment delivery rates (Engstrom and Wright, 1993); and second, the low DOC content of the inorganic fraction of soils lost from agricultural and developed watersheds renders these soils less able to bind and transport Hg. That said, agricultural systems indeed export significant quantities of DOC in the form of animal wastes, which may serve to carry sediment HgT. This helps explain the diminished magnitude of the sediment HgT correlation with agricultural land relative to the sediment HgT correlation observed with E911.

These relationships to land-use, taken in concert with results of the principal components analyses (above) speak to the ultimate source of the meHg which bioaccumulates to fish tissues in these study lakes. The literature indicates that meHg production occurs both in lake watersheds (e.g., Hurley et al., 1995), and in lake sediments (e.g., Regnell, 1994). Both signals are evident within the present dataset. While our study cannot answer the question as to which is most important, the lack of a statistical relationship between hypolimnetic meHg and perch tissue HgT, in concert with increases in tissue HgT with increased acidity, suggest that transport of meHg from acidic, forested watersheds may be a more important predictor of tissue HgT than is hypolimnetic water chemistry.

Table 8.10. Spearman correlations between epilimnetic and sediment Hg parameters, and simplified land-use categories. Shaded values represent significant correlations (p<0.05), while bold values are highly significant (p <0.01).

Parameter	Statistic	Forested	Agri-cultural	Wetland and openwater	Developed	VT E911 (count of dwellings)
HgT	R	0.173	-0.164	0.107	-0.182	-0.318
	n	92	92	92	92	44
meHg	R	0.228	-0.0933	0.0881	-0.198	-0.174
	n	92	92	92	92	44
SHgT	R	0.0237	**-0.33**	0.129	-0.136	**-0.533**
	n	92	**92**	92	92	**44**
SMeHg	R	-0.107	-0.14	0.178	0.09	-0.154
	n	72	72	72	72	35
Zooplankton HgT	R	-0.103	-0.0677	-0.23	0.146	0.301
	n	36	36	36	36	21
Whole yellow perch HgT	R	0.359	-0.114	0.365	-0.525	-0.134
	n	45	45	45	45	21
Fillet yellow perch HgT, for age 4.6 year fish	R	**0.377**	-0.216	0.0751	**-0.412**	-0.239
	n	**47**	47	47	**47**	23

8.11 Development of candidate linear discriminant functions to predict tissue Hg levels in fillets given physicochemical data

The analyses described above indicate that Hg in waters, sediments, and fish tissue can vary depending on numerous factors, including trophic status, land use, and the levels of several individual physico-chemical parameters. Principal components analysis provides insight into how these parameters simultaneously covary to influence Hg concentrations. One very useful application of these data is to construct a statistical model which can predict whether fillets of yellow perch in individual study lakes will contain sufficient Hg to violate the EPA tissue meHg criterion of 0.3 $\mu g\ g^{-1}$.

Classification analysis using linear discriminant functions (Rencher, 1995) is a multivariate technique which can be used to allocate fillet tissue HgT concentrations to pre-defined classes given an array of covarying parameters. To construct this statistically-based model, lakes were a-priori classified into two groups: one meeting the EPA standard, and a second failing the EPA standard, based on age-corrected yellow perch fillet HgT concentrations. Stepwise discriminant analysis was used to select those variables which most strongly accounted for membership of study lakes to each class of tissue HgT. Variables initially entered into the stepwise selection procedure (SAS Proc Stepdisc, SAS Institute 2002) were those found to correlate significantly to the age-adjusted yellow perch fillet HgT concentrations (Table 5). Significance levels (*p*) to enter and remove variables were set a-priori at 0.15, a conservative value intended to maximize the incremental increase in variability explained by each additional parameter retained by the analysis.

The variables retained by the stepwise analysis were then used to construct linear discriminant functions, using SAS Proc Discrim (SAS Institute 2002). Classification error analysis was performed using resubstitution and crossvalidation, to provide a range of likely misclassification error rate, accounting for the prior proportions of lakes occupying each class. The assumption of equality of covariance matrices between classes was tested using the Chi-square statistic.

The stepwise linear discriminant analysis yielded a combination of five variables (ANC, DOC, pH, conductivity, and flushing rate) which maximized the generalized distance between lakes meeting and failing the USEPA criterion (Wilks' $\Lambda = 0.32$, $p<0.0001$). Equations one and two provide linear discriminant functions to model a lake's likelihood that muscle tissues of average age 4.6-year yellow perch will meet or violate the USEPA criterion. Lakes can be attributed to a class by simultaneously solving the equations, with the function yielding the largest solution indicating the classification for the lake in question.

<u>Yellow perch fillets <0.3 μg g^{-1} HgT, Meets USEPA Criterion:</u>

-1,580 – 82.92(lnANC) + 45.35(lnDOC) + 1,658(ln_pH) - 18.99(lnCond) – 35.09(invrtFlush) Eq. 1

<u>Yellow perch fillets ≥0.3 μg g^{-1} HgT, Violates USEPA Criterion:</u>

-1,494 – 81.94(lnANC) + 48.49(lnDOC) + 1,610(ln_pH) – 18.65(lnCond) – 33.02(invrtFlush) Eq. 2

Where:

lnANC = ln (1+acid neutralizing capacity, in mg l^{-1}, measured from the epilimnion)
lnDOC = ln (1+dissolved organic carbon, in mg l^{-1}, measured from the epilimnion)
ln_pH = ln (1+pH, in standard units, average of total water column)
lnCond = ln (1+conductivity, in us cm^{3}, average of total water column)
invrtFlush = (Flushing rate, in # yr^{-1})$^{-2}$

The overall classification error rate was 11.9% and 14.3% based on the resubstitution and crossvalidation methods, respectively. This means that, for Vermont and New Hampshire lakes of greater than 20 acres, we can be confident in using the discriminant functions to predict whether a lake will violate the USEPA tissue Hg criterion, with approximately a 13% chance of misclassifying an individual lake.

These models were applied to in a descriptive capacity to classify the remaining 45 REMAP study lakes which did not contain yellow perch, and also to characterize the generalized level of criterion compliance across the entire REMAP dataset. For the lakes without yellow perch, the model indicated that 46.6% (+/- 13.1%) of these lakes would have average age-4.6 year yellow perch fillet concentrations of ≥0.3 μg g^{-1}. Broken down by state, 28.6% of Vermont lakes would show violations of the USEPA criterion, while 62.5% of New Hampshire lakes would be in violation of the criterion. Across the pooled REMAP study lake set (e.g., those lakes with and without yellow perch), the model indicates that 40.2% of lakes may be in violation of the criterion (54% in NH, 25% in VT). The greatest utility of these linear discriminant models is as a screening tool to identify lakes where tissue HgT concentrations are likely to be elevated. Lakes identified as having conditions that support bioaccumulation could be prioritized for sampling to determine actual concentrations, assess model performance, and refine state tissue consumption advisories.

A limited test of the statistical model performance can be achieved by applying these models to a separate, independently derived set of lakes with the appropriate parameters and yellow perch tissue data. The Maine REMAP dataset (MEDEP, 1995) provides one such opportunity. In conjunction with the Maine REMAP project, tissues of at least one middle and one upper trophic-level fish species were composited from between two and five fish per lake, across up to 125 lakes over the period 1993-1994. From these 125 lakes, ancillary data sufficient to classify the lakes using the present models were available on 68 lakes. Although the number of these 68 lakes from which yellow perch were available is small (n=10 lakes), data were available for two other piscivorous warmwater species, the largemouth and smallmouth bass *Micropterus salmides* and *M. dolomieui* (n=13 lakes for each species).

When evaluated using Eq. 1 and 2, 33% of the 68 Maine lakes were found to have a high likelihood of having yellow perch fillet HgT concentrations in excess of EPA criterion of 0.3 μg g^{-1} w.w. meHg. For the subset of these from which perch or bass data are available, predictions were compared to actual tissue Hg concentrations.

Results of these comparisons were unsatisfactory for yellow perch, but were more promising where largemouth and small mouth bass Hg concentrations formed the basis of comparison. Means and standard deviations for these three species are shown in relation to their modeled tissue-Hg status in Figure 8.11. For yellow perch, actual tissue concentrations are indistinguishable between lakes which were modeled to have perch tissue meeting the criterion, and those where the model indicated non-attainment of the criterion. However, for largemouth and smallmouth bass, lakes modeled to meet the criterion show lower overall concentrations than lakes modeled to violate the criterion.

Absolute application of the linear discriminant models developed for the VT and NH lakes to the Maine (or other) lake sets is problematic owing to several factors. First, the study lake sets for VT/NH and for Maine represent separate, randomly selected samples of *different lake populations*, occupying different landscapes, and characterized by varying atmospheric Hg deposition rates. Second, significant differences existed in target species and sampling collection strategies between the two studies. Specifically, available yellow perch data from the Maine study were derived from composites of two to five fillets from 20+ centimeter fish, whereas in VT and NH, age-adjusted individual-lake mean perch concentrations were calculated from fillets of five individual 15+ centimeter fish, for all lakes where perch were understood to be present. Finally and most importantly, largemouth and smallmouth bass are species of higher trophic order than yellow perch, and thus necessarily differ in their specific Hg bioaccumulation rates. Thus, even though the discriminant model performance for Maine lakes was marginal at best, the differences noted between both bass species from that lake set suggest that the models do indeed incorporate factors which are universally important to estimating tissue Hg concentrations within broad classes.

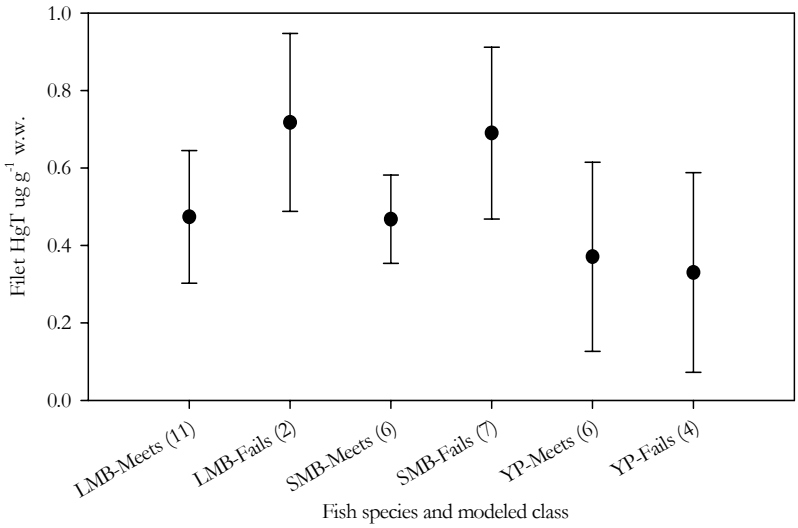

Figure 8.11. Means and standard deviations for HgT in fillets of three species of freshwater fish from Maine lakes, in relation to the EPA 0.3 μg g^{-1} tissue Hg criterion. LMB: largemouth bass; SMB: smallmouth bass; YP: yellow perch. Meets: model indicates attainment of criterion; fails: model indicates criterion exceeded.

8.12 Summary of statistical analyses

The analyses presented above permit the following summary findings:

Yellow perch fillet mean HgT concentrations for the present study lakes are most accurately estimated using age as a covariate. The overall average yellow perch fillet HgT concentration, adjusted to an age 4.6 year fish, is 0.225 $\mu g\ g^{-1}$ w.w.

Reviewed geographically, the raw data on Hg in waters, sediments, and biota indicate that New Hampshire lakes have elevated epilimnetic meHg, hypolimnetic HgT and meHg. Concentrations of hypolimnetic meHg are highest in southern NH. There is a 'hotspot' in yellow perch fillet HgT (age-adjusted means) in southwestern NH. The same hotspot is reflected in sediment meHg concentrations, and may reflect a localized Hg source.

Evaluation of the stratification imposed upon the random lake selection indicated that no variation in any Hg parameters can be attributed to strata, at a 95% or greater probability level. The stratification was therefore not included in subsequent statistical analyses, although individual lake weighting factors were included in subsequent analyses.

Cumulative frequency diagrams based on weighted individual lake mean observations show the distribution of Hg in waters, sediments, and biota across the region, as well as by state. Based on these diagrams, approximately 25% of lakes across the region possess yellow perch which violate the EPA criterion of 0.3 $\mu g\ g^{-1}$ w.w. meHg in fish tissues. Significant differences between hypolimnetic HgT and meHg, prey and fillet tissue HgT, and zooplankton HgT are apparent between the states, with New Hampshire displaying generally higher overall values. Comparisons are available from the Maine REMAP project, which indicate that while sediment HgT concentrations in Maine are lower than in the Vermont-New Hampshire region, yellow perch tissue concentrations are generally consistent with those of New Hampshire lakes.

A formal evaluation of interannual variability indicates that only one parameter – epilimnetic HgT, varied significantly between years. This variability appears to relate to seasonal rainfall, in that the average HgT concentration across the region was elevated in 1998, coincident with a very wet summer. Year 2000 resamplings of several lakes in 2000 produced results which were largely unchanged from those in 1998, when the effect of individual lake variation was accounted for. Observed differences in HgT between year 1998 and 2000 measurements also are related to differences in rainfall.

A formal statistical evaluation of the role of trophic status on Hg in waters, sediments, and biota indicated that: 1) epilimnetic HgT and meHg was elevated in both eutrophic and dystrophic lakes; 2) yellow perch fillet HgT are greatest in dystrophic lakes, and lowest in eutrophic lakes; and, 3) in general, dystrophic lakes can be expected to have HgT fillet concentrations that are 0.218 $\mu g\ g^{-1}$ w.w. greater than in all other lake types. These findings support the hypothesis that Hg is biodiluted in lakes with significant algal production.

Mean log-bioconcentration factors range from a low of 4.37 for concentration from hypolimnetic HgT to yellow perch fillets, to a high of 6.94 from epilimnetic meHg to loon blood. The bioconcentration factors calculated from this studies' data re consistent with those published elsewhere in the literature.

Numerous water chemistry parameters show significant ($p<0.05$) correlations to a variety of Hg measurements, in both waters and sediments. Data reduction techniques such as principal components analysis are useful to reduce the variability in the dataset, and show how covariance among parameters influences Hg in the study lakes. Such an analysis showed that while HgT and meHg concentrations are higher both in more acidic lakes and more eutrophic lakes, tissue HgT only becomes enhanced in lakes of increased acidity. Sediment HgT increases with increasing lake acidity, and decreases with increasing productivity. This is either the result of bloom dilution and subsequent accumulation to the broad trophic webs characteristic of eutrophic lakes, or related to the reduced ability of algal-derived DOC to bind Hg relative to the higher molecular-weight allocthonous DOC characteristic of acidic lake watersheds.

Land use characteristics also influence Hg in the present study lakes. As is characteristic of numerous studies, meHg and tissue Hg is elevated in lakes with larger forested and wetland areas. Age-adjusted perch fillet mean HgT is reduced in developed watersheds. Sediment HgT decreases with increasing agricultural area and increased watershed building count.

Statistical models were developed permitting the prediction of a lakes attainment or violation of the 0.3 $\mu g\ g^{-1}$ w.w fish tissue meHg criterion with a 13% likelihood of misclassifying an individual lake. Application of this model to lakes across the Vermont-New Hampshire region indicates that 40.2% of lakes should violate the criterion (54% in NH, 25% in VT). Evaluation of model performance using the independently derived Maine REMAP dataset produced mixed results, which were poor when performance was evaluated using yellow perch data, but better when smallmouth and largemouth bass were used. This can be explained by several factors, and does not indicate that the model is overly flawed for use in the Vermont-New Hampshire region. Overall , the statistical models capture those factors which the present study indicates are important in estimating whether lakes will have fish tissues in excess of the EPA criterion. Lacking a more detailed, mechanistic model, the statistical model can be used to select lakes outside of the REMAP study set for future sampling, both to verify model performance, and to refine fish tissue advisories.

9.0 Estimation and mapping of atmospheric Hg deposition

9.1 Summary

This section describes the methods used by Ecosystems Research Group, Ltd. to develop estimates of wet and dry mercury deposition to the Vermont and New Hampshire REMAP Lakes Study Area. Estimates were derived at 30-meter ground resolution, allowing the representation at this scale of the effects of geographic location, land cover, forest type, topography, and climate on Hg deposition to the REMAP lake-watersheds. Existing data on total Hg in precipitation, suspended aerosol particles, and Hg-vapor from two monitoring networks (MDN and NESCAUM-REMAP) were assimilated and used to interpolate regional concentration fields for seasonal average Hg concentrations in precipitation, suspended particles, and vapor-phase Hg in air. The concentration fields were applied to high-resolution estimates of deposition velocities and precipitation rates calculated by Ecosystems Research Group, Ltd.'s High Resolution Deposition Model (HRDM) to yield localized estimates of Hg transfer to the landscape.

Total estimated Hg deposition to the REMAP lake-watersheds was dominated by Hg_0 assumed to be assimilated by plant foliage, reactive gaseous Hg deposition, and Hg delivered by precipitation. Particulate-phase and cloud-water Hg deposition were generally unimportant compared to the other pathways. Estimated Hg deposition to the REMAP watersheds ranged from 10.3 $\mu g\ m^{-2}\ y^{-1}$ to 32.9 $\mu g\ m^{-2}\ y^{-1}$, averaging 22.6 $\mu g\ m^{-2}\ y^{-1}$. Estimated total direct deposition to surface waters within the REMAP watersheds ranged from 7.6 $\mu g\ m^{-2}\ y^{-1}$ to 16.4 $\mu g\ m^{-2}\ y^{-1}$, averaging 9.4 $\mu g\ m^{-2}\ y^{-1}$.

9.2 Concentrations of Hg species in the atmosphere

There are few direct measurements of mercury in precipitation and the atmosphere relative to the information currently available for estimation of other important air pollutants (S, N, O_3) in the study region. However, what information is available is perhaps one of the best regional data sets currently available for atmospheric Hg. The data used to estimate the regional concentration fields for atmospheric Hg species were obtained from the National Atmospheric Deposition Program, Mercury Deposition Network (MDN) and regional studies conducted by NESCAUM.

9.2.1 Hg in precipitation

There are 10 locations within or adjacent to the study area where Hg has been measured in precipitation (Table 9.2.1.1) as part of two Hg monitoring networks. Both MDN and NESCAUM network sites measure total Hg in precipitation but use different samplers, protocols and analytical laboratories. The MDN protocol specifies weekly sample collections, while the NESCAUM stations followed the University of Michigan Air Quality Laboratory (UMAQL) protocol which specifies event collections (Burke et al. 1995). Alter (2000) identified a 9 to 22% weekly bias (UMAQL higher) in Hg concentration between collocated samplers using the different samplers, protocols and analytical laboratories for weeks with single and multiple events, respectively. Subsequent collocation trials involving the two differing samplers and protocols but the same (MDN) analytical laboratory found smaller bias (Ann Chalmers and Clyde Sweet, personal communication 2002). Our analysis of the collocated data from the MDN and NESCAUM site at Acadia National Park indicates that on a monthly volume-weighted average basis, the UMAQL protocol determined an average of 38% higher Hg concentrations than the MDN protocol. The relationship between the monthly averages of the two protocols was best modeled by

$$MDN = -1.575634 + 1.3019375*UMAQL - 0.0269445*UMAQL^2 \qquad \text{[Eq. 3]}$$

($r^2 = 0.97$, $p < 0.0001$, n=11, 1 outlier removed) where MDN and UMAQL represent the respective monthly volume-weighted average concentrations of Hg in precipitation in ng l^{-1} determined by those protocols.

Concentrations measured at NESCAUM sites were adjusted for this bias using equation 3 for comparison with the MDN network and generation of regional concentration fields.

Due to differences in the objectives and funding of the two Hg monitoring networks, there was no year when all 10 stations operated simultaneously. Most stations operated during 1997 or 1998 to 1999 (Table 9.2.1.1). Alter (personal communication 2001) examined the year-to-year variance in monthly concentrations at long operating sites from both networks and determined that there was no evidence for significant year-to-year differences in concentrations during the period encompassing all observations. The coefficient of variation of annual volume weighted mean concentrations was 9.2% for Underhill (1993-1999) and 9.6% for Acadia (1997-2000), approaching the likely precision of the measurement. As a first approximation, and given the lack of large year-to-year variance, it is reasonable to pool the observations from different years at different sites as a basis for forming the most dense network possible for spatial interpolation of the Hg precipitation concentration field. The objective of this project was to estimate the differences in Hg atmospheric deposition to lake watersheds across the VT-NH region for comparison with differences in Hg burdens of various ecosystem compartments. Because most measures of ecosystem Hg accumulation will integrate across several years (or decades) of Hg deposition, it seemed more reasonable to pool all years of data available for each station rather than to limit the analysis to the 1997-1999 period.

Table 9.2.1.1. Mercury monitoring stations used to interpolate regional atmospheric mercury concentration fields.

Station	State	Network	Latitude	Longitude	Years Available
Greenville	ME	MDN	45.4897	69.6644	1997-2000
St. Anicet	PQ	MDN	45.2000	74.0333	1998-2000
Underhill	VT	UMAQL	44.5283	72.8962	1993-1999
Bridgton	ME	MDN	44.1075	70.7289	1997-2000
Huntington	NY	MDN	43.9725	74.2208	2000
Freeport	ME	MDN	43.8319	70.0628	1998-2000
Laconia	NH	MDN	43.5000	71.5000	1998-2000
New Castle	NH	MDN	43.1667	70.8667	1998-1999
Quabbin	MA	UMAQL	42.2983	72.3347	1997-1999
East Providence	RI	UMAQL	41.8403	71.3617	1997-1999

Monthly precipitation-weighted average concentrations (adjusted to an MDN basis) were further averaged to seasonal precipitation-weighted concentrations (Table 9.2.1.2). Data were not available for the Huntington, NY station to form the summer and fall season averages. The seasonal concentrations for 10 stations (winter, spring) or 9 stations (summer, fall) were spatially interpolated to a 1-km grid over the region using distance^3-weighting of observations (for example, see Figure 9.2).

Table 9.2.1.2. Seasonal precipitation-weighted average concentrations for the Hg monitoring sites. Values for the UMAQL protocol sites were adjusted to an MDN basis (equation 3). Concentrations are reported in ng l^{-1}.

Station	state	winter	spring	summer	fall
Bridgton	ME	4.51	6.58	9.85	5.55
Freeport	ME	4.89	7.11	11.59	7.69
Greenville	ME	2.79	4.80	9.32	4.82
Quabbin	MA	5.66	7.35	8.96	6.73
Laconia	NH	4.81	8.10	8.43	6.20
New Castle	NH	4.11	7.08	11.82	6.08
Huntington	NY	5.10	7.20		
Saint Anicet	PQ	5.26	9.09	10.50	8.77
East Providence	RI	5.68	8.63	8.93	7.09
Underhill	VT	4.64	7.64	8.19	6.52

9.2.2 Hg in cloud water, frost or dew

In the few measurements of Hg in cloud water, frost or dew (Lawson 1999, Malcolm and Keeler 2002) Hg was not elevated or enriched with respect to its concentration in precipitation as is the case for rapidly scavenged compounds. This behavior is expected given the low RGM and H_p concentrations in the atmosphere and the very low solubility of Hg_0 in water. We estimated the concentration of Hg in cloud water from the precipitation concentration corrected for a slight enrichment (1.1, the maximum observed by Malcolm and Keeler 2002) and spatial variations in cloud liquid water content (cf. Miller et al. 1993a,b).

9.2.3 Particulate-phase Hg

Total suspended particle (<2.5 micron) mercury concentrations (Hg_p) in air were determined at three of the NESCAUM sites: Quabbin Reservior (QBN), East Providence (PRV), and Underhill (LKC) using UMAQL protocols (Burke et al. 1995). Hg_p concentrations were lower in summer and higher in winter at all three sites, with seasonal differences more pronounced than site-to-site differences. The site-to-site and temporal variation in Hg_p concentrations could be modeled across all three sites as a function of the Hg concentrations in precipitation and month of the year ($r^2=0.96$, $p<0.001$, n=33, 1 outlier removed, Appendix B.1). Monthly Hg_p concentrations were estimated at the 7 other network sites using this model. Nine percent of the monthly values (5 October, 3 January, and 1 December) predicted by this model for MDN sites were less than zero. Values for these sites and time periods were estimated by temporally interpolating between adjacent monthly values at each site. This method of estimation honored the seasonal trends indicated by the NESCAUM sites, but recognized somewhat of a departure from the relationship between Hg_p and precipitation Hg indicated by the statistical model. Seasonal average Hg_p concentrations were formed from the monthly observations or estimates and spatially interpolated to a regional concentration field following the method used for precipitation.

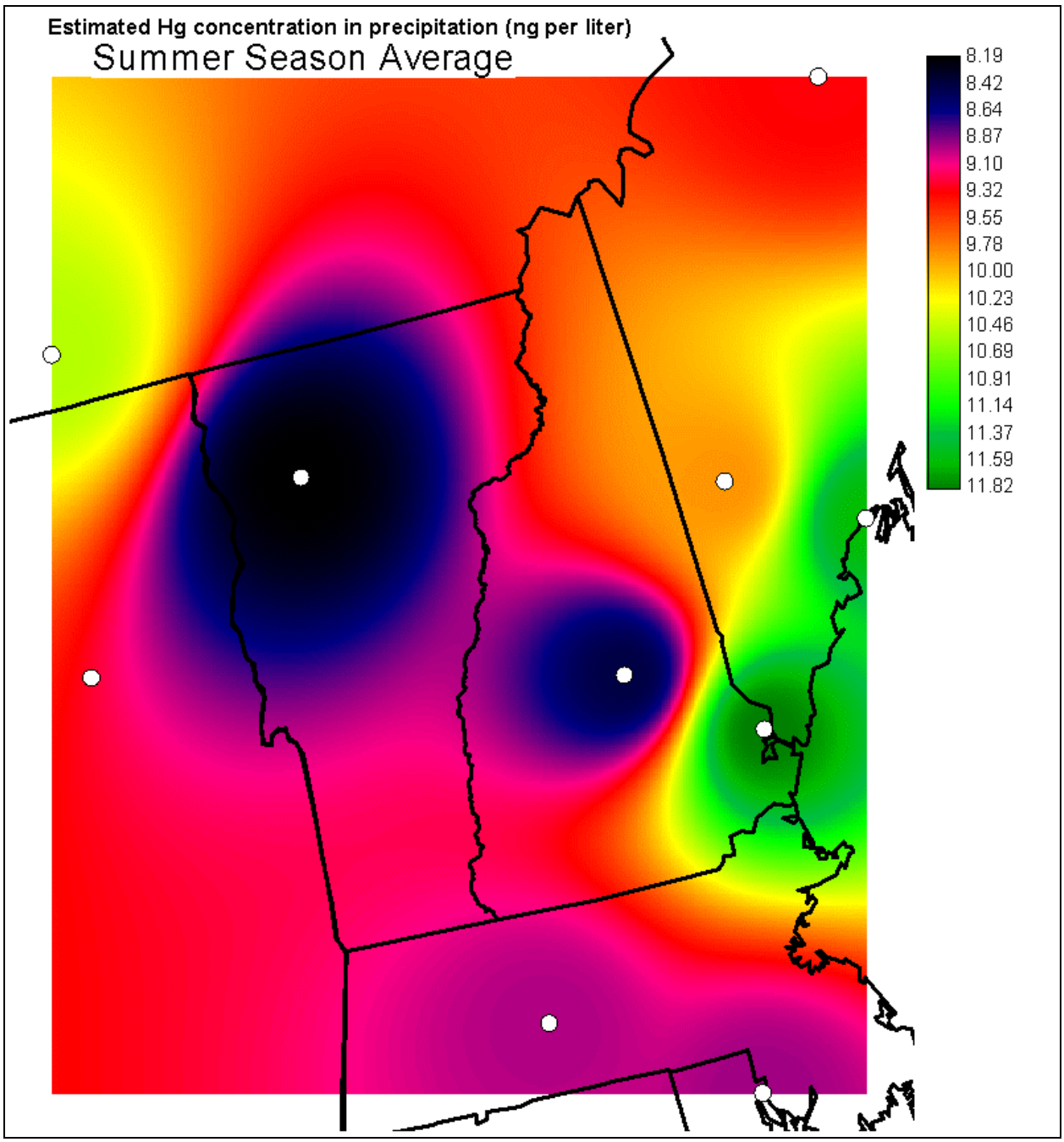

Figure 9.2. Estimated Hg concentration (ng l^{-1}) field for summer precipitation. White circles represent the location of mercury monitoring stations (Table 9.2.1.1) used in the interpolation of the regional concentration field. Note: the location of the Huntington, NY site is included in this figure for reference, but there were no summer data available for use in interpolating the concentration field pictured (see text).

9.2.4 Hg_0 vapor

Total mercury vapor concentrations (Hg_v = Hg_0+RGM) in air were determined at three of the NESCAUM sites: Quabbin Reservoir (QBN), East Providence (PRV), and Underhill (LKC) using UMAQL protocols (Burke et al. 1995). In contrast to the Hg_p observations, Hg_v showed no significant seasonal variation within individual sites. However, individual months were sometimes higher than the mean, indicating the possible importance of significant emission or transport events. Hg_v concentrations were significantly different between the sites (ANOVA $p<0.0001$) with the annual means significantly different between each site (Tukey-Kramer HSD), suggesting a south-to-north or urban-to-rural trend (PRV>QBN>LKC). Analysis of covariance of seasonal mean Hg_v with the seasonal average precipitation Hg concentration as the covariate and season as the main effect, revealed the expected seasonal relationship between Hg_v and precipitation Hg ($r^2=0.95$, $p=0.016$, $n=12$). Hg_v was positively correlated with Hg in precipitation, reflecting spatial patterns in atmospheric Hg burdens, while the residuals of this effect were lower in summer and higher in winter reflecting greater oxidation and scavenging rates in summer (Lin and Pekonen 1999). This model formed the basis for estimating Hg_v concentrations at the other network sites (Appendix B.2). Seasonal average Hg_v concentration observations and estimates were spatially interpolated to a regional concentration field following the method used for precipitation.

9.2.5 Reactive gaseous Hg

Reactive gaseous Hg (RGM = $HgCl_2$ + $HgBr_2$) was not measured by either network. Recent studies suggest that RGM can represent 1-3% of Hg_v at continental sites (Lindberg and Stratton, 1998; Landis et al. 2002). Because RGM is highly reactive and rapidly scavenged by moist particles and surfaces, RGM concentrations likely fall off rapidly with distance from their primary sources, incinerators and power plants (Lindberg and Stratton, 1998). Thus, RGM concentrations in the study region are likely to be highly variable and related to point sources. Estimation of the effect of point sources on the spatial distribution of RGM in the atmosphere is beyond the scope of this project. For the purpose of providing bounded estimates of total Hg deposition we estimated RGM deposition for the region assuming RGM represents either 1% or 3% of Hg_v.

9.3 Atmosphere-land surface transfers of Hg

The exchange of Hg between the atmosphere and ecosystems is bidirectional. Precipitation, dry particle deposition, RGM deposition and Hg_0-vapor deposition contribute Hg to landscape burdens. Oxidized forms of Hg in soils, soil waters, surface waters and aquatic sediments are reduced by both biotic and abiotic processes to form Hg_0. Because Hg_0 is sparingly soluble in water, most of the Hg_0 produced in terrestrial and aquatic systems is partitioned into the vapor phase and reemitted to the atmosphere. The primary controls on Hg_0 emissions from different landscape elements are just beginning to be well understood. The accumulated landscape burden, bioavailability, and persistence Hg in the environment are all affected by the balance of Hg deposition and reemission. Modeling Hg reemission processes is beyond the scope of this project. The deposition component of atmosphere-surface exchange processes were modeled using Ecosystems Research Group, Ltd.'s High-Resolution Deposition Model (HRDM, Miller 2000). Important data sources for the HRDM are described in Appendix C. We also developed a provisional method to estimate the net Hg_0 deposition (net of canopy assimilation and reemission) using foliar Hg accumulation rates, although the mechanisms governing Hg_0 exchange processes and foliar sequestration of Hg are currently poorly understood.

9.3.1 Precipitation

We estimated the spatial distribution of Hg deposition due to precipitation by multiplying the seasonal average Hg precipitation concentration fields (described above) by the seasonal 30-y normal precipitation fields derived for the HRDM (Miller 2000). Briefly, a regression model was developed to extract the elevation component of the variance in seasonal precipitation rates measured in the NOAA cooperative observer network for the Northeastern US (619 stations). The elevation regression model captures local

orographic effects on the precipitation rate. The residuals of this model were spatially interpolated to provide local estimates of medium-scale orographic and moisture source effects (Dingman 1981). The regression model is then applied to a high-resolution digital elevation model (DEM) and combined with the residual field to provide a localized estimate of seasonal precipitation rate.

9.3.2 Cloud water deposition

The cloud water deposition model of Miller et al. (1993a,b) was parameterized with representative canopy configurations for the major surface types expected to receive cloud water deposition. Multiple sensitivity analyses were conducted with the multi-layer model in order to characterize model response to a large set of possible canopy by meteorological condition interactions. We then statistically apportioned the multi-layer model response to key environmental parameters that can be obtained for each 30-m pixel (wind speed, temperature, LWC, cloud frequency). Cloud frequency is taken to be a function of elevation as observed at Whiteface Mountain, NY (Miller et al. 1993b) but adjusted for regional variation in atmospheric water vapor content using the ratio of sea level precipitation rate at a given location relative to the value at Whiteface Mountain. LWC was estimated from cloud frequency (Miller and Friedland 1999).

9.3.3 Dry deposition of Hg_p, RGM, and Hg_0

Dry deposition of Hg_p, RGM, and Hg_0 were estimated using the approach of Lindberg et al. (1992) with some differences and additions described below. Dry deposition velocities for aerosol particles and gasses were estimated using a big leaf model designed for complex terrain and multi-species canopies (Miller et al. 1993a,b). This model includes appropriate physics to simulate deposition to a complex landscape with a wide range of elevations, pressures, temperatures, and receptor surface types. A big-leaf model is preferred over a multi-layer model for this application because of the limited information available to properly characterize the receptor surface at each 30-m pixel.

The meteorological data required to drive the dry deposition model (temperature, relative humidity, wind speed, percent of possible solar radiation) were derived from hourly observations at 3 stations within the region of interest, extrapolated on the basis of terrain functions (for example see Miller et al. 1993b) and regional climatology fields (Miller 2000). Total potential solar radiation at a site was calculated taking into account the effects of terrain, and atmospheric optical properties on direct and diffuse solar radiation. The total possible solar radiation was multiplied by the value of percent possible radiation interpolated for a location from the values observed for that hour at the 3 observation stations. The meteorological stations used for this analysis were the Underhill (VT) NOAA site, the Lye Brook Wilderness (VT) CASTNET site, and the Woodstock (NH) CASTNET site.

Dry deposition to water surfaces was calculated following the method of Xu et al. (1999). RGM was assumed to behave similarly to nitric acid vapor (Lindberg et al. 1992, Rea et al. 2001) and Hg_0 deposition was computed without regard to a compensation point (see below).

9.3.4 Net Hg_0 deposition inferred from Hg accumulation in foliage and leaf litter fall rates

The Lindberg et al. (1992) model clearly overestimates Hg_0 deposition (S.E. Lindberg personal communication 2002) because it does not include a compensation point for Hg (Hanson et al. 1995) as is necessary for modeling other atmospheric species with bi-directional fluxes (e.g. van Hove et al. 2002) and it lacks representation of canopy emission of Hg_0 (Lindberg et al. in press, Lindberg and Meyers 2002, Lindberg et al. 1998). Xu et al. (1999) side-stepped modeling a compensation point by separately calculating Hg_0 deposition according to Lindberg et al. (1992) and formulating a separate model for canopy emission of Hg_0 that is consistent with the very limited pre-1999 understanding of controls on this process. Net Hg_0 deposition was taken to be the net of the two model results. Unfortunately several key parameters in Xu et al.'s (1999) canopy emission model – such as the supersaturated concentration of Hg_0 dissolved in soil water – remain highly uncertain, are likely quite variable, and are difficult to model with available information. Also, recent experimental evidence (Johnson et al. in press, Mae Gustin personal communication 2002) indicates

that soil emission of Hg_0 is not limited by diffusion through soil as was previously thought (see Johnson and Lindberg 1995, Lindberg et al. 1998) and therefore, supersaturation of soil water with dissolved gaseous Hg_0 as assumed by Xu et al. (1999) appears unlikely. Recent, intensive measurements of Hg_0 emission from vascular plant canopies suggests that some biological process at the root-soil interface may be responsible for the production of Hg_0 (bioreduction) and apparent supersaturation of Hg_0 in the xylem of plants exhibiting net Hg_0 emission (Lindberg in press, S.E. Lindberg personal communication 2002).

Rea et al. (2002) measured the accumulation of Hg in the foliage of deciduous trees over the course of the growing season and found that total accumulation was substantially less than Hg_0 deposition estimated following Lindberg et al. (1992). Rea et al. (2001) determined that Hg_p and RGM dry deposition are rapidly washed off foliar surfaces, and therefore foliar accumulation of Hg most likely represents Hg_0 assimilation. Rea et al. (2002) and Grigal (2002) reach the conclusion that accumulation of Hg in foliage most likely represents a net Hg_0 flux from the atmosphere to the canopy. However, given the observations of large Hg emissions from a variety of plant canopies (Lindberg et al. 1998, Lindberg and Meyers 2002, Cobos et al. 2002) and strong indications that the source of Hg_0 emitted is from (or involves passage through) the roots of the plants (Lindberg and Meyers 2002, Lindberg et al. in press) it seems equally plausible that foliar accumulation of Hg and its transfer to the soil via litterfall could represent Hg recycling rather than atmospheric deposition. In fact, the rate of Hg accumulation in foliage was highly linear with no significant difference between accumulation rates measured by Rea et al. (2002) in two widely separated forests, in two different years, with significantly different meteorological conditions and Hg_0 deposition velocities at each site (Figure 3). Hg retained in plant foliage is presumably sequestered in the vacuole space by phytochelatins that bind Hg^{2+} (Cobbett 2000). The lack of difference in foliar accumulation rates given the difference in deposition velocities for the two sites studied by Rea et al. (2002) suggests that foliar Hg accumulation might be limited by biological processes mediating sequestration of Hg such as the production of phytochelatins or the oxidation of Hg_0 to Hg^{2+} necessary for Hg to be bound and sequestered by phytochelatins. Such limitations would apply to accumulation of Hg_0 with either a soil or atmospheric source.

Given the possibility that the annual transfer of Hg from foliage to forest floor via litter fall represents net Hg_0 deposition (Rea et al. 2002, Grigal 2002), we developed a method to model the accumulation of Hg in foliage of the study area. Observed Hg contents in foliage at Underhill, VT (Rea et al. 2002) are described well by

$$Hg_{foliage}(ng\ g^{-1}) = DOY * 0.20137 - 26.203 \qquad \text{[Eq. 4]}$$

(r^2= 0.99, $p<0.0001$, n= 4). Foliar Hg accumulation was also linear with a similar accumulation rate (slope of equation 4) at the Pellston, MI site studied by Rea et al. (2002) (Figure 9.3.4). The zero Hg intercept of equation 4 suggests the onset of accumulation occurred on day 130 (May 10th) at the Underhill site (44.53 N) and 5 days later at the Pellston site (45.57 N), both plausible dates for initial swelling of buds at these locations. The Hg accumulation period constitutes the time between the zero Hg intercept and majority leaf fall, and amounts to 140 to 150 days at these two sites, approximating the length of the growing season. The accumulation period was both shorter and the total Hg accumulation less at the more northerly Pellston site. Thus, as a first approximation, we expect the Hg content of deciduous foliage to be a linear function of the length of the growing season.

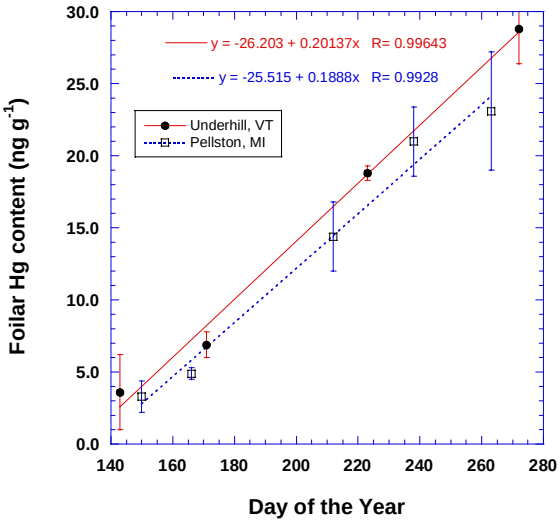

Figure 9.3.4. Growing season Hg accumulation in foliage of several deciduous species measured in VT and MI by Rea et al. (2001). Hg accumulation was highly linear with similar daily accumulation rates at both sites. Points are collection period means (with standard errors) of several species.

We analyzed data on growing season length and mean annual temperature (MAT) from 28 stations in Vermont and New Hampshire. In this region, the length of the growing season was extended by 6.2 days for each 1°C increase in MAT (r^2 = 0.77 $p<0.0001$ n=28). This result falls between the recent estimate by White et al. (1999) of an increase of 5 days per 1°C MAT derived for stations between 32.8N and 45.5N in the eastern US and a value of 9.6 days per 1°C we calculated from Canadian data (CANSIS 2002) representing 43.73N to 46.94N, 63.29W to 73.69W (r^2= 0.95 $p<0.0001$ n=38) and, therefore, seems appropriate for the study region.

Using the Underhill site as the basis (30-year MAT = 10.75°C), the Hg foliar accumulation period is then

$$\text{Period} = 83.4 + 6.2*\text{MAT} \qquad \text{[Eq. 5]}$$

The concentration of Hg in foliage at the end of the accumulation season was calculated from equations 4 and 5. This accumulation rate is applicable for the major deciduous species of the study area (see Rea et al. 2001). We also estimated the Hg accumulation in foliage of evergreen species that retain needles for 2 to 7 years and exhibit continued accumulation of Hg in the years after foliage formation (Rasmussen 1995, Grigal 2002). Evergreen foliage generally exhibits higher Hg concentrations than deciduous foliage from the same site due to the greater needle life span of evergreens (Rasmussen 1991, Grigal 2002). Rasmussen (1995) found that the Hg concentration of balsam fir and white spruce needles increased by 5-10 ng g^{-1}, during the year after foliage formation. We assume that evergreens accumulate Hg at the same rate as deciduous foliage during the first year and increase by 10 ng g^{-1} for each subsequent year of needle retention.

The flux of Hg to the forest floor is computed from the estimated foliar Hg concentration at senescence and an estimate of litter fall mass. Litter fall mass is proportional to total productivity and related to climate at continental to global scales (Schlesinger 1977). However, in a well distributed sample of Vermont forests (Miller et al. in prep) foliar biomass was primarily related to basal area of the plot (age and other growth factors) and forest type (r^2=0.73, $p<0.0001$, n=210), but not to mean annual temperature. Within the VT-NH region, variance in standing biomass and production is dominated by stand age (management history)

rather than climatic factors (Miller et al. in preparation). Because it is currently impossible to estimate forest age at the spatial resolution of the model, we use the mean foliage biomass (adjusted for evergreen needle retention) to estimate litter fall mass by forest type (Table 9.3.4).

Table 9.3.4. Characteristics of regional forest types used in the dry deposition and litter fall Hg accumulation models. Leaf biomass estimates are from the forest survey conducted by Miller et al. (in preparation).

	Forest Type	Leaf Biomass t ha-1	+/-se	g litterfall per g leaf biomass	Leaf Area (m2 m-2) per g leaf biomass	LAI	Sources of allometric equations
	Deciduous Forest						
1	Paper Birch - White Birch	4.39	1.3	1.0000	0.0180	**7.90**	Whittaker et al. 1974
2	White Birch - Northern Hardwoods	3.46	0.32	1.0000	0.0180	**6.23**	Whittaker et al. 1974
3	Sugar Maple - Northern Hardwoods	3.46	0.32	1.0000	0.0180	**6.23**	Whittaker et al. 1974
4	Northern Hardwoods	3.66	0.26	1.0000	0.0203	**7.43**	Whittaker et al. 1974
5	Central Hardwoods	3.49	0.82	1.0000	0.0096	**3.35**	Whittaker et al. 1974
6	Coastal Oaks	3.27	na	1.0000	0.0096	**3.14**	Whittaker et al. 1974
	Evergreen Forest						
7	Coastal Pines	4.67	na	0.8672	0.0075	**3.50**	Whittaker et al. 1974
8	White Pine	2.18	0.65	0.8672	0.0113	**2.46**	Whittaker et al. 1974
9	White Pine - Hemlock - Red Spruce	2.39	0.55	0.6123	0.0113	**2.70**	estimated from properties of classes 8 and 11
10	Hemlock - Red Spruce	3.23	1.3	0.4849	0.0113	**3.65**	estimated from properties of classes 8 and 11
11	Balsam Fir - Red Spruce	6.65	0.33	0.3574	0.0113	**7.51**	Miller and Friedland 1992
	Mixed Forest						
12	Coastal Oak - Coastal Pine	4.67	na	0.8672	0.0075	**3.50**	Whittaker et al. 1974
13	White Pine - Central Hardwoods	2.61	1.84	0.8672	0.0075	**1.96**	Whittaker et al. 1974
14	White Pine - Hemlock - Red Spruce - Central Hardwoods	2.02	0.65	0.8672	0.0075	**1.52**	Whittaker et al. 1974
15	Balsam Fir - Red Spruce - Hemlock - White Pine - Northern Hardwoods	3.33	0.33	0.8331	0.0150	**5.00**	Whittaker et al. 1974
16	Balsam Fir - Red Spruce - Sugar Maple - Northern Hardwoods	4.66	0.4	0.5953	0.0132	**6.13**	estimated from properties of classes 15 and 17
17	Balsam Fir - Red Spruce - Paper Birch	6.98	0.75	0.3574	0.0113	**7.89**	Miller and Friedland 1992

9.4 Tabulation of deposition results for the REMAP Lake-Watersheds

VTDEC supplied GIS-coverages containing polygons delineating either segments or the full watershed for lakes of VT and NH. VTDEC also provided a coverage containing the centroids of lakes included in the REMAP study. We selected the study watershed polygons based on the study lake centroids. There was an error in the basin delineation of North Pond near Brookfield, VT. This basin was digitized manually from USGS topographic maps. Unique polygon identifiers were assigned to each of the watershed basin segments and a mask was produced to allow extraction of the deposition estimates by watershed or basin segment.

9.5 Discussion

The modeled deposition velocities and corresponding fluxes of Hg_p, Hg_v, and RGM were consistent with values reported by other investigators using the Lindberg et al. (1992) approach to modeling dry deposition. Assuming that dry-deposited Hg_p and RGM are washed off the canopy with 100% efficiency during subsequent rains (Rea et al. 2002), the sum of modeled precipitation, Hg_p and RGM fluxes should approximate the Hg flux that would be measured in canopy throughfall. In field measurements from a variety of forest types and locations, the ratio of throughfall to precipitation Hg flux ranged from 1 – 3 Grigal (2002). The modeled values for this ratio (assuming the RGM = 1% Hg_v scenario) fall between 1.2 and 1.92 (Figure 9.5.1). If the RGM3 scenario (RGM = 3% Hg_v) were used, the modeled ratio of throughfall to precipitation Hg flux would be in excess of 3 for most of the study watersheds (Figure 9.5.2). This comparison suggests that the RGM1 scenario is likely to be more realistic.

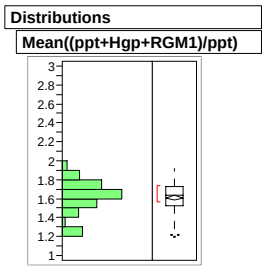

Quantiles

100.0%	maximum	1.9200
99.5%		1.9200
97.5%		1.8985
90.0%		1.8040
75.0%	quartile	1.7300
50.0%	median	1.6400
25.0%	quartile	1.5300
10.0%		1.2900
2.5%		1.2400
0.5%		1.2000
0.0%	minimum	1.2000

Moments

Mean	1.6103962
Std Dev	0.1690923
Std Err Mean	0.0131638
upper 95% Mean	1.6363886
lower 95% Mean	1.5844038
N	165

Figure 9.5.1. Ratio of modeled "throughfall" (see text) to modeled precipitation flux of Hg. The model results are consistent with field studies that indicate the ratio of throughfall to precipitation typically ranges from 1 – 3 (Grigal 2002).

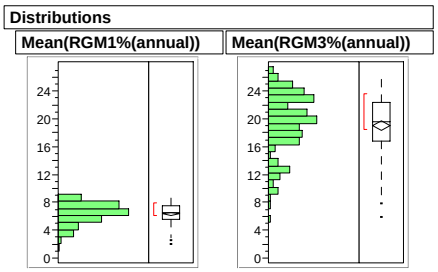

Quantiles

100.0%	maximum	8.7400	100.0%	maximum	26.220
99.5%		8.7400	99.5%		26.220
97.5%		8.4240	97.5%		25.281
90.0%		7.9940	90.0%		23.992
75.0%	quartile	7.4700	75.0%	quartile	22.410
50.0%	median	6.5400	50.0%	median	19.620
25.0%	quartile	5.6100	25.0%	quartile	16.830
10.0%		4.1540	10.0%		12.452
2.5%		3.0665	2.5%		9.198
0.5%		1.9800	0.5%		5.950
0.0%	minimum	1.9800	0.0%	minimum	5.950

Moments

Mean	6.3324417	Mean	18.997919
Std Dev	1.433084	Std Dev	4.2987611
Std Err Mean	0.1115654	Std Err Mean	0.3346581
upper 95% Mean	6.5527315	upper 95% Mean	19.658713
lower 95% Mean	6.1121519	lower 95% Mean	18.337125
N	165	N	165

Figure 9.5.2. Frequency distributions of modeled RGM flux (μg m^{-2} y^{-1}) assuming that RGM concentrations are either 1% or 3% of observed total gaseous mercury concentrations.

Model estimates of Hg accumulation in foliage and subsequent deposition via litterfall were generally less than the estimated Hg_0 flux (Figure 9.5.3). As discussed above, the modeled Hg_0 flux is clearly an overestimate of the Hg_0 deposition. The litterfall Hg flux may also overestimate Hg_0 deposition if some fraction of the Hg fixed in the leaf is derived from dissolved Hg^{2+} and Hg_0 entrained in the transpiration stream (Lindberg et al. 1998).

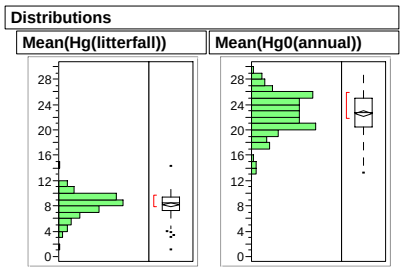

Quantiles

100.0%	maximum	14.290	100.0%	maximum	29.870
99.5%		14.290	99.5%		29.870
97.5%		11.520	97.5%		28.403
90.0%		10.046	90.0%		26.300
75.0%	quartile	9.335	75.0%	quartile	25.025
50.0%	median	8.530	50.0%	median	22.800
25.0%	quartile	7.325	25.0%	quartile	20.490
10.0%		5.728	10.0%		18.378
2.5%		3.917	2.5%		15.079
0.5%		1.110	0.5%		13.220
0.0%	minimum	1.110	0.0%	minimum	13.220

Moments

Mean	8.2196805	Mean	22.595173
Std Dev	1.8024703	Std Dev	3.0865424
Std Err Mean	0.1403221	Std Err Mean	0.240287
upper 95% Mean	8.4967514	upper 95% Mean	23.069628
lower 95% Mean	7.9426096	lower 95% Mean	22.120718
N	165	N	165

Figure 9.5.3. Frequency distributions of modeled Hg fluxes (μg m^{-2} y^{-1}) via litterfall (may represent net Hg0 deposition) and Hg0 deposition modeled without regard to a compensation point following Lindberg et al. (1992).

A provisional estimate of total Hg flux (Total*) was made by assuming:

1. dry-deposited Hg_p and RGM are washed off the canopy with 100% efficiency during subsequent rains,
2. the RGM1 scenario is a reasonable estimate of RGM flux, and
3. the accumulation of Hg in foliage and transfer to the forest floor via leaf litterfall represents the net flux of Hg_0 from the atmosphere to the land.

The estimated total Hg deposition to the REMAP watersheds ranged from 10.3 μg m^{-2} y^{-1} to 32.9 μg m^{-2} y^{-1}, averaging 22.6 μg m^{-2} y^{-1}. Precipitation, litterfall, and the RGM fluxes all contributed substantially to the total deposition. Cloudwater and Hg_p fluxes were of minor importance to the REMAP lake watersheds. Litterfall Hg flux and the RGM flux were more variable across the study watersheds than the precipitation flux (Figure 9.5.4). Estimated total direct deposition to surface waters within the REMAP watersheds ranged from 7.6 μg m^{-2} y^{-1} to 16.4 μg m^{-2} y^{-1}, averaging 9.4 μg m^{-2} y^{-1}. Maps of annual Hg deposition across the region, by type, are shown in Section 9.6.

Precipitation flux was highest in the summer and lowest in the winter, following the seasonal patterns in Hg concentration in precipitation (Figure 9.5.5). Particulate Hg fluxes were higher in winter and fall than spring or summer (Figure 9.5.6). Both RGM (Figure 9.5.7) and Hg_0 (Figure 9.5.8) exhibited maximum fluxes in the summer due to the increased leaf area and decreased canopy resistance to transfer during the growing season.

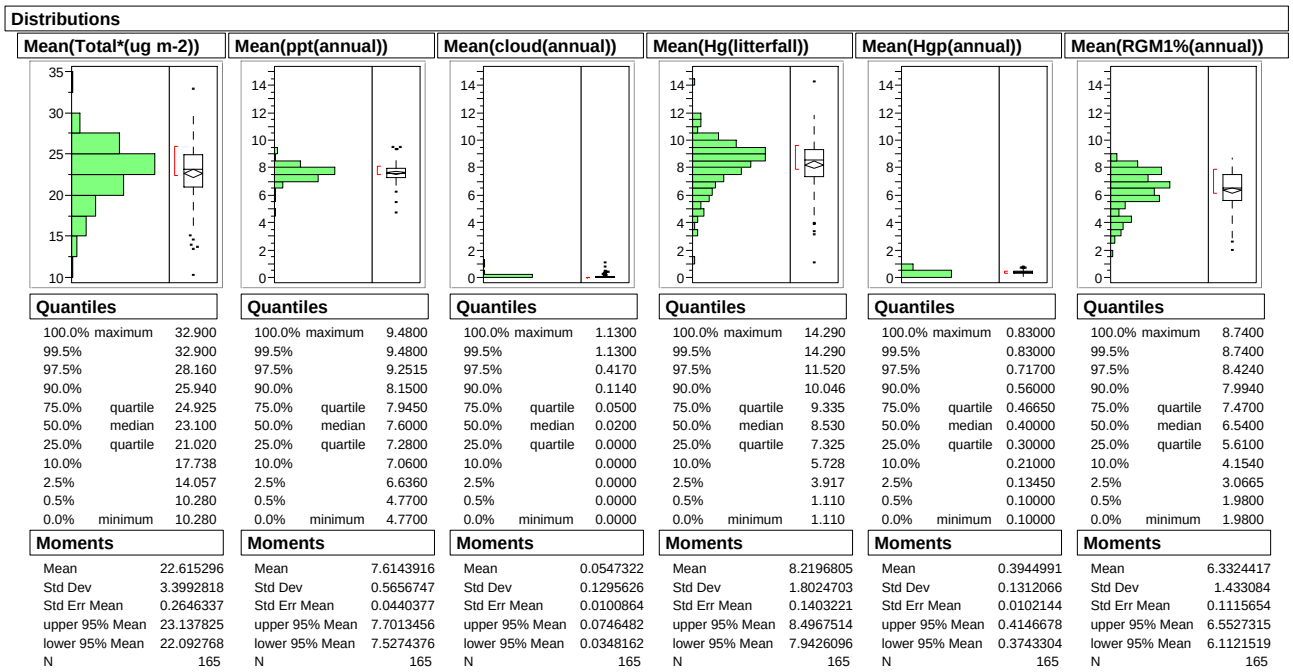

Figure 9.5.4. Frequency distributions of the total and component Hg fluxes to the REMAP study watersheds. Total Hg flux (Total*) assumes: dry-deposited Hgp and RGM are washed off the canopy with 100% efficiency, the RGM1 scenario is a reasonable estimate of RGM flux, and the accumulation of Hg in foliage and transfer to the forest floor via leaf litterfall represents the net flux of Hg0 from the atmosphere to the land. All fluxes are reported in μg m^{-2} y^{-1}.

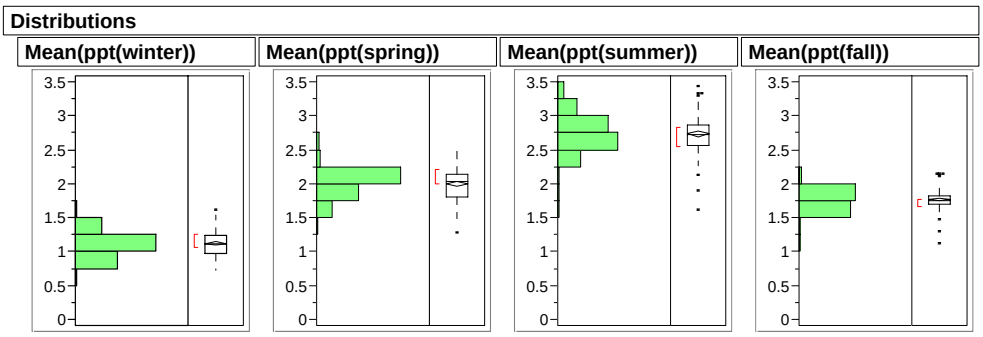

Quantiles

		Mean(ppt(winter))	Mean(ppt(spring))	Mean(ppt(summer))	Mean(ppt(fall))
100.0%	maximum	1.6200	2.5300	3.4400	2.1500
99.5%		1.6200	2.5300	3.4400	2.1500
97.5%		1.4685	2.4460	3.2985	2.0990
90.0%		1.3040	2.2064	3.0740	1.8900
75.0%	quartile	1.2300	2.1400	2.8600	1.8259
50.0%	median	1.1200	2.0400	2.7300	1.7500
25.0%	quartile	0.9750	1.8100	2.5700	1.7000
10.0%		0.9300	1.7260	2.4078	1.6600
2.5%		0.8730	1.6400	2.2705	1.5845
0.5%		0.7300	1.2900	1.6200	1.1200
0.0%	minimum	0.7300	1.2900	1.6200	1.1200

Moments

	Mean(ppt(winter))	Mean(ppt(spring))	Mean(ppt(summer))	Mean(ppt(fall))
Mean	1.1201135	1.9998055	2.7328859	1.7615549
Std Dev	0.1549536	0.2024024	0.2668163	0.1189188
Std Err Mean	0.0120631	0.015757	0.0207716	0.0092578
upper 95% Mean	1.1439325	2.0309182	2.7739002	1.7798348
lower 95% Mean	1.0962944	1.9686927	2.6918716	1.743275
N	165	165	165	165

Figure 9.5.5. Frequency distributions of precipitation Hg flux to the REMAP study watersheds by season. All fluxes are reported in µg m^{-2} season^{-1}.

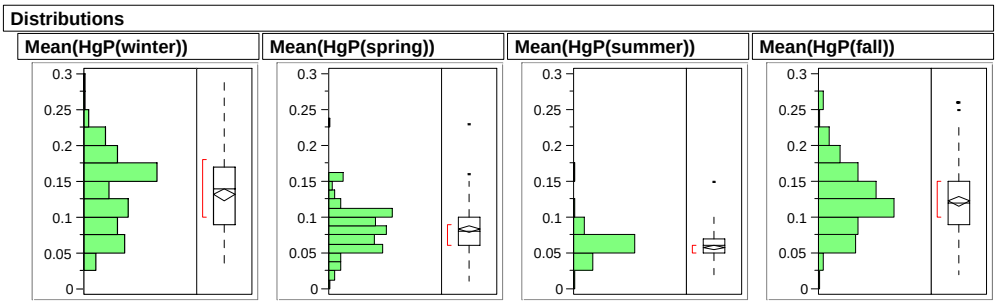

Quantiles

		Mean(HgP(winter))	Mean(HgP(spring))	Mean(HgP(summer))	Mean(HgP(fall))
100.0%	maximum	0.29000	0.23000	0.15000	0.26000
99.5%		0.29000	0.23000	0.15000	0.26000
97.5%		0.23000	0.15000	0.09850	0.22850
90.0%		0.20000	0.12000	0.08000	0.18000
75.0%	quartile	0.17000	0.10000	0.07000	0.15000
50.0%	median	0.14000	0.08000	0.06000	0.12000
25.0%	quartile	0.09000	0.06042	0.05000	0.09000
10.0%		0.06000	0.04600	0.04000	0.06133
2.5%		0.04000	0.02150	0.03000	0.04150
0.5%		0.03000	0.01000	0.02000	0.02000
0.0%	minimum	0.03000	0.01000	0.02000	0.02000

Moments

	Mean(HgP(winter))	Mean(HgP(spring))	Mean(HgP(summer))	Mean(HgP(fall))
Mean	0.1312978	0.0834533	0.0574866	0.1222606
Std Dev	0.0530829	0.031017	0.0175314	0.0458953
Std Err Mean	0.0041325	0.0024147	0.0013648	0.0035729
upper 95% Mean	0.1394576	0.0882212	0.0601815	0.1293155
lower 95% Mean	0.1231381	0.0786855	0.0547917	0.1152057
N	165	165	165	165

Figure 9.5.6. Frequency distributions of particulate-phase Hg flux to the REMAP study watersheds by season. All fluxes are reported in µg m^{-2} season^{-1}.

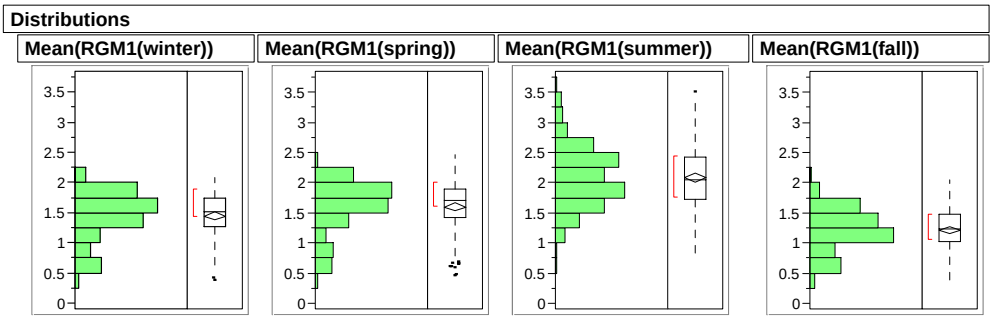

Quantiles

		Mean(RGM1(winter))	Mean(RGM1(spring))	Mean(RGM1(summer))	Mean(RGM1(fall))
100.0%	maximum	2.0800	2.4700	3.5100	2.0500
99.5%		2.0800	2.4700	3.5100	2.0500
97.5%		2.0440	2.1785	3.2380	1.7700
90.0%		1.8940	2.0459	2.6680	1.6100
75.0%	quartile	1.7499	1.8851	2.4300	1.4750
50.0%	median	1.5200	1.7000	2.0400	1.2300
25.0%	quartile	1.2700	1.4150	1.7232	1.0200
10.0%		0.7419	0.7827	1.4560	0.6424
2.5%		0.5915	0.6115	1.1075	0.5015
0.5%		0.3900	0.4700	0.7200	0.3800
0.0%	minimum	0.3900	0.4700	0.7200	0.3800

Moments

	Mean(RGM1(winter))	Mean(RGM1(spring))	Mean(RGM1(summer))	Mean(RGM1(fall))
Mean	1.4469665	1.5953003	2.0772576	1.2133252
Std Dev	0.3976743	0.429896	0.5111194	0.3414236
Std Err Mean	0.0309589	0.0334674	0.0397906	0.0265798
upper 95% Mean	1.5080959	1.6613827	2.1558255	1.2658079
lower 95% Mean	1.3858371	1.5292178	1.9986897	1.1608425
N	165	165	165	165

Figure 9.5.7. Frequency distributions of RGM Hg flux (assuming RGM = 1% of measured Hg_O) to the REMAP study watersheds by season. All fluxes are reported in μg m^{-2} $season^{-1}$.

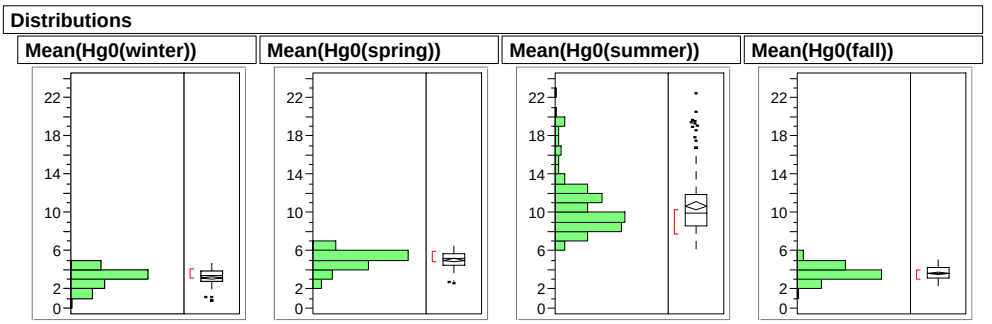

Quantiles

		Mean(Hg0(winter))	Mean(Hg0(spring))	Mean(Hg0(summer))	Mean(Hg0(fall))
100.0%	maximum	4.8400	6.9700	22.430	5.3600
99.5%		4.8400	6.9700	22.430	5.3600
97.5%		4.3985	6.4185	19.573	5.1455
90.0%		4.1580	6.0700	14.732	4.6700
75.0%	quartile	3.8550	5.7350	11.830	4.2396
50.0%	median	3.3700	5.2400	9.890	3.6400
25.0%	quartile	2.7700	4.5300	8.640	3.2100
10.0%		1.4340	3.4860	7.862	2.6560
2.5%		1.1430	2.8615	6.980	2.0890
0.5%		0.8100	2.6000	6.180	1.8500
0.0%	minimum	0.8100	2.6000	6.180	1.8500

Moments

	Mean(Hg0(winter))	Mean(Hg0(spring))	Mean(Hg0(summer))	Mean(Hg0(fall))
Mean	3.1668358	5.0288239	10.720164	3.6796111
Std Dev	0.927026	0.9350405	3.0710596	0.7491405
Std Err Mean	0.0721689	0.0727928	0.2390817	0.0583205
upper 95% Mean	3.3093358	5.1725558	11.192239	3.7947669
lower 95% Mean	3.0243359	4.8850919	10.248089	3.5644552
N	165	165	165	165

Figure 9.5.8. Frequency distributions of Hg0 flux to the REMAP study watersheds by season. All fluxes are reported μg m^{-2} $season^{-1}$.

9.6 Deposition maps

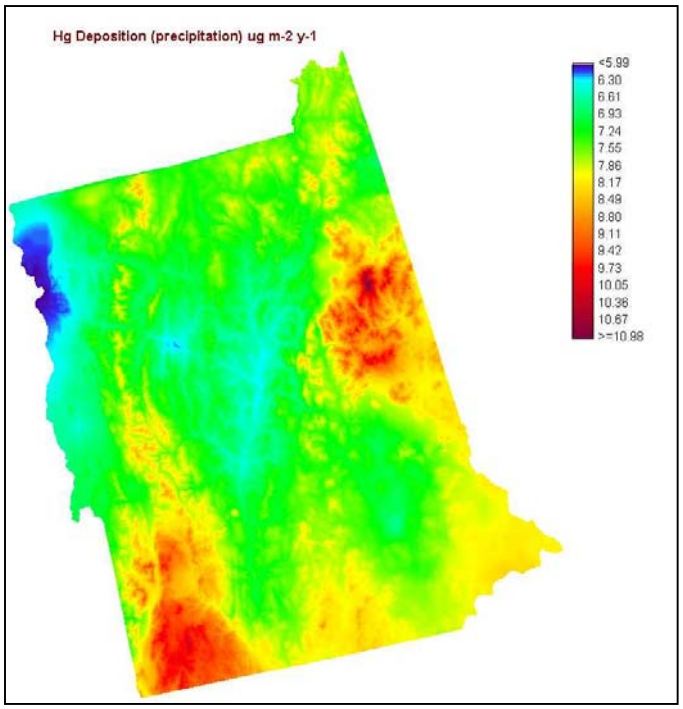

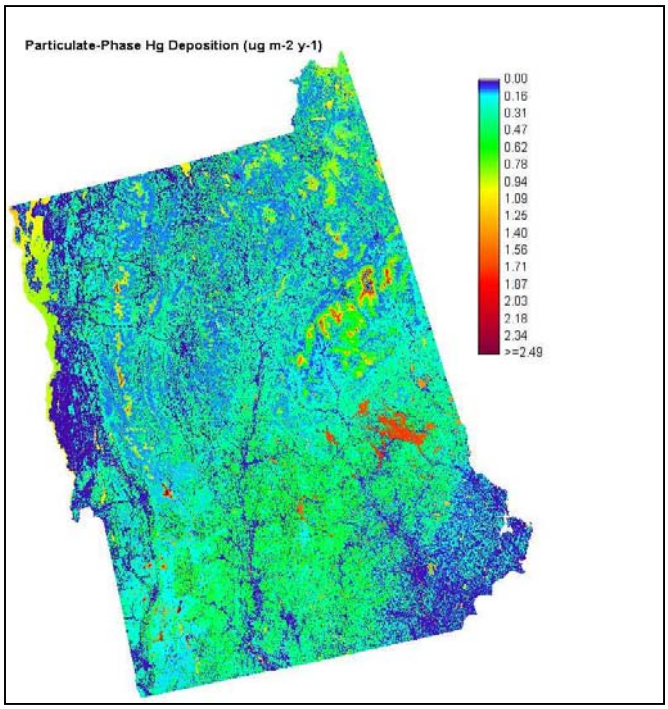

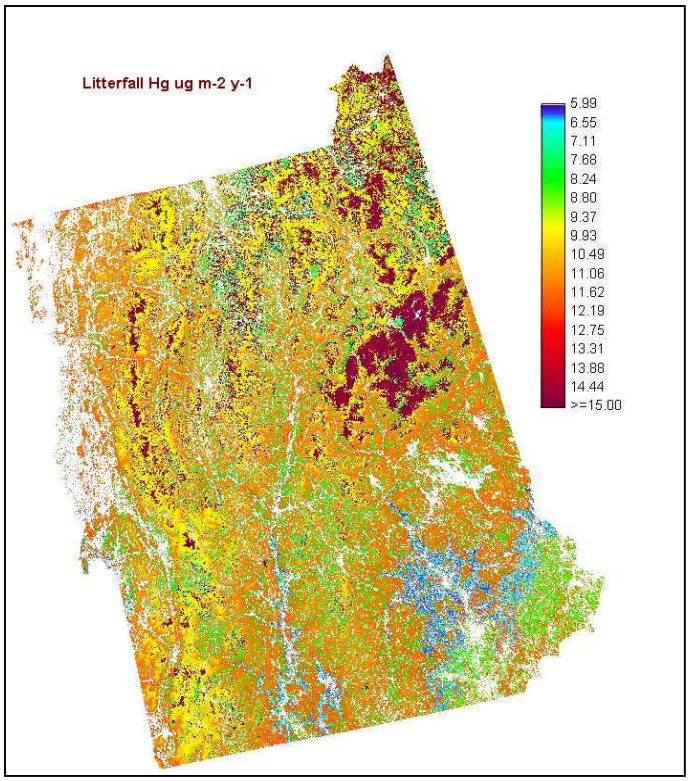

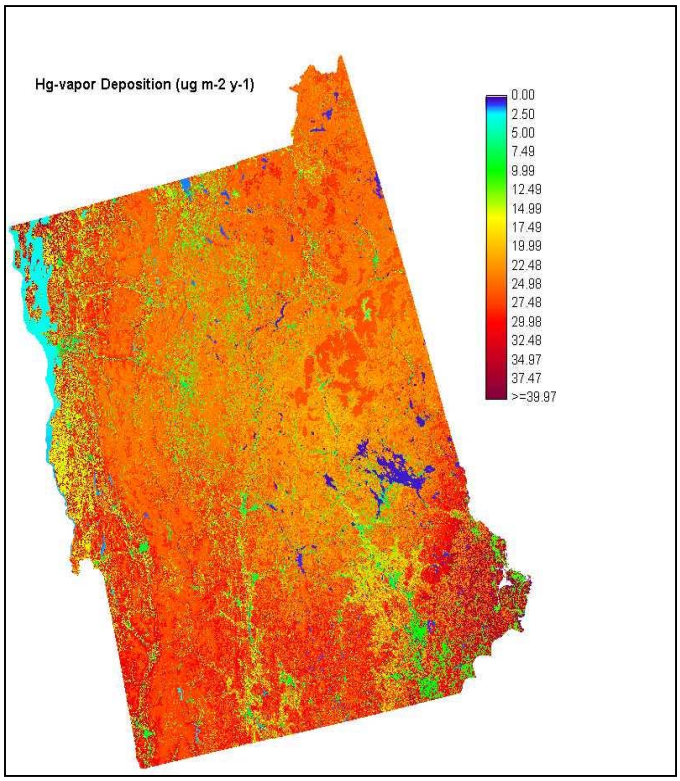

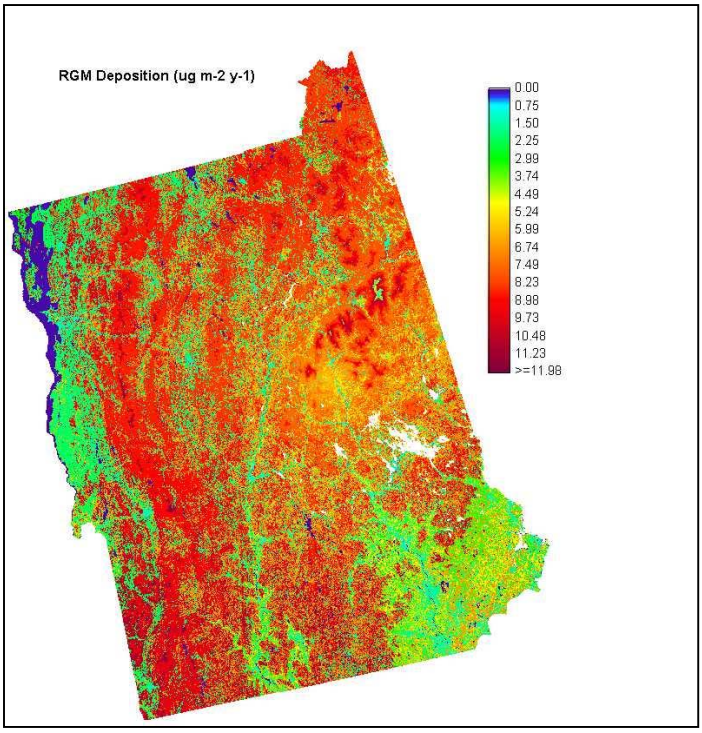
RGM Deposition (ug m-2 y-1)
0.00
0.75
1.50
2.25
2.99
3.74
4.49
5.24
5.99
6.74
7.49
8.23
8.98
9.73
10.48
11.23
>=11.98

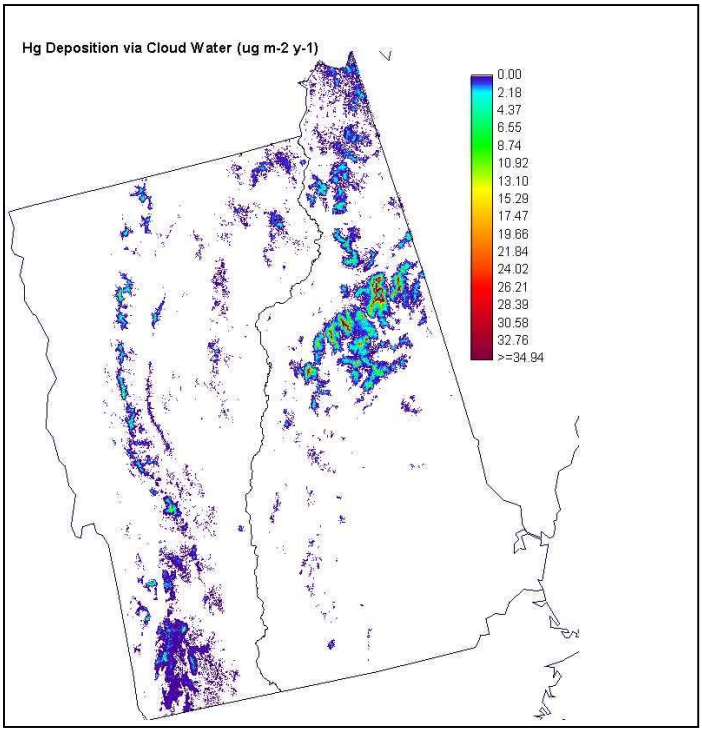
Hg Deposition via Cloud Water (ug m-2 y-1)
0.00
2.18
4.37
6.55
8.74
10.92
13.10
15.29
17.47
19.66
21.84
24.02
26.21
28.39
30.58
32.76
>=34.94

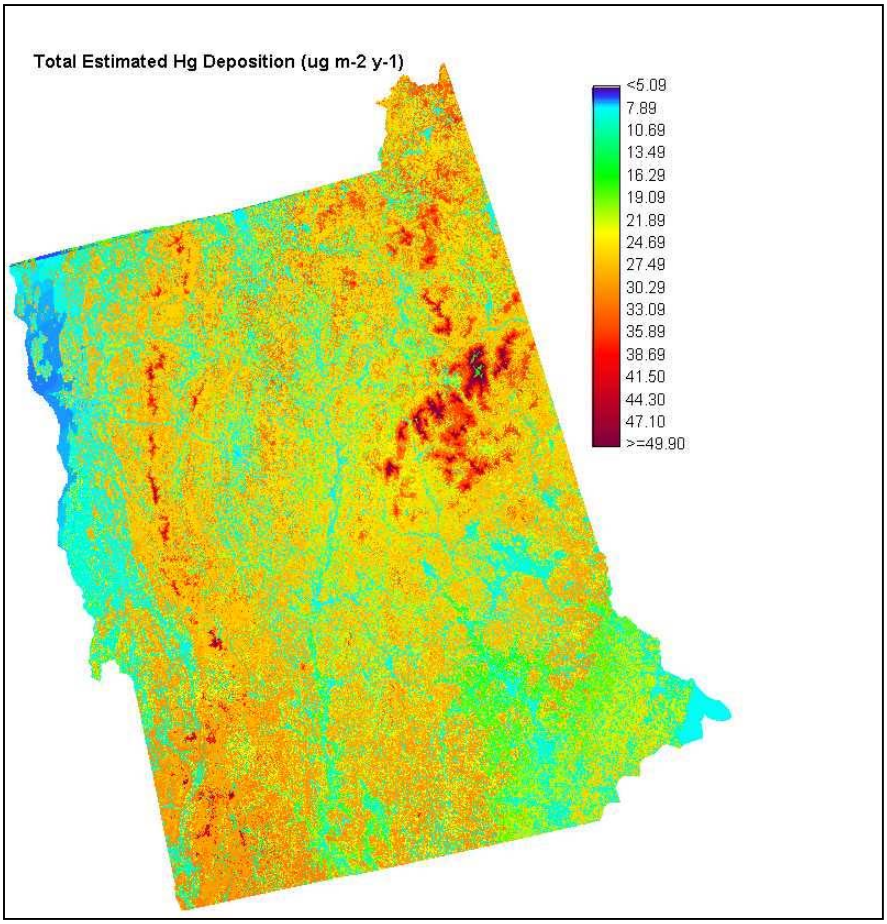
Total Estimated Hg Deposition (ug m-2 y-1)
<5.09
7.89
10.69
13.49
16.29
19.09
21.89
24.69
27.49
30.29
33.09
35.89
38.69
41.50
44.30
47.10
>=49.90

9.7 Relationship of deposition to in-lake Hg measures

The relationships between air Hg deposition estimates and in-lake Hg measurements were preliminarily assessed using correlations. SAS Proc Corr (SAS Institute 2002) was used to derive Spearman correlations between annualized measures of total, wet, litterfall, particulate, and reactive gaseous Hg, and epilimnetic Hg and meHg, and Hg in zooplankton, and prey and fillet perch. There was a statistically significant relationship between wet Hg deposition and prey-sized yellow perch (R = 0.423, p=0.007), and the relationship to meHg was marginally significant. The resulting correlation matrix is shown in Table 9.7.

Table 9.7. Spearman correlation matrix between atmospheric Hg deposition estimates, and in-lake Hg measures.

	Statistic	Epilimnetic Hg	Epilimnetic meHg	Zooplankton Hg	Yellow perch – prey sized	Yellow perch – age 4.6 yr fish
Total Hg deposition	R	-0.207	0.075	0.060	0.080	0.125
	p-value	0.195	0.641	0.763	0.628	0.437
Wet Hg deposition	R	0.167	0.280	-0.182	0.423	0.240
	p-value	0.298	0.076	0.353	0.007	0.130
Litterfall Hg deposition	R	-0.253	0.075	0.015	0.042	0.132
	p-value	0.111	0.641	0.939	0.798	0.410
Particulate Hg deposition	R	0.249	0.057	-0.064	-0.019	0.166
	p-value	0.116	0.722	0.748	0.910	0.300
Reactive gaseous Hg exchange	R	-0.255	0.000	0.128	-0.097	0.005
	p-value	0.108	0.999	0.516	0.558	0.974

10.0 Data Archive

All data collected in conjunction with this project are presently archived in a dedicated Microsoft Access© database. This database is housed on the VTDEC information systems network, on the 'Jupiter' data server. Information and data housed in 'Jupiter' are backed up daily to tape media, with archival backup tapes stored off-site. Backup tapes are maintained for two years prior to present. The specific 'REMAP' database housing the project data is relational and has several levels of built-in validity checking. Core data tables stored in the database include site and sample tables, tables for water, sediment, and plankton and piscivore collections, and results of the same. Paleolimnology data results are also housed in this database. The structures and field names for the core tables within the REMAP database are shown by Figure 10.0.

In addition to archiving on the VTDEC server, all project data have been delivered to the USEPA Environmental Effects Research Laboratory in Narragansett, R.I., where they have been archived to a larger regional database addressing Hg contamination at multiple trophic levels.

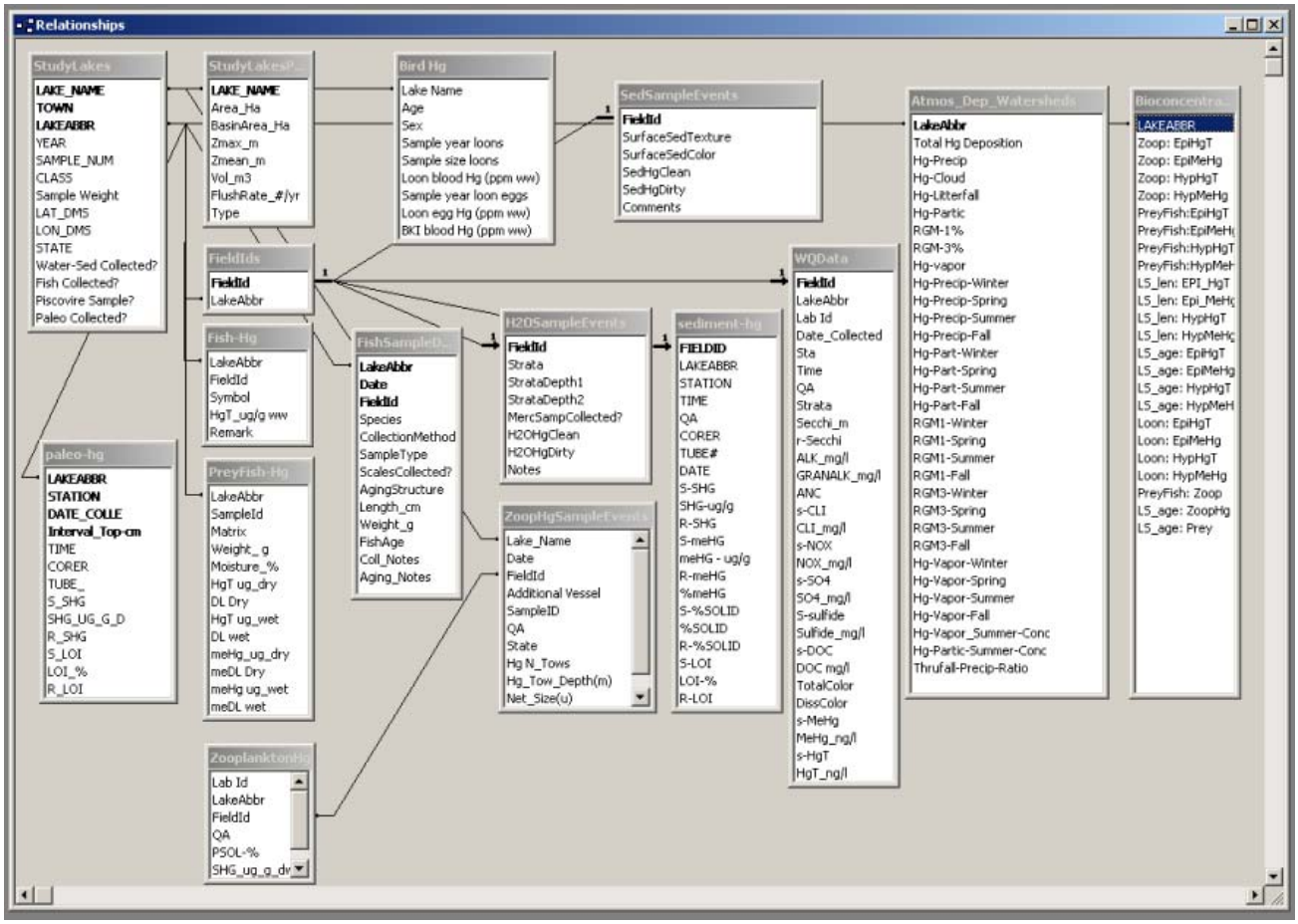

Figure 10.0. Data tables and structure for all information collected in conjunction with the Assessment of Hg in Waters, Sediments, and Biota of VT and NH Lakes Project.

11.0 References

Alter, L. 2000. Mercury Deposition and Atmospheric Concentrations in New England: Year 1 Data and Quality Assurance Report to Ray Thompson, REMAP Coordinator, USEPA, New England Region. North East States for Coordinated Air Use Management, Boston, MA.

American Public Health Association. 1995. Standard Methods for the Analysis of Water and Wastewater, Ed. 19. Washington, D.C.

Black, A.P. and R.F. Christman. 1963. Characteristics of Colored Surface Waters. American Water Works Association.

Bloom, N.S. 1995. Considerations in the Analysis of Water and Fish for Mercury. *in* United States Environmental Protection Agency. 1995. Proc. National Forum on Mercury in Fish. EPA/823/R-95/002.

Branfireun, B.A., A. Heyes, and N. Roulet. 1996. The Hydrology and methylmercury dynamics of a precambrian shield headwater peatland. *Water Resources Research* **32**: 1785-1794.

Burke, J., M. Hoyer, G. Keeler, and T. Scherbatskoy (1995) Wet deposition of mercury and ambient mercury concentrations at a site in the Lake Champlain Basin. *Water Air and Soil Pollution* **80**:353-362.

Canadian Soil Information System [CANSIS] (2002) Canadian ecosdistrict climate normals 1961-1990. http://sis.agr.gc.ca/cansis/nsdb/ecostrat/climate_normals_1961-90.html Agriculture and Agrifood Canada.

Carter, J. C. Drysdale, N. Burgess, S. Beauchamp, G. Brun, and A. d'Entremont. 2001. Mercury concentrations in yellow perch (*Perca flavescens*) from 24 lakes at Kejimkujik National Park, Nova Scotia. Parks Canada Technical Reports in Ecosystem Science # 031. Halifax, Nova Scotia, CA.

Chen, C.Y., R. Stemberger, B. Klauje, J. Blum, P. Pickhardt, and C. Folt. 2000. Accumulation of heavy metals across a gradient of lakes. *Limnol. Oceanog.* **45**: 1525-1536.

Cobbett, C.S. (2000) Phytochelatins and their roles in heavy metal detoxification. *Plant Physiology* **123**:825-832.

Cobos, D.R., J.M. Baker, and E.A. Nater (2002) Conditional sampling for measuring mercury vapor fluxes. *Atmos. Environ.* **36**:4309-4321.

Dingman, S.L. 1981. Elevation: a major influence on the hydrology of New Hampshire and Vermont, USA. *Hydrological Sciences Bulletin* **26**:399-413.

Driscoll, C.T., C. Yan, C. L. Schofield, R. Munson, J. Holsapple. 1994. The Mercury Cycle and Fish in the Adirondack Lakes. *Environ. Sci. Technol.* 28:3, 136A-143A.

Electric Power Research Institute, 1996. Protocol for Estimating Historic Atmospheric Mercury Deposition. EPRI/TR-106768. Palo Alto, CA.

Evers, D.C., Kaplan, J., Meyer, M., Reaman, P., Braselton, W., Major, J.A., Burgess, N., Sheuhammer., A., 1998. Geographic trend in mercury measured in common loon feathers and blood. *Env. Tox. Chem.* **17:** 173-183.

Evers, D. C., C. DeSorbo, and L. Savoy. 2000. Assessing the impacts of methylmercury on piscivorous wildlife as indicated by the Common Loon, 1998-99. Maine Dept. Environ. Protection, Augusta, Maine.

Evers, D.C.. 2003 in prep. Development of a wildlife criterion value to protect against methylmercury exposure to piscivorous wildlife in Maine. Maine Dept. Environ. Protection, Augusta, Maine.

Gilmour, C. C. and G. Reidel. 2000. A survey of size-specific mercury concentrations in game fish from Maryland fresh and estuarine waters. *Arch. Environ. Contam. Toxicol.* **39**: 53-59.

Gilmour, L.C., E. Henry, R. Mitchell. 1992. Sulfate Stimulation of Mercury Methylation on Freshwater Sediments. *Environ. Sci. Technol.* 26:11.

Grigal, D.F. (2002) Inputs and outputs of mercury from terrestrial watersheds: a review. *Environ. Reviews* **10**:1-39.

Hanson, P.J., S.E. Lindberg, T.A. Tabberer, J.G. Owens, K.-H. Kim (1995) Foliar exchange of mercury vapor: evidence for a compensation point. *Water, Air , and Soil Pollution* **80**:373-382.

Herrin, RT, R.C. Lathrop, P.R. Gorski, A.W. Andren. 1998. Hypolimnetic methylmercury and its uptake by plankton during fall destratification: A key entry point of mercury into lake food chains? *Limnol. Oceanog.* **43**: 1476-1486.

Johnson, D.W. and S.E. Lindberg (1995) The biogeochemical cycling of Hg in forests: alternative methods for quantifying total deposition and soil emission. *Wat. Air Soil Poll.* **80**:1069-1077.

Kamman, N.C. and D. R. Engstron. 2002. Fluxes of Mercury to Vermont and New Hampshire Lakes Inferred from ^{210}Pb-dates Sediment Cores. *Atmos. Environ.* **36**: 1599-1609

Kuehl, R.O. 2000. Design of experiments: statistical principles of research design and analysis. Duxbury Press. Pacific Grove, CA, USA.

Landis M.S., R.K. Stevens, F. Schaedlich, and E.M. Prestbo (2002) Development and characterization of an annular denuder methodology for the measurement of divalent inorganic reactive gaseous mercury in ambient air. *Environ. Sci. Technol.* **36**: 3000-3009.

Lawson, S.T. (1999) Cloud Water Chemistry and Mercury Deposition in a High Elevation Spruce-Fir Forest. M.S. Thesis. Univ. of Vermont School of Natural Resources, Burlington, VT 05405. 105 p.

Lee, Y., and A. Iverfeldt. 1991. Measurement of Methylmercury and Mercury in Run-off, Lake, and Rain Waters. *Wat. Air. Soil Poll.* **56**: 309-321.

Liang, L. 1996. Chemist, Brooks Rand LTD. Seattle, WA. Personal communication.

Lin, C.-J. and S. O. Pehkonen (1999) The chemistry of atmospheric mercury: a review. *Atmos. Environ.* **33**: 2067-2079.

Lindberg, S.E. and T.P. Meyers (2001) Development of an automated micrometeorological method for measuring the emission of mercury vapor from wetland vegetation. *Wetlands Ecol. and Manage.* **9**:333-347.

Lindberg, S.E. and W.J. Stratton (1998) Atmospheric mercury speciation: concentrations and behavior of gaseous mercury in ambient air. *Environ. Sci. Technol.* **32**: 49-57.

Lindberg, S.E., P. J. Hansen, T.P. Meyers, and K.-H. Kim. 1998. Air/Surface Exchange of Mercury over Forests – the need for a Reassessment of Continental Biogenic Emissions. *Atmos. Environ.* **32**:895-908.

Lindberg, S.E., T.P. Meyers, G.E. Taylor, R.R. Turner, and W.H. Schroeder. 1992. Atmosphere-Surface Exchange of Mercury in a Forest: Results of Modeling and Gradient Approaches. *J. Geophys. Res.* **97**:2519-2528.

Lindberg, S.E., W. Dong, and T. Meyers (in press) Transpiration of gaseous elemental mercury through vegetation in a subtropical wetland in Florida. *Atmos. Environ.*

Lorey, P. M. 2002. The determination of trace levels of mercury in environmental samples in the northeastern U.S. Inferring the past, present, and future of atmospheric mercury deposition. Unpublished PhD dissertation. Syracuse University, Department of Civil, Environmental and Chemical Engineering. Syracuse, N.Y.

Maine Department of Environmental Protection. 1995. Fish tissue contamination in Maine lakes, data report. Regional environmental monitoring and assessment program (REMAP). Augusta, Maine, USA.

Malcolm, E.G. and G.J. Keeler (2002) Measurements of mercury in dew: atmospheric removal of mercury species to a wetted surface. *Environ. Sci. Technol.* **36**: 2815-2821.

Mason, R. P. and K. A. Sullivan. 1998. Mercury and Methylmercury Transport through an urbanized watershed. *Wat. Res.* **32**: 321-330.

Mierle, G. and R. Ingram. 1991. The Role of Humic Substances in the Mobilization of Mercury from Watersheds. *Wat. Air. Soil Poll.* **56**: 349-357.

Miller, E.K., A. J. Friedland, E.A. Arons, V.A. Mohnen, J.J. Battles, J.A. Panek, J. Kadlecek and A.H. Johnson (1993b) Atmospheric Deposition to Forests Along an Elevational Gradient at Whiteface Mountain, NY USA. *Atmos. Environ.*, **27A**: 2121-2136.

Miller, E.K. (2000) Atmospheric Deposition to Complex Landscapes: HRDM – A Strategy for Coupling Deposition Models to a High-Resolution GIS. Proceedings of the National Atmospheric Deposition Program Technical Committee Meeting, October 17-20, 2000, Saratoga Springs, New York.

Miller, E.K. and A.J. Friedland (1999) Local Climate Influences on Precipitation, Cloud Water, and Dry Deposition to an Adirondack Subalpine Forest: Insights from Observations 1986-1996. *J. Environ. Qual.* **28**:270-277.

Miller, E.K., J.A. Panek, A.J. Friedland, J. Kadlecek and V.A. Mohnen (1993a) Atmospheric deposition to a high-elevation forest at Whiteface Mountain, New York, USA. *Tellus*, **45B**, 209-227.

Morrison, M.L. 1991. Part 1: Quality Assurance Plan for the Long-term Monitoring Project, *in* Data User's Guide for the U.S. EPA Long-term Monitoring Project: Quality Assurance Plan and Data Dictionary. EPA/600/3-91/072. Corvallis, Oregon.

National Weather Service, 2002. Burlington VT Local Climatology. Internet URL http://www.erh.noaa.gov/btv/html/climo2.shtml. Last accessed 9-2002.

Oldfield, F. and P. Appleby. 1984. Empirical Testing of ^{210}Pb dating models for lake sediments, in Lake Sediments and Environmental History. Univ. of Minnesota Press. Minneapolis.

Pickhardt, P.C., C.L. Folt, C. Y. Chen, B. Klaue, and J.D. Blum. 2002 Algal blooms reduce the uptake of toxic methylmercury in freshwater food webs. *Proc. Nat. Acad. Sci.* **99**(7). 4419-4223.

Rasmussen, P.E. (1995) Temporal variation of mercury in vegetation. *Wat. Air Soil Poll.* **80**:1039-1042.

Rea, A.W., S.E. Lindberg, and G.J. Keeler (2001) Dry deposition and foliar leaching of mercury and selected trace elements in deciduous forest throughfall. *Atmos. Environ.* **35**:3453-3462.

Rea, A.W., S.E. Lindberg, T. Scherbatskoy, and G.J. Keeler (2002) Mercury accumulation in foliage over time in tow northern mixed hardwood forests. *Wat. Air Soil Poll.* **133**:49-67.

Rencher, A.C. 1995. Methods of Multivariate Analysis. J Wiley and Sons. N.Y. New York USA.

SAS Institute Inc. 2002. SAS Version 8.2a. Users Manual. Cary, N.C. USA.

Schlesinger, W.H. (1977) Carbon balance in terrestrial detritus. *Annual Rev. Ecol. and Systematics* **8**:51-81.

Shanley, J.B., T. Scherbatskoy, A. Donlon, G. Keeler. 1999. Mercury Cycling and Transport in the Lake Champlain Basin *in* Manley, T. O. and P. Manley, *eds.* Lake Champlain in Transition: From Research

Toward Restoration. American Geophysical Union Water Resources Monograph Series, Volume 14, 1999.

SPSS Science Inc. 2000. SigmaStat v. 2.03 users manual. SPSS Science Inc. Chicago, Il. USA.

Tejasen, K. 1999. Assessment of Mercury in Lake Waters in Vermont and New Hampshire. Unpublished masters thesis, Syracuse University, Department of Civil, Environmental and Chemical Engineering. Syracuse, NY, USA

Ullrich, S.M., T.W. Tanton, and S. Abdrashitova. 2001. Mercury in the aquatic environment: a review of factors affecting methylation. *Crit. Rev. Environ. Sci.* **31**: 241-293.

United States Environmental Protection Agency, 1979 (revised 1983). Chemical Analysis of Water and Wastes. EPA/600/4-79/020 Washington D.C.

United States Environmental Protection Agency, 1994. Methods for the Analysis of Metals in Water and Wastewater EPA/600/R-94/111 Washington D.C.

United States Environmental Protection Agency, 1996a. Method 1669 Sampling Ambient Water for Determination of Trace Metals at Water Quality Criteria Levels. EPA/821/R 96/011 Washington D.C.

United States Environmental Protection Agency, 1996b. Method 1631: Mercury in Water by Oxidation, Purge and Trap, and Cold Vapor Atomic Fluorescence Spectrometry EPA/821/R 96 012 Washington D.C.

United States Environmental Protection Agency, 1997. Mercury Study Report to Congress. EPA 425-R97-003. Washington D.C.

United States Environmental Protection Agency, 2001. Water Quality Criterion for the Protection of Human Health. EPA-823-F-01-001. Washington DC

United States Environmental Protection Agency, 2002. EMAP Site Selection protocols. URL: http://www.epa.gov/wed/pages/EMAPDesign/site_selection.htm

United States Environmental Protection Agency, 1998. Ambient Water Quality Criteria Derivation Methodology - Human Health, Technical Support Document. EPA/822/B-98/005. Washington, D.C.

United States Geological Survey, 1992. Multi Resolution Land Characteristics. Internet URL http://edc.usgs.gov/glis/hyper/guide/mrlc. Last accessed 9-2002. Washington D.C.

Van Hove, L.W.A, P. Heeres, and M.E. Bossen (2002) The annual variation in stomatal ammonia compensation point of rye grass (*Lolium perenne* L.) leaves in an intensively managed grassland. *Atmos. Environ.* **36**:2965-2977.

Vermont Center for Geographic Information, 1996. Land Use and Cover for VT and the Lake Champlain Basin. Internet URL http://www.vcgi.org/metadata/view_meta.cfm?metafile=landlandcover_lclu.htm. Last accessed 9-2002. Waterbury, VT USA.

Vermont Department of Environmental Conservation. 1996. 1996 Water Quality Assessment -305(b) Report. Appendix A. Lake Water Quality Assessment. Waterbury, VT. Available online at http://www.vtwaterquality.org/Planning/LakeAssessment1996.PDF.

Vermont Department of Environmental Conservation. 1992 revised 2001. Laboratory Quality Assurance Plan. Waterbury.

Vermont Department of Environmental Conservation. 1998 rev. 2000. Assessment of Hg in Lake-bed Sediments of Vermont and New Hampshire. Quality Assurance Project Plan. Waterbury, VT, USA.

White, M.A., S.W. Running and P.E. Thornton (1999) The impact of growing-season length variability on carbon assimilation and evapotranspiration over 88 years in the eastern US deciduous forest. *Int. J. Biometeorology* **42**: 139-145.

Xu, X., X. Yang, D.R. Miller, J.J. Helble, and R.J. Carley (1999) Formulation of bi-directional atmosphere-surface exchanges of elemental mercury. *Atmos. Environ.* **33**:4345-4355

Appendix A. Historical and present fluxes of mercury to Vermont and New Hampshire lakes inferred from ^{210}Pb dated sediment cores

Reprinted from *Atmos. Environ.* 36: 1599-1609. Copyright 2002.

PERGAMON

Atmospheric Environment 36 (2002) 1599–1609

ATMOSPHERIC ENVIRONMENT

www.elsevier.com/locate/atmosenv

Historical and present fluxes of mercury to Vermont and New Hampshire lakes inferred from ^{210}Pb dated sediment cores

Neil C. Kamman[a,*], Daniel R. Engstrom[b]

[a] *Vermont Department of Environmental Conservation, 103 S. Main 10N, Waterbury, VT, 05671-0408 USA*
[b] *St. Croix Watershed Research Station, Science Museum of Minnesota, Marine on St. Croix, MN, 55047 USA*

Received 22 April 2001; accepted 5 November 2001

Abstract

Lakes across the Northern Hemisphere have experienced enhanced atmospheric deposition of anthropogenically derived Hg for over 100 years. In the present study, we quantified Hg fluxes to the sediments of ten small drainage lakes across Vermont and New Hampshire, USA, for the period ~1800 to present. Dates were established by ^{210}Pb. Total Hg (HgT) fluxes to sediments ranged from 5 to 17 $\mu g\,m^{-2}\,yr^{-1}$ during pre-industrial times, and from 21 to 83 $\mu g\,m^{-2}\,yr^{-1}$ presently. Present-day HgT fluxes are between 2.1 to 6.9 times greater than pre-1850 fluxes. Current-day direct atmospheric Hg deposition to the study region was estimated at 21 $\mu g\,m^{-2}\,yr^{-1}$, which agrees well with measured HgT deposition, when re-evasion of Hg is accounted for. Our data suggest that Hg fluxes to lake sediments have declined in recent decades, owing to reductions in atmospheric Hg deposition to the lake surface. Watershed export of atmospherically deposited Hg remains elevated relative to present-day deposition rates, which contributes to the impression that Hg retention by watershed soils has declined. © 2002 Elsevier Science Ltd. All rights reserved.

Keywords: Mercury; Paleolimnology; Atmospheric deposition; Sediment; Watershed

1. Introduction

Environmental mercury (Hg) contamination of aquatic ecosystems is a pervasive environmental problem, with potentially severe toxicological consequences for humans and piscivorous wildlife (USEPA, 1997; Evers et al., 1998; National Academy of Sciences, 2000). The majority of Hg contaminating aquatic ecosystems is understood to be anthropogenically derived and atmospherically deposited (Fitzgerald et al., 1998). In poorly buffered, undisturbed lakes, Hg is transported through watersheds by high molecular weight dissolved organic matter, and the proportion of this Hg which is neither methylated nor re-evaded as Hg^0 is deposited to the sediments (Lee and Iverfeldt, 1991; Mierle and Ingram, 1991; Driscoll et al., 1994a; Hurley et al., 2000). Several studies have underscored the importance of watershed size in controlling Hg fluxes to sediments (Engstrom et al., 1994; Mielli, 1995; Lorey and Driscoll, 1999). Wetland area (Driscoll et al., 1994a; St. Louis et al., 1994), land use (Hurley et al., 2000), and pH (Rada et al., 1993) have also been shown to influence delivery of Hg to sediments.

Paleolimnological studies have been used to estimate whole-lake surficial sediment Hg burdens (Gilmour et al., 1992; Rada et al., 1993), and, when coupled with fine-resolution ^{210}Pb dating, to estimate fluxes of Hg to lake sediments for both modern and historical time frames (Ouellet and Jones, 1983; Engstrom et al., 1994; Von Gunten et al., 1997; Hermanson, 1998; Lockhart et al., 1998; Lorey and Driscoll, 1999). Numerous multiple lake-sediment studies show anthropogenic Hg contamination to be a recent phenomenon (~1850 to present), coincident with industrialization, and fossil fuel and waste combustion (Landers et al., 1998; Pirrone et al., 1998). Engstrom and Swain (1997) have shown that Hg deposition to lakes down-gradient of Midwestern urban centers is declining in response to recent reductions in

*Corresponding author. Tel.: +1-802-241-3795.
E-mail addresses: neil.kamman@state.vt.us (C. Kamman), dengstrom@smm.org (R. Engstrom).

1352-2310/02/$ - see front matter © 2002 Elsevier Science Ltd. All rights reserved.
PII: S1352-2310(02)00091-2

Hg emissions. While there exists significant uncertainty in the estimation of Hg fluxes to individual lakes (Mielli, 1995; Gottgens et al., 1999), the pattern evident in so many paleolimnological Hg studies is clear: anthropogenically derived Hg has increased by a factor of 2–8 × in the sediments of lakes throughout the Northern Hemisphere (Landers et al., 1998).

In the present study, we analyzed a series of single, short-cores taken from undisturbed lakes in Northern New England, to evaluate four specific hypotheses: (1) that Hg fluxes have increased proportionally to increases observed in other studies; (2) that Hg fluxes have decreased in recent years; (3) that Hg fluxes increase with increasing watershed area to lake area ratio; and, (4) that paleolimnologically inferred atmospheric total Hg deposition estimates compare well with measured total wet + dry Hg deposition.

2. Methods

2.1. Site characteristics

The lakes selected for this study lie within the borders of Vermont and New Hampshire, and are characteristic of undisturbed lakes within the Northeastern Highlands Ecoregion (Omernik, 1987; USEPA, 2000). All are small, 8.1–38.9 hectare drainage lakes occupying undisturbed forested catchments, which are a mix of deciduous or coniferous vegetation overlying soils ranging from stony to silty loams. Bedrock geology is largely schistose or granitic, and most watersheds are poorly buffered. Some shales and slates are in evidence near High Pond in Vermont, and the buffering capacity of this watershed is enhanced accordingly. These watersheds have experienced varying degrees of deforestation during settlement, but have regrown to forest in the past 75–150 years. Limnological attributes of the study lakes are provided in Table 1, and their location across the study region is shown in Fig. 1.

2.2. Field techniques

Sixty cm by six cm diameter lexan coring tubes were prepared for sampling by cleaning in a commercial laboratory dishwasher with Alcanox®, followed by soaking in 10% HNO_3, copious rinsing with ASTM Type-II deionized water, and air drying in a metal-free hood. In the field, two sediment cores were acquired from the lake's deep hole using a Glew-design gravity corer (Glew, 1989). The core reflecting the least disturbed stratigraphy and most distinct sediment-water interface was selected for sectioning immediately in the field, which minimized disturbance. Subsamples were extruded at 1-cm intervals to the core bottom, and split, with one half used for Hg analysis, and the other for

Table 1
Location and limnological attributes of 10 Vermont and New Hampshire lakes used to estimate current and historical mercury deposition

Lake	Lat. DDMMSS	Long. DDMMSS	Lake area (Ha)	Basin area (Ha)	Max. depth (m)	Mean depth (m)	Volume (m^3)	Flushing rate (#/yr)	Alkalinity (meq)
Dudley	430730	715030	12.1	673.4	6.1	3.7	444,183	7.8	121.0
Gilman	433030	711200	13.0	255.4	5.2	2.1	276,380	5.0	146.0
High	434510	730914	8.1	70.0	16.0	7.9	641,598	0.5	1,195.0
Intervale	434730	713130	17.4	466.2	14.9	7.0	1,220,269	1.9	94.0
McConnell	444904	714806	35.2	1465.4	5.5	2.3	809,805	17.3	160.0
Sessions	444220	711150	14.2	207.2	10.3	4.9	690,951	1.5	124.0
Spring	432942	725512	26.7	111.3	24.0	10.7	2,850,174	0.7	737.0
Wallingford	432341	725432	35.2	594.9	7.0	2.1	749,950	20.2	114.0
Wheeler	444230	713829	26.7	1683.1	10.0	4.0	1,055,053	42.3	150.4
Willard	430130	720130	38.9	414.4	17.7	8.0	3,137,500	0.8	31.6

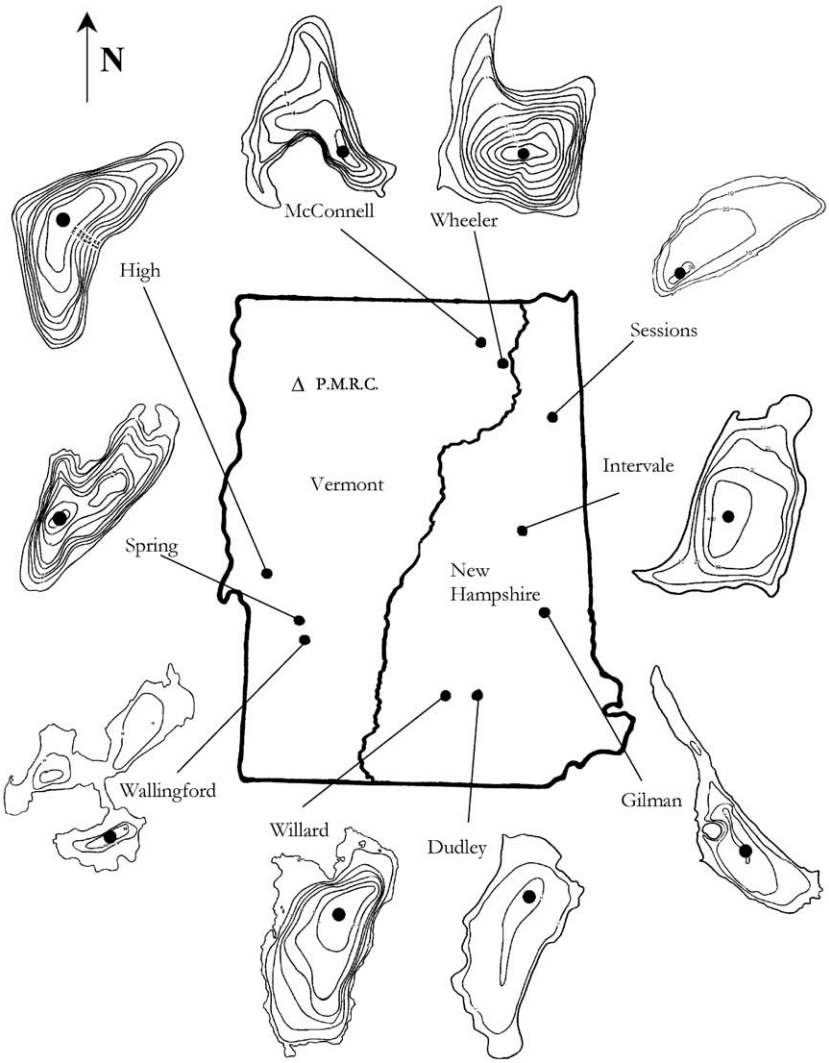

Fig. 1. Geographic location and bathymetry of ten Vermont and New Hampshire lakes used to estimate current and historical mercury deposition. Coring locations are indicated by (●). Map scales differ, and acreages are shown in Table 1. Proctor Maple Research Center (PMRC), an atmospheric monitoring station located in Underhill, VT, is also shown.

^{210}Pb determinations. Mercury-clean sampling procedures (USEPA, 1996) were used throughout the sampling and subsequent sample handling procedures. Sediment aliquots for Hg determinations were stored wet in pre-cleaned, lot-certified 250 ml PETE Nalgene® round vessels, individually bagged in zip-style PETE bags. Sampling was performed during the summer and fall of 1998.

2.3. Sample processing and analysis procedures

2.3.1. ^{210}Pb dating

Sediment cores were analyzed for ^{210}Pb activity to determine age and sediment accumulation rates for the past 150–200 years. Lead-210 was measured at 17–22 depth intervals in each core through its grand-daughter product ^{210}Po, with ^{209}Po added as an internal yield tracer. The polonium isotopes were distilled from 0.3–2.8 g dry sediment at 550°C following pretreatment with concentrated HCl and plated directly onto silver planchets from a 0.5 N HCl solution (Eakins and Morrison, 1978). Activity was measured for $1–8 \times 10^5$ s with ion-implanted or Si-depleted surface barrier detectors and an EG&G Nuclear alpha spectroscopy system. Unsupported ^{210}Pb was calculated by subtracting supported activity from the total activity measured at each level; supported ^{210}Pb was estimated from the asymptotic activity at depth (the mean of the lowermost

samples in a core). Supported ^{210}Pb values for Spring Lake were confirmed by gamma spectrometry on an EG&G Nuclear ultra-low background well-detector. Dates and sedimentation rates were determined according to the constant rate of supply model (OldField and Appleby, 1984) with confidence intervals calculated by first-order error analysis of counting uncertainty (Binford, 1990). All dating analyses were performed at the Science Museum of Minnesota's St. Croix Watershed Research Station.

2.3.2. Mercury in sediment

A small aliquot of homogenized wet sediment was extracted for percent solids determination (APHA, 1999, method 2540B). The remaining sediment was dried at 60°C, a 0.5 g portion of which was then digested in 5 ml aqua-regia for 2 min at 95°C, and brought to 55 ml with ASTM Type-II deionized water. Hg in the sample was converted to Hg^{2+} by oxidation with 15 ml $KMnO_4$, and further brought to 110 ml. This aliquot was mixed with $SnCl_2$ to reduce Hg^{2+} to Hg^0, which was carried by Ar into a Leeman® automated cold vapor atomic absorption spectrometer (USEPA, 1994, method 245.1 and 245.5). Following initial calibration, standards were run before and after all sample runs, and every tenth sample during the run, as were reagent blanks and matrix spikes. Individual samples were run in duplicate. Standard reference material (SRM, Standard Soil CRM008-050, Resource Technology Corp., Laramie, WY, USA) was analyzed to ensure the completeness of the digestion process. The method detection limit for sediment HgT was $0.05\,\mu g\,g^{-1}$. The analytical accuracy of the mercury data, estimated as relative percent difference between duplicates, was $\pm 1.7\%$. Analytical precision, estimated as the mean percent recovery for matrix spikes, was 97.4%. The average residual concentration of SRM relative to their certified values was $+0.01\,\mu g\,g^{-1}$, representing a mean relative difference of 3.4%. These analyses were performed at the Vermont Department of Environmental Conservation's (VTDEC) LaRosa Environmental Laboratory.

2.3.3. Other parameters

Long-term mean alkalinity values (Table 1) were calculated from available data within the VTDEC Lake Inventory Database and the New Hampshire Department of Environmental Services Lake Trophic Status Database. Original samples were analyzed following standard methods (APHA, 1999). Long-term atmospheric Hg deposition values were measured at the Proctor Maple Research Center (PMRC), in Underhill, VT (Fig. 1), and taken from Scherbatskoy et al. (1999) and Shanley et al. (1999).

2.3.4. Calculations

Fluxes of total Hg to lakes were calculated as the product of the ^{210}Pb-derived sedimentation rates and dry-weight total Hg concentrations, for each core interval, and these are assumed to represent net sedimentation of Hg to the individual lake sediment focal centers. Background fluxes were estimated as the average of pre-1850 fluxes. Linear regressions estimating the relationship between time-averaged Hg fluxes and the ratio of watershed:lake area were calculated using SAS PROC REG. Watershed retention of atmospherically deposited Hg was calculated as the ratio of the regression slope to the regression $y-$intercept (Engstrom et al., 1994). The variance of this ratio was based on the following algorithm (Mickey, 2001):

$$\mathrm{var}(b/a) = b^2/a^2\{[\mathrm{var}(b)/b^2] - [2\,\mathrm{cov}(a,b)/ab] - [\mathrm{var}(a)/a^2]\},$$

where a is the regression $y-$intercept, for the independent variable value 0; and, b is the regression slope.

3. Results and discussion

3.1. ^{210}Pb dating and sedimentation rates

For all ten lakes, supported ^{210}Pb concentrations ranged from 0.28 to $2.5\,pCi\,g^{-1}$, and the number of deeper core intervals from which supported ^{210}Pb was estimated ranged from one (McConnell Pond) to six (Intervale Pond). Inventories of unsupported ^{210}Pb in the ten cores ranged from 6.77 to $22.02\,pCi\,cm^{-2}$, which is equivalent to ^{210}Pb fluxes of 0.22–0.71 $pCi\,cm^{-2}\,yr^{-1}$ (Fig. 2 and Table 2). These ^{210}Pb fluxes are similar to regional estimates of atmospheric ^{210}Pb deposition ($0.5\,pCi\,cm^{-2}\,yr^{-1}$), which implies that core-specific sedimentation rates are not appreciably amplified by sediment focusing. The underlying assumption for this conclusion is that direct atmospheric deposition dominates the ^{210}Pb budgets of these lakes (i.e., little watershed contribution) (Oldfield and Appleby, 1984). Dates corresponding to the bottom-most unsupported ^{210}Pb strata ranged from 1787 (Wallingford Pond), to 1861 (Spring Lake), with a lake set-wide average value of 1825 (S.D. = 21 yr). Sedimentation rates for strata below the supported ^{210}Pb horizon were extrapolated using averaged baseline sedimentation rates.

Sedimentation rate profiles (Fig. 3) are variable in nature. For Dudley, Intervale, McConnell, Wallingford, and Wheeler Ponds, sedimentation rates increase with time, with maximum values near or at the core tops, indicating possible recent disturbances in these ponds' watersheds. High and Willard Ponds display mid-core peak sedimentation, while Sessions Pond shows two distinct sedimentation peaks at ~1900 and 1970. Spring

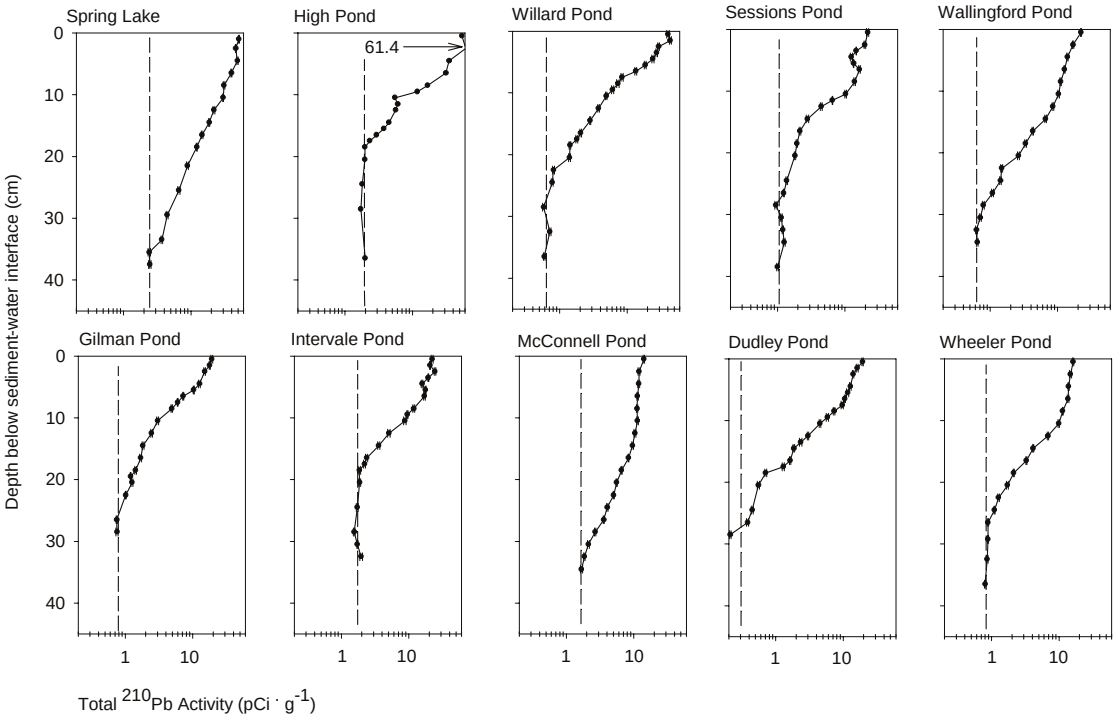

Fig. 2. Total ^{210}Pb, by depth downcore, for sediments of 10 Vermont and New Hampshire lakes.

Table 2
Supported and unsupported ^{210}Pb concentrations, densities, and fluxes, for 10 Vermont and New Hampshire lakes

	Supported ^{210}Pb, pCi g^{-1} (S.E.)	*N* supported samples	Cumulative unsupported ^{210}Pb, (pCi cm^{-2})	Unsupported ^{210}Pb flux, (pCi cm^{-2} yr^{-1})
Dudley	0.28 (0.07)	3	11.08	0.36
Gilman	0.75 (0.01)	2	6.77	0.22
High	1.88 (0.06)	5	14.73	0.47
Intervale	1.74 (0.06)	6	12.49	0.40
McConnell	1.68 (0.06)	1	11.32	0.36
Sessions	1.09 (0.06)	5	10.63	0.35
Spring	2.50 (0.05)	4	22.02	0.71
Wallingford	0.64 (0.02)	2	12.34	0.40
Wheeler	0.64 (0.05)	4	10.54	0.34
Willard	0.85 (0.02)	4	12.60	0.41

Lake and Gilman Pond have low, nearly flat sedimentation profiles over the period of record. Standard errors for baseline sedimentation rates for Sessions and Dudley Ponds are large.

3.2. Hg concentrations and Hg fluxes

Total Hg concentrations ranged from 0.06 to 0.66 μg g^{-1} (d.w.), with peak concentrations in all cases coinciding with dates of 1950 or later. Profiles of Hg concentrations in sediment reveal striking similarities (Fig. 3). For all lakes, baseline Hg concentrations of 0.06–0.21 μg g^{-1} d.w. begin to rise circa 1875, and peak between 1950 and modern times, at between 0.22 and 0.66 μg g^{-1} d.w. Most of the lakes show a decline in sediment Hg concentrations in the most recent sediments. These declines are most pronounced in Spring Lake, and High and Willard Ponds.

Mercury concentration profiles are strongly influenced by sedimentation rate, in that concentrations of elemental constituents are accentuated under periods of reduced sedimentation, and vice versa (Engstrom and Wright, 1983). Flux rates normalize this covariance, and permit comparisons across lakes. Examination of

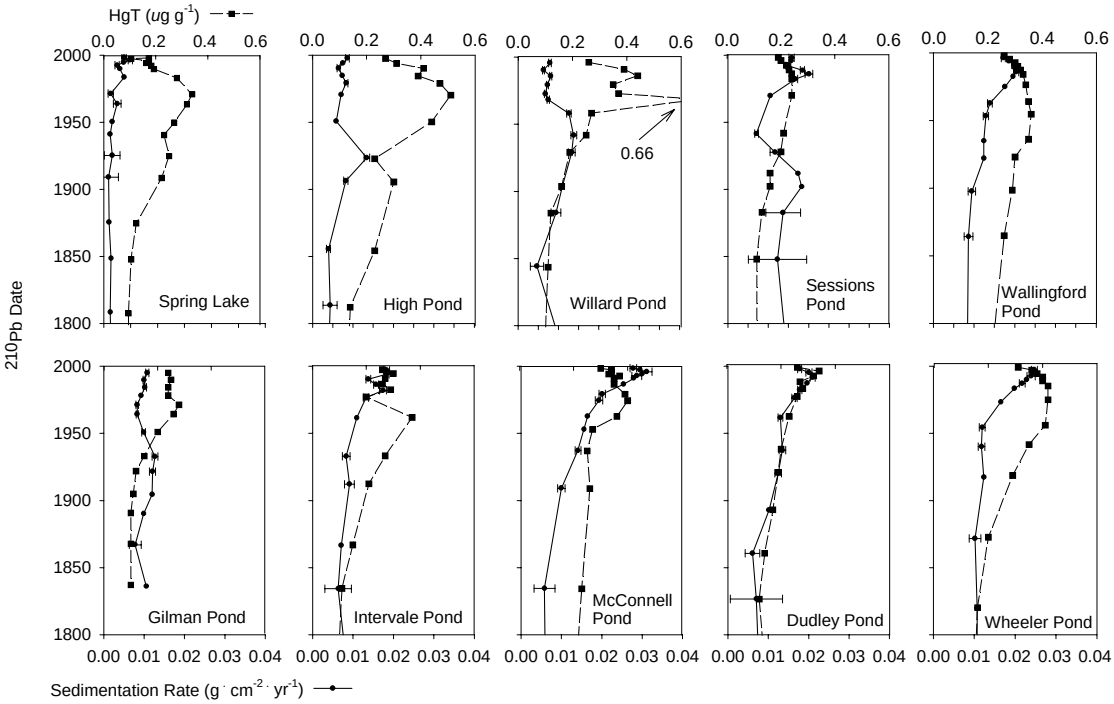

Fig. 3. Total Hg concentrations and sedimentation rates (estimated using the constant rate of supply dating model), by ^{210}Pb inferred date, for sediment cores from 10 Vermont and New Hampshire lakes. Error bars about sedimentation rates represent standard errors propagated from counting uncertainty. Rates estimated from baseline supported ^{210}Pb are shown only to the year 1800. Lakes are arrayed in order of increasing watershed:lake area.

Table 3
Total Hg fluxes, in $\mu g\,m^{-2}\,yr^{-1}$, for baseline, peak, and modern time periods, for 10 Vermont and New Hampshire lakes

	Modern (1998) Hg flux $\mu g\,m^{-2}\,yr^{-1}$	Peak flux (year of occurrence) $\mu g\,m^{-2}\,yr^{-1}$	Baseline flux (years used to estimate) $\mu g\,m^{-2}\,yr^{-1}$	Ratio of modern to baseline
Dudley	46	68 (1992)	10 (1777–1860)	4.6
Gilman	26	26 (1998)	11 (1863)	2.4
High	23	39 (1979)	5 (1693–1813)	4.6
Intervale	48	55 (1995)	7 (1626–1834)	6.9
McConnell	83	106 (1992)	13 (1777–1834)	6.4
Sessions	30	48 (1985)	14 (1766–1848)	2.1
Spring	25	41 (1963)	11(1755–1808)	2.3
Wallingford	45	66 (1987)	17 (1731–1787)	2.6
Wheeler	78	92 (1990)	16 (1715–1819)	4.9
Willard	21	50 (1968)	10 (1704–1844)	2.1
Average	42.5	52.9	11.4	3.9

baseline (pre-1850), peak, and modern (1998) fluxes (Table 3) and flux profiles (Fig. 4) reveals striking similarities. For all lakes, there was an increase in Hg fluxes, beginning by 1875. The greatest post-industrial Hg flux enhancement was observed in McConnell Pond, and the smallest, at Gilman Pond. Averaged pre-1850 Hg flux rates ranged from 5 to 17 $\mu g\,m^{-2}\,yr^{-1}$. Peak fluxes, which occurred between 1963 and modern times, varied from 26 to 106 $\mu g\,m^{-2}\,yr^{-1}$. Modern flux ratios (the ratio of modern:baseline flux) ranged from 2.1 to 6.9 (Table 3). Seven lakes displayed a continual decline in Hg flux, across four or more of the most recent core sections. This pattern has been interpreted by Engstrom and Swain (1997) as indicating a significant decline in

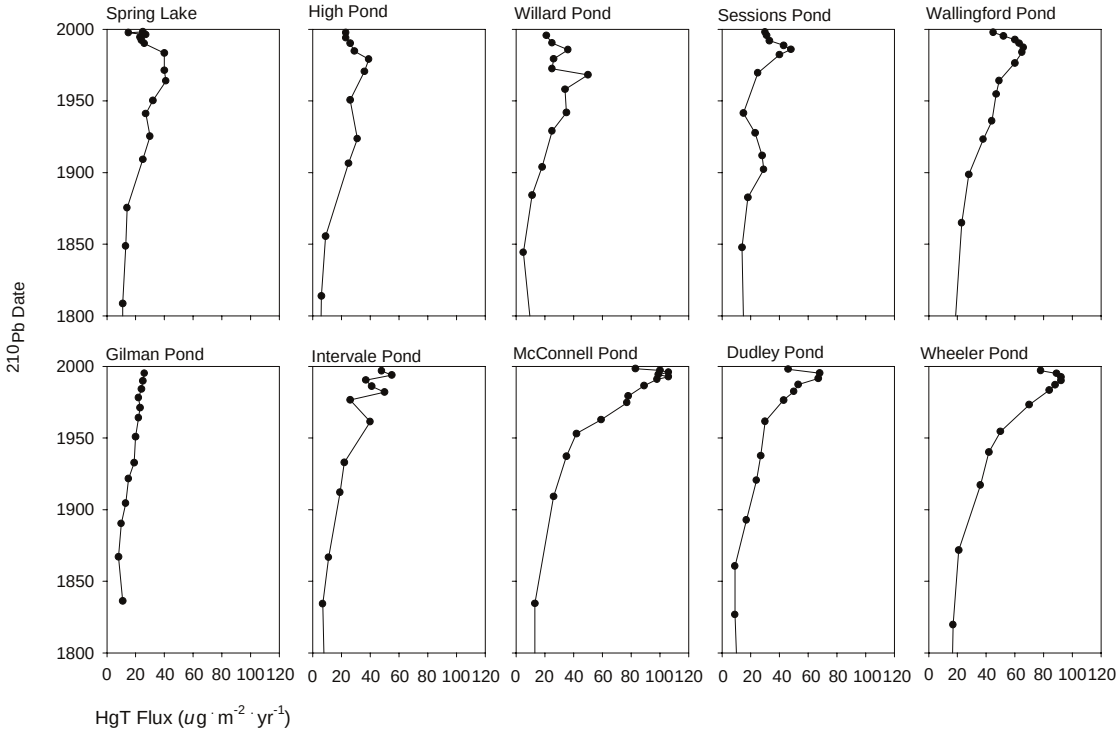

Fig. 4. Total Hg fluxes, by ^{210}Pb inferred date, to the sediments of 10 Vermont and New Hampshire lakes. Lakes are arrayed in order of increasing watershed:lake area.

atmospheric Hg loadings to several Minneapolis area lakes. Their argument that reductions in atmospheric Hg emissions from coal combustion, waste incineration, and industrial sources are responsible for reduced Hg fluxes may also apply to the present study lakes.

Our Hg fluxes and flux ratios are in excellent agreement with those reported for lakes in Northern Quebec (Lucotte et al., 1995), and the upper Midwest (Engstrom and Swain, 1997), for eight ponds and an ombrotrophic bog in Maine (Norton et al., 1997; Perry et al., 2001), for lakes in Finland, Sweden, and Western Canada (as compiled by Landers et al., 1998), and for Adirondack drainage and seepage lakes (Lorey and Driscoll, 1999). The average flux ratio (ratio of modern:baseline) for the entire lake set of 3.9 suggests that lakes across Vermont and New Hampshire have experienced a nearly four-fold increase in Hg fluxes since before 1850.

3.3. Inferring Hg fluxes attributable to atmospheric loading

Across a set of lakes, the relationship between the ratio of watershed:lake area and Hg flux can be used to estimate the proportion of the flux attributable to direct atmospheric contributions for any given time period (Swain et al., 1992). By this elegantly simple technique, an estimated linear function between the watershed:lake area ratio and Hg flux is backcast to a watershed:lake area ratio of one, with the corresponding flux providing an estimate of the direct atmospheric component. This assumes that evasion of Hg from lake surfaces is minimal and consistent across lakes, and that, across watersheds, a consistent proportion of the Hg transported from upstream is retained within the lake sediments. While evasion of Hg from lake surfaces has not completely been studied, the former assumption appears validated by Fitzgerald et al. (1991), who estimated that evasion accounted for no more than 10% of the Hg flux from Little Rock Lake, Wisconsin. The latter assumption is supported by Hurley et al. (2000), and Shanley et al. (2001), who have shown that the export of particulate-bound Hg varies consistently in relation to watershed DOC and sediment export, across multiple watershed scales in the upper Midwest and Northeast, respectively. However, Driscoll et al. (2001) indicate that this may not be the case for dissolved Hg moving through Adirondack systems. Thus, sediment Hg flux estimates derived by this study most accurately reflects sedimentation of particulate-bound Hg.

Fig. 5a shows linear regression models for averaged pre-1850 and modern (1998) times, across our study

lakes. Prior to 1850, there exists no significant relationship between watershed-lake area ratio and Hg flux. By contrast, for 1998, the relationship is highly significant ($F = 14.97$, $p = 0.0047$), with the variation in watershed:lake area explaining 65% of the variation in Hg flux. The estimated Hg flux attributable to direct atmospheric contributions for the pre-1850 period is $10\,\mu g\,m^{-2}\,yr^{-1}$ (S.E. = 2.0, $p = 0.001$ for Ho: atmospheric flux = 0) while the estimate for 1998 is $21\,\mu g\,m^{-2}\,yr^{-1}$ (S.E. = 7.5, $p = 0.032$ for Ho: atmospheric flux = 0). Modern atmospheric fluxes compare reasonably well to direct measurements made at a relatively high elevation Vermont site by Scherbatskoy et al. (1999). Shanley et al. (1999) used these data to estimate average annual terrestrial atmospheric fluxes of 46.3, $37.0\,\mu g\,m^{-2}\,yr^{-1}$ of which are thought to be deposited dry. These authors acknowledge that the proportion of dry-deposited Hg which is re-evaded as Hg^0 both from terrestrial and lakewater surfaces is presently unknown. Thus, our estimated modern atmospheric flux estimate of $21\,\mu g\,m^{-2}\,yr^{-1}$ is within the range of likely values for wet + dry total Hg, minus that Hg which is re-evaded from the lake surface.

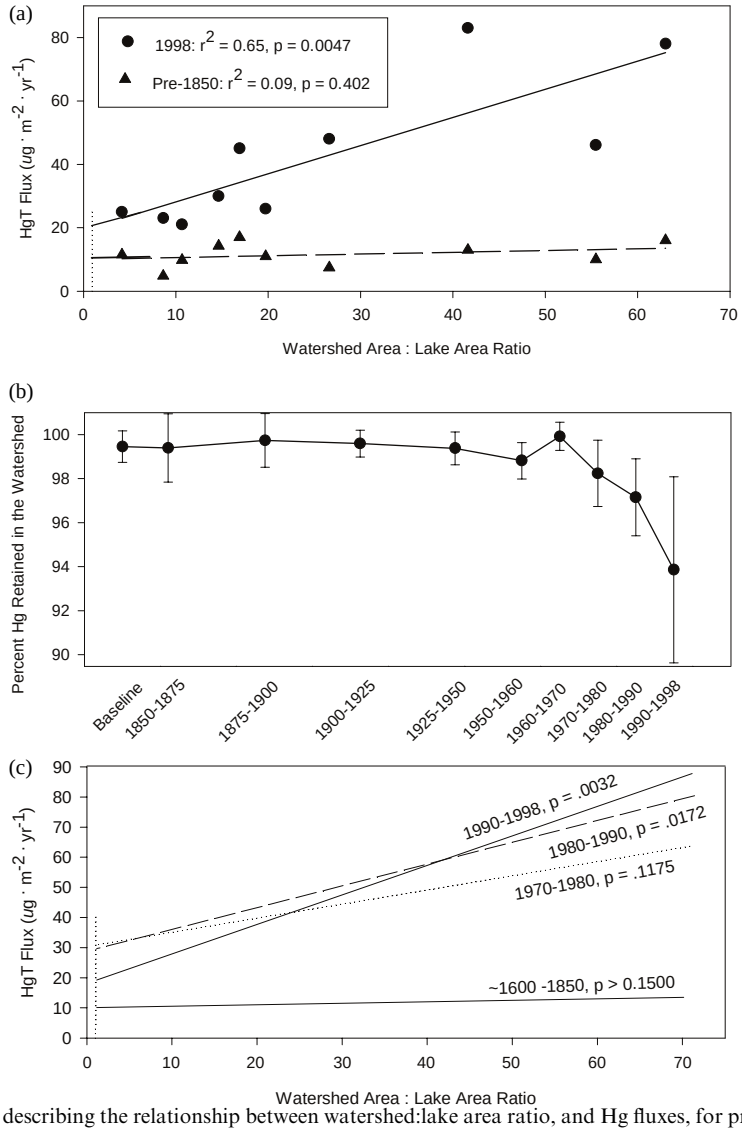

Fig. 5. (a) Linear models describing the relationship between watershed:lake area ratio, and Hg fluxes, for pre-1850 and modern (1998) time periods, for 10 Vermont and New Hampshire lakes. (b) Percent of atmospherically deposited Hg retained in these watersheds, from pre-1850 to present. (c) Linear models for the baseline period, 1970–1980, 1980–1990, and 1990–1998. Regressions are backcast to a ratio of 1:1 (shown by the dotted line), which represents the flux attributable to direct atmospheric deposition. Bars represent the standard error of the watershed retention estimates.

3.4. The role of watershed:lake area ratios in the control of Hg fluxes to lakes

Models of watershed:lake area in relation to decade-averaged fluxes from 1950 to present produce intriguing, although statistically less satisfying results. In these lakes, the relationships between watershed:lake area and Hg flux are non-significant ($p > 0.05$ for Ho: $b = 0$) except for the periods 1980–1990, and 1990–1998. During these periods, 1.2 and 0.86 $\mu g\,Hg\,m^{-2}\,yr^{-1}$ were delivered for each unit of watershed:lake area respectively; rates which are lower than the 3.27 and 1.93 $\mu g\,m^{-2}\,yr^{-1}$ reported by Engstrom et al. (1994) and Lorey and Driscoll (1999) in the Midwestern and Adirondack lakes. Thus, even though average fluxes for the 1950s and subsequent decades are significantly elevated over pre-1850 levels ($F = 4.13$, $p < 0.02$), the influence of watershed size in controlling Hg flux to this study set only becomes clear in recent years.

Viewed from the perspective of Hg retained in the watersheds (Fig. 5b), our results appear to suggest that watershed retention of atmospherically deposited Hg has declined progressively from the 1950s to the present. In reality, this trend is more likely a function of declining atmospheric Hg deposition to lake surfaces than an actual increase in export of Hg from watershed soils. A decrease in atmospheric Hg deposition should be reflected most immediately in the sediments of lakes with very small watersheds, while lakes with relatively large watersheds should continue to receive large Hg inputs (relative to direct Hg deposition to the lake surface), owing simply to a greater quantity of runoff from soils that have become saturated with anthropogenic Hg. The effect of this lag between declines in direct Hg deposition and watershed delivery is that watershed Hg loading as a percent of direct atmospheric deposition will increase, especially for lakes with large watershed:lake area ratios. This point was first proposed by Mielli (1995), and is well illustrated by the linear functions describing the relationship of Hg flux to watershed:lake area for each of the last three decades (Fig. 5c). These linear models suggest that the atmospheric component of Hg fluxes derived from larger watersheds continues to increase, even as the overall atmospheric deposition rate (e.g. model prediction at a watershed:lake area ratio of 1) appears to be declining.

Our estimate of 93.8% atmospheric Hg retention in the watersheds of the study lakes is significantly elevated over the 78% reported by both Engstrom et al. (1994) and Lorey and Driscoll (1999) for their Midwestern and Adirondack study lakes. The cause of this difference may relate either to the biogeochemistry of the watersheds, or to physical factors. Driscoll et al. (1994a, b, 1998) indicate that Hg delivery through watersheds is controlled by a variety of factors, including DOC, pH, alkalinity, and the proportion of wetlands in the watershed. Other influential factors include bedrock geology (Coker et al., 1995) and land use (Hurley et al., 2000). Alkalinity, taken here as a general indicator of DOC and pH in the watersheds, varies significantly between our study lakes, and the Adirondack and Midwestern ones ($F = 6.89$, $p = 0.005$), with log-adjusted alkalinity values significantly lower in the Adirondack lakes. However, there is no significant relationship between the estimated modern atmospheric Hg retained in the watersheds, and alkalinity ($p \geqslant 0.05$, $n = 3$). The geology underlying the lakes of all three lake sets, while varied, does not differ strongly, except by the presence of two highly alkaline Minnesota lakes cored by Engstrom et al. (1994). Land cover in the watersheds of all three study lake sets is predominantly forested, however, only the Adirondack lake set may have escaped the influence of deforestation in the past 150 years. No data are available regarding wetlands for either the Adirondack or Midwestern study lakes. Thus, given the available information, variation in watershed chemistry, bedrock geology, or land use cannot alone explain the high atmospheric Hg retention observed in these Vermont and New Hampshire lakes.

Morphologically, however, the study lakes are different. Watershed:lake area ratios vary significantly among these three studies ($F = 7.098$, $p = 0.004$). The present study lakes have significantly larger watershed ratios than the Midwestern sites ($p < 0.05$), which are predominantly seepage lakes. Watershed ratios for the Adirondack sites are intermediate in size, and the lakes are mixed drainage and seepage. Therefore, the larger watershed:lake area ratios in this study may explain why these Vermont and New Hampshire lakes display higher Hg retention than do the Adirondack and Midwestern study lakes. Our estimate of 93.8% Hg retained in the watersheds is in good agreement with mass-balance estimates of 92% to 94% provided by Scherbatskoy et al. (1998) for a small forested watershed adjacent to the PMRC.

4. Summary

Estimated Hg fluxes across the 10 lakes sampled in this study provide three distinct signals. First, there exists a synchronous increase in Hg fluxes across all lakes corresponding to the period 1850–1875, and Hg fluxes peak between 1955 and the present. Peak Hg fluxes are on average 3.9 times greater than average pre-1850 values, which is attributable to increased atmospheric deposition of Hg over the core record. Second, the relationship between the watershed:lake area ratio and Hg flux has become increasingly important in the past 30 years, and the modern direct atmospheric estimate of 21 $\mu g\,m^{-2}\,yr^{-1}$ is in reasonable agreement with measured atmospheric fluxes. Finally, watershed

retention of atmospherically deposited Hg, estimated at 93.8%, is elevated relative to Adirondack and Midwestern lakes, but is in good agreement with mass-balance measurements made near PMRC. A great deal of effort is presently being accorded to reduction and virtual elimination of Hg. Indeed, burning of cleaner coal and reductions in other industrial emissions may have resulted in the reduced Hg fluxes observed in this dataset in recent times. However, high watershed Hg retention, coupled with a continually increasing influence of watershed size in the downstream delivery of Hg, indicate that a significant time lag can be expected between implementation of Hg use and emission controls, and significant reductions in Hg accumulation to lake sediments. Quantification of this lag may be possible given the number of paleolimnological datasets presently available across North America, and represents a fruitful area for further analysis and inquiry.

Acknowledgements

We thank Steve Couture, Bob Estabrook, and Steve Landry of the NH Department of Environmental Services for their project support; Ed Glassford, Kate Peyerl, and Kellie Merrell of the VT Department of Environmental Conservation, for analytical chemistry, coordinating both field sampling and lab processing, and for figure preparation; Kelly Thommes of the St. Croix Watershed Research Station for assistance in the ^{210}Pb dating; and, Dr. Ruth Mickey of the University of Vermont for assistance with statistics and Dr Mary C. Watzin, also of UVM, for her thoughtful manuscript review. We gratefully acknowledge Rochelle Araujo, Ray Thompson, and Alan VanArsdale of USEPA for their continued interest and support of this research. Finally, we thank our anonymous reviewer for informative comments to earlier manuscript drafts. This project was funded largely by USEPA, under cooperative agreement CR-82549501, and the results of this research do not necessarily reflect the views of USEPA.

References

APHA, 1999. Standard Methods for the Examination of Water and Wastewater. 19th Edition, American Public Health Association, Washington, D.C.

Binford, M.W., 1990. Calculation and uncertainty analysis of ^{210}Pb dates for PIRLA project lake sediment cores. Journal of Paleolimnology 3, 253–267.

Coker, W.B., Kettles, I.M., Shilts, W.W., 1995. Comparison of mercury concentrations in modern lake sediments and glacial drift in the Canadian shield in the region of Ottawa/Kingston to Georgian Bay, Ont., Canada. Water, Air, and Soil Pollution 80, 1025–1029.

Driscoll, C.T., Blette, V., Yan, C., Schofield, C.L., Munson, R., Holsapple, J., 1994a. The role of dissolved organic carbon in the chemistry and bioavailability of mercury in remote Adirondack Lakes. Water, Air, and Soil Pollution 80, 499–508.

Driscoll, C.T., Yan, C., Schofield, C.L., Munson, R., Holsapple, J., 1994b. The mercury cycle and fish in the Adirondack lakes. Environmental Science and Technology 28, 136A–143A.

Driscoll, C.T., Holsapple, J., Schofield, C.L., Munson, R., 1998. The chemistry and transport of mercury in a small wetland in the Adirondack Region of New York, USA. Biogeochemistry 40, 137–146.

Driscoll, C.T., Kalicin, M., Lindeman, M., Liuzzi, C., Newton, R., Munson, R., 2001. Chemical and biological control of mercury cycling in Upland, Wetland and Lake Ecosystems in the Adirondack region of New York, E.O.S. Transactions, American Geophysical Union 82, 20.

Eakins, J.D., Morrison, T., 1978. A new procedure for the determination of lead-^{210} in lake and marine sediments. International Journal of Applied Radiation and Isotopes 29, 531–536.

Engstrom, D.R., Wright, H.E., 1983. Chemical stratigraphy of lake sediments as records of environmental change. In: Haworth, E.Y., Lund, J.W. (Eds.), Lake Sediments and Environmental History. University of Minnesota Press, Minneapolis, MN.

Engstrom, D.R., Swain, E.B., 1997. Recent declines in atmospheric mercury deposition in the Upper Midwest. Environmental Science and Technology 31, 960–967.

Engstrom, D.R., Swain, E.B., Henning, T.A., Brigham, M.E., Brezonik, P.L., 1994. Atmospheric mercury deposition to lakes and watersheds: a quantitative reconstruction from multiple sediment cores. In: Baker, L.A. (Ed.), Environmental Chemistry of Lakes and Reservoirs. American Chemical Society, Washington, D.C.

Evers, D.C., Kaplan, J., Meyer, M., Reaman, P., Braselton, W., Major, J.A., Burgess, N., Sheuhammer, A., 1998. Geographic trend in mercury measured in common loon feathers and blood. Environmental Toxicology and Chemistry 17, 173–183.

Fitzgerald, W.F., Mason, R.P., Vandal, G.M., 1991. Atmospheric cycling and air–water exchange of mercury over mid-continental lacustrine regions. Water, Air, and Soil Pollution 56, 745–767.

Fitzgerald, W.F., Engstrom, D., Mason, R., Nater, E., 1998. The case for atmospheric mercury contamination in remote areas. Environmental Science and Technology 32, 1–7.

Gilmour, L.C., Henry, E., Mitchell, R., 1992. Sulfate stimulation of mercury methylation on freshwater sediments. Environmental Science and Technology 26, 2281–2287.

Glew, J., 1989. A new trigger mechanism for sediment samplers. Journal of Paleolimnology 2, 241–243.

Gottgens, J.F., Rood, B., Delfino, J., Simmers, B., 1999. Uncertainty in paleoecological studies of mercury in sediment cores. Water, Air, and Soil Pollution 110, 131–333.

Hermanson, M., 1998. Anthropogenic mercury deposition to arctic lake sediments. Water, Air, and Soil Pollution 101, 309–321.

Hurley, J.P., Barbiaz, C.L., Cleckner, L.B., Rolfhus, K., Shafer, M.M., Back, R.C., 2000. Partitioning of mercury and methylmercury in Lake Superior tributaries. In: Proceedings

of the 43rd Conference on Great Lakes and St. Lawrence River Research, 2000 Annual Symposium. International Association of Great Lakes Research, 2205 Commonwealth Blvd., Ann Arbor, MI.

Landers, D.H., Gubala, C., Verta, M., Lucotte, M., Johansson, K., Lockhart, W., 1998. Using lake sediment mercury flux ratios to evaluate the regional and continental dimensions of mercury deposition in arctic and boreal ecosystems. Atmospheric Environment 32, 919–928.

Lee, Y., Iverfeldt, A., 1991. Measurement of methylmercury and mercury in run-off, lake, and rain waters. Water, Air, and Soil Pollution 56, 309–321.

Lockhart, W.L., Wilkinson, P., Billeck, B., Danell, R., Hunt, R., Brunskill, G., Delaronde, J., St. Louis, V., 1998. Fluxes of mercury to lake sediments in central and Northern Canada inferred from dated sediment cores. Biogeochemistry 40, 163–173.

Lorey, P., Driscoll, C., 1999. Historical trends of mercury deposition in Adirondack lakes. Environmental Science and Technology 33, 718–722.

Lucotte, M., Mucci, A., Hillaire-Marcel, C., Pichet, P., Grondin, A., 1995. Anthropogenic mercury enrichment in remote lakes of Northern Quebec. Water, Air, and Soil Pollution 80, 467–476.

Mickey, R., 2001. University of Vermont, Department of Mathematics and Statistics. Burlington, VT. Personal communication.

Mielli, M., 1995. Preindustrial atmospheric deposition of mercury: uncertain rates from lake sediment and peat cores. Water, Air, and Soil Pollution 80, 637–640.

Mierle, G., Ingram, R., 1991. The role of humic substances in the mobilization of mercury from watersheds. Water, Air, and Soil Pollution 56, 349–357.

National Academy of Sciences, 2000. Toxicological Profile for Methylmercury. National Academy Press, Washington, D.C.

Norton, S., Evans, G.C., Kahl, J.S., 1997. Comparison of Hg and Pb fluxes to hummocks and hollows of ombrotrophic Big Heath bog and to nearby Sargent Mt. Pond, Maine, USA. Water, Air, and Soil Pollution 100, 271–286.

Oldfield, F., Appleby, P.G., 1984. Empirical testing of ^{210}Pb-dating models for lake sediments. In: Haworth, E.Y., Lund, J.W.G. (Eds.), Lake Sediments and Environmental History. University of Minnesota Press, Minneapolis, pp. 93–124.

Omernik, J.M., 1987. Ecoregions of the conterminous United States. Map (scale 1:7,500,000). Annals of the Association of American Geographers 77, 118–125.

Ouellet, M., Jones, H., 1983. Historical changes in acid precipitation and heavy metals deposition originating from fossil fuel combustion in eastern North America as revealed by lake sediment geochemistry. Water Science and Technology 15, 115–130.

Perry, E.R., Norton, S., Cangelosi, J., Hess, C., Norris, M., 2001. Mercury storage, release, and transport in the watersheds of eight Maine lakes. In: Proceedings of the 2001 Annual Symposium of the Geological Society of America, Northeastern Section, Burlington, VT. Geological Society of America, Boulder, CO.

Pirrone, N., Allegrini, I., Keeler, G., Nriagu, J., Rossman, R., Robbins, J., 1998. Historical atmospheric mercury emissions and depositions in North America compared to mercury accumulations in sedimentary records. Atmospheric Environment 32, 929–940.

Rada, R.G., Powell, D., Wiener, J., 1993. Whole-lake burdens and spatial distribution of mercury in surficial sediments in Wisconsin seepage lakes. Canadian Journal of Fisheries and Aquatic Sciences 50, 865–873.

Scherbatskoy, T.D., Shanley, J.B., Keeler, G., 1998. Factors controlling mercury transport in an upland forested catchment. Water, Air, and Soil Pollution 105, 427–438.

Scherbatskoy, T.D., Poirot, R.L., Stunder, B.J., Artz, R., 1999. Current knowledge of air pollution and air resource issues in the Lake Champlain basin in Lake Champlain in transition: from research toward restoration. Water Science Applications 1, 1–23.

Shanley, J.B., Donlon, A.F., Scherbatskoy, T., Keeler, G., 1999. Mercury cycling and transport in the lake champlain basin in lake champlain in transition: from research toward restoration. Water Science Applications 1, 1–23.

Shanley, J.B., Scherbatskoy, T., Schuster, P., Reddy, M., Chalmers, A., 2001. Commonalities in mercury behavior in contrasting Northeastern USA landscapes. EOS Transactions, American Geophysical Union 82, 20.

St. Louis, V.L., Rudd, J., Kelly, L., Beaty, K., Bloom, N.S., Flett, R.J., 1994. Importance of wetlands as sources of methylmercury to boreal forest ecosystems. Canadian Journal of Fisheries and Aquatic Sciences 51 (5), 1065–1076.

Swain, E.B., Engstrom, D.R., Brigham, M.E., Henning, T.A., Brezonik, P.L., 1992. Increasing rates of atmospheric mercury deposition in mid-continental North America. Science 257, 784–787.

United States Environmental Protection Agency, 1994. Methods for the determination of metals in environmental samples. EPA/600/R–94/111, Washington, D.C.

United States Environmental Protection Agency, 1996. Method 1669: Sampling ambient water for determination of trace metals at water quality criteria levels. EPA/821/R–96/011, Washington, D.C.

United States Environmental Protection Agency, 1997. Mercury study report to Congress. EPA 425-R97-003, Washington, D.C.

US Environmental Protection Agency, 2000. Level III ecoregions of the continental United States (revision of Omernik, 1987). US Environmental Protection Agency, National Health and Environmental Effects Research Laboratory, Western Ecology Division, Corvallis, OR.

Von Gunten, H.R., Sturm, M., Moser, R., 1997. 200-Year record of metals in lake sediments and background concentrations. Environmental Science and Technology 31, 2193–2197.

Appendix B: Statistical Models of Atmospheric Hg Concentrations

Appendix B.1: Particulate-phase Hg concentration dependence on MDN basis Hg concentration in precipitation and month of the year. Based on observations at Underhill (VT), Quabbin (MA), and East Providence (RI).

Response Hg(p)pg/m3

Whole Model

Actual by Predicted Plot

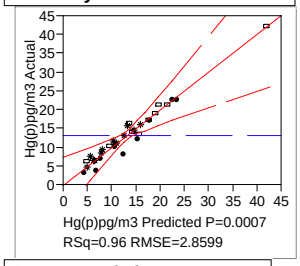

Summary of Fit

RSquare	0.960201
RSquare Adj	0.858491
Root Mean Square Error	2.859878
Mean of Response	13.13805
Observations (or Sum Wgts)	33

Analysis of Variance

Source	DF	Sum of Squares	Mean Square	F Ratio
Model	23	1775.9197	77.2139	9.4406
Error	9	73.6101	8.1789	Prob > F
C. Total	32	1849.5298		0.0007

Parameter Estimates

Term	Estimate	Std Error	t Ratio	Prob>|t|
Intercept	24.063971	3.186585	7.55	<.0001
month[apr]:(MDN wet Hg conc-7.44624)	-4.201733	2.175047	-1.93	0.0854
month[aug]:(MDN wet Hg conc-7.44624)	5.4423957	1.962899	2.77	0.0217
month[dec]:(MDN wet Hg conc-7.44624)	18.330477	2.19489	8.35	<.0001
month[feb]:(MDN wet Hg conc-7.44624)	0.9255783	1.359456	0.68	0.5131
month[jan]:(MDN wet Hg conc-7.44624)	26.652794	9.292814	2.87	0.0185
month[jul]:(MDN wet Hg conc-7.44624)	3.0426317	3.308101	0.92	0.3817
month[jun]:(MDN wet Hg conc-7.44624)	-2.686522	12.29857	-0.22	0.8320
month[mar]:(MDN wet Hg conc-7.44624)	2.776505	1.589077	1.75	0.1145
month[may]:(MDN wet Hg conc-7.44624)	4.97326	2.3257	2.14	0.0612
month[nov]:(MDN wet Hg conc-7.44624)	8.2486153	2.248827	3.67	0.0052
month[oct]:(MDN wet Hg conc-7.44624)	25.858019	27.04712	0.96	0.3640
month[sep]:(MDN wet Hg conc-7.44624)	2.2039207	2.920546	0.75	0.4698
month[apr]	-3.397039	5.331244	-0.64	0.5399
month[aug]	-13.83678	3.779381	-3.66	0.0052
month[dec]	29.285928	4.734761	6.19	0.0002
month[feb]	-4.746843	4.216313	-1.13	0.2894
month[jan]	55.269179	20.22232	2.73	0.0231
month[jul]	-24.03358	8.037734	-2.99	0.0152
month[jun]	-16.64159	11.95041	-1.39	0.1972
month[mar]	-4.775426	4.604059	-1.04	0.3267
month[may]	-23.1879	4.94757	-4.69	0.0011
month[nov]	8.1044788	5.839844	1.39	0.1986
month[oct]	12.737304	23.16449	0.55	0.5958

Effect Tests

Source	Nparm	DF	Sum of Squares	F Ratio	Prob > F
MDN wet Hg conc[month]	12	12	926.7676	9.4427	0.0011
month	11	11	1146.6266	12.7448	0.0003

Residual by Predicted Plot

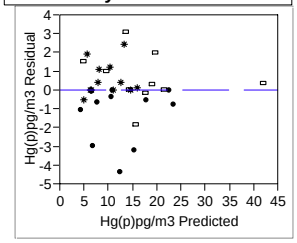

MDN wet Hg conc[month]

Leverage Plot

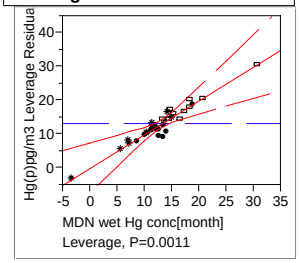

month

Leverage Plot

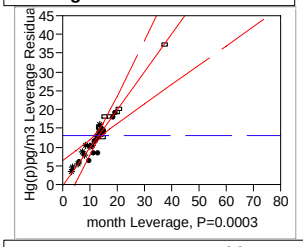

Least Squares Means Table

Level	Least Sq Mean	Std Error	Mean
apr	20.666932	4.682030	12.2033
aug	10.227193	2.226046	14.3667
dec	53.349899	3.836191	24.4317
feb	19.317127	3.024495	17.5919
jan	79.333150	21.875679	16.8600
jul	0.030387	8.083379	7.3083
jun	7.422386	12.617032	4.6900
mar	19.288545	3.640281	13.6200
may	0.876071	4.145956	9.0083
nov	32.168450	5.360909	13.9575
oct	36.801275	25.134177	12.8500
sep	9.286237	4.183184	12.1867

Appendix B.2: Vapor-phase Hg concentration dependence on MDN basis Hg concentration in precipitation and season of the year. Based on observations at Underhill (VT), Quabbin (MA), and East Providence (RI).

Response Mean(vapor Hg conc)

Whole Model

Actual by Predicted Plot

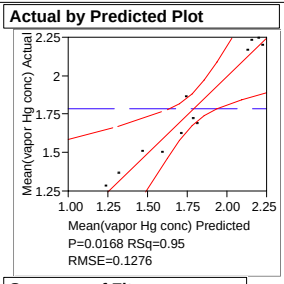

Summary of Fit

RSquare	0.951872
RSquare Adj	0.867649
Root Mean Square Error	0.127605
Mean of Response	1.785759
Observations (or Sum Wgts)	12

Analysis of Variance

Source	DF	Sum of Squares	Mean Square	F Ratio
Model	7	1.2881821	0.184026	11.3017
Error	4	0.0651319	0.016283	Prob > F
C. Total	11	1.3533140		0.0168

Parameter Estimates

Term	Estimate	Std Error	t Ratio	Prob>|t|
Intercept	1.6071951	0.080965	19.85	<.0001
season[fall]:(Mean(MDN wet Hg conc)-7.38807)	0.6722334	0.126204	5.33	0.0060
season[spring]:(Mean(MDN wet Hg conc)-7.38807)	0.6708197	0.183619	3.65	0.0217
season[summer]:(Mean(MDN wet Hg conc)-7.38807)	0.7303141	0.155903	4.68	0.0094
season[winter]:(Mean(MDN wet Hg conc)-7.38807)	0.2957931	0.080425	3.68	0.0212
season[fall]	0.3581972	0.101665	3.52	0.0244
season[spring]	-0.146945	0.123369	-1.19	0.2995
season[summer]	-0.90059	0.186419	-4.83	0.0085

Effect Tests

Source	Nparm	DF	Sum of Squares	F Ratio	Prob > F
Mean(MDN wet Hg conc)[season]	4	4	1.2568783	19.2974	0.0070
season	3	3	0.6816598	13.9544	0.0138

Residual by Predicted Plot

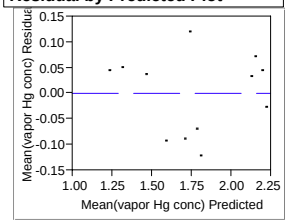

Mean(MDN wet Hg conc)[season]

Leverage Plot

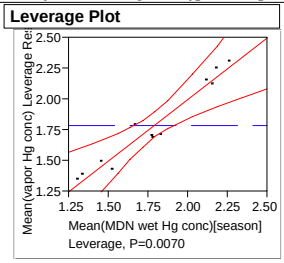

season

Leverage Plot

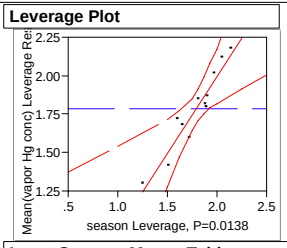

Least Squares Means Table

Level	Least Sq Mean	Std Error	Mean
fall	1.9653923	0.08695377	1.71937
spring	1.4602499	0.13164023	1.85881
summer	0.7066052	0.23747299	1.76414
winter	2.2965332	0.15362677	1.80072

Appendix C: Overview of the High Resolution Deposition Model

Project Overview – For informational purposes only
Please Do Not Cite or Distribute Without Permission

Atmospheric Deposition to Complex Landscapes: HRDM - A Strategy for Coupling Deposition Models to a High-Resolution GIS

Eric K. Miller, Ph. D.

Ecosystems Research Group, Ltd., Norwich, VT 05055
Environmental Studies Program, Dartmouth College, Hanover, NH 03755

Summary

A spatially distributed modeling environment was developed that couples detailed physical models of atmosphere-surface heat, mass and momentum transfer processes to a high-resolution geographic information system and regional climatology for the northeastern United States (ME, NH, VT, MA, RI, NY, NJ, PA). The high-resolution distributed model (HRDM) was developed for a series of applications which include: providing high-resolution estimates of total atmospheric deposition to lake-watershed ecosystems, regional studies of pollutant accumulation in soils, and regional studies of air pollution effects on ecosystem health, productivity and carbon sequestration. The distributed model can produce estimates of atmospheric deposition at seasonal and annual time steps with 30-meter ground resolution subject to the constraints of positional and characterization accuracy of underlying land surface and atmospheric descriptive data. The modeling environment is designed to be flexible enough to accommodate alternative approaches to estimating meteorological and atmospheric chemistry fields.

Project Rational and Objectives

HRDM provides high-resolution (30x30 meter ground area) estimates of total atmospheric deposition (wet + dry + cloud water) in complex terrain.

High spatial resolution atmospheric deposition estimates are useful for:
- Estimates of total atmospheric loading to watersheds
- Assessment of land-cover effects on regional deposition rates
- Identification of sensitive landscape segments and ecoregions
- Ranking of landscape regions with respect to historic and current deposition loads
- Characterization of deposition at locations remote from NADP or CASTNet stations

HRDM improves upon existing approaches for regionally consistent estimates of local atmospheric deposition rates. Most existing spatial models of deposition were developed to operate at much coarser spatial and temporal scales than would be desired for addressing many important questions in ecosystem science.

Existing estimates of atmospheric deposition fields for the northeastern US have one or more of the following limitations for application to local and regional ecological problems:
- Incomplete estimates of total atmospheric deposition (models may be wet-only or wet+dry, but all lack estimates of cloud water deposition).
- Limited temporal resolution (a few months to a few years represented)
- Low spatial resolution (80km to 1km)
- Omission of terrain and land cover effects on deposition rate (direct spatial interpolations of network observations)
- Weak interpolations of dry-deposition fields from a sparse observation network
- Oversimplification of terrain effects (due to terrain averaging at low spatial resolutions)
- Oversimplification of receptor surface effects (surface type averaging at low resolutions)
- Oversimplification of receptor surface/terrain interactions

Applications of the high-resolution total deposition model include:
- Estimation of current and historical total nitrogen and sulfur deposition to watersheds in support of a study of terrestrial ecosystem influences on N and P supply to aquatic ecosystems in the Northeast (USEPA - http://es.epa.gov/ncerqa_abstracts/grants/98/ecological/stemberger.html)
- Comparison of historical total nitrogen and sulfur deposition to total ecosystem pools of N and S at a series of forest sites throughout the Northeast. (USDA)
- Estimation of current and historical total nitrogen and sulfur deposition to New England in support of the Forest Mapping Initiative Program of the NEG/ECP Acid Rain Action Plan (NESCAUM, USDA-FS)
- Characterization of N and S deposition for Vermont Acid Impaired Lakes (VTDEC).
- Characterization of wet and dry mercury deposition to the watersheds of the VT/NH REMAP Lakes (VTDEC)

Overview of the Spatially Distributed Modeling Environment

The complexity in patterns of rainfall, vegetation (dry and cloud deposition receptor surface) and deposition at sub-kilometer scales in the mountainous northeastern US states (Figure 1) requires a high spatial-resolution approach to atmospheric deposition estimates. Miller (2000) developed a spatially-distributed modeling environment which couples detailed physical models of atmosphere-land surface heat, mass and momentum transfer processes (Miller et al. 1993a,b) to a high-resolution geographic information system and regional climatology for the northeastern US. The model provides estimates of wet, dry and cloud water deposition at 30-meter resolution. Key features of the HRDM include:

1. Wet, dry and cloud-water deposition processes are represented – providing a true "total deposition" regional model for mountainous landscapes.
2. Statistical modeling of regional spatial gradients is combined with surface interpolation of residual fields to obtain 10-km grid resolution estimates of atmospheric chemistry with a high degree of fidelity to network observations.
3. Wet deposition is calculated as a combination of the 10-km resolved precipitation chemistry, 1-km resolved regional precipitation field, and 30-m (90-m in older versions) resolved terrain corrected precipitation amount.
4. Either point observational records or gridded meteorological model output can be spatially interpolated to 30-m resolution, corrected for local topographic and landscape positional effects and monthly regional climatology to drive the dry and cloud water deposition models.
5. The receptor surface for dry and cloud water deposition is represented at 30-m resolution. The biophysical characteristics of the receptor surface (leaf area, aerodynamic properties, stomatal response to light, temperature and humidity) are estimated in terms of the proportion of leaf area expected to be attributable to specific plant species. Species proportions are estimated by a forest species distribution submodel with guidance from the USGS/EPA NLCD data set.
6. Deposition estimates are generated on a seasonal basis using sub-season time steps including representations of diurnal fluctuations employed in the dry deposition process model.
7. Depositing species represented in the model include: aqueous H^+, K^+, Na^+, NH_4^+, Mg^{2+}, Ca^{2+}, SO_4^{2-}, NO_3^-, Cl^-, $Hg_{(total)}$; dry particle phase H^+, K^+, Na^+, NH_4^+, Mg^{2+}, Ca^{2+}, SO_4^{2-}, NO_3, Cl^-, $Hg_{(total)}$; and vapor-phase HNO_3, NO_2, SO_2, O_3, $Hg_{(0)}$, RGM.

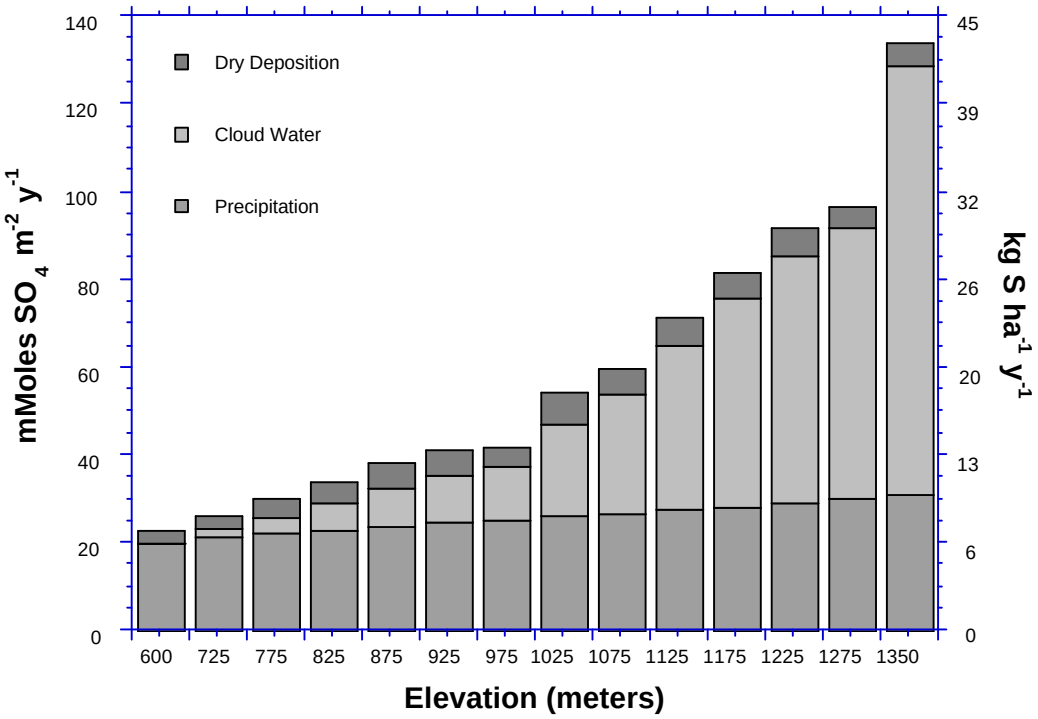

Figure 1. Variation in wet, dry, cloud, and total sulfur deposition over ~2km ground distance as a function of elevation on Whiteface Mt., NY, 1986-1989 (from Miller et al. 1993).

The relationships between the primary model components and data layers in the modeling environment are shown in Figure 2 and described briefly below.

Spatial Data Layers

Digital Elevation Model – USGS 3 arcsec (nominal resolution of 60x90m at 45° latitude) – exisiting data sets produced by the HRDM are based on this DEM. All new data sets being generated with the HRDM are based on the USGS NED 30-m ground resolution DEM.

General Land Cover – USGS/EPA NLCD 30-m ground resolution, 23 general land-cover classes derived from LANDSAT TM+ (1992/1993)

Regional Climatology – regional temperature and precipitation fields interpolated from climate data at 619(ppt), 323(T) stations from the NOAA cooperative observation network

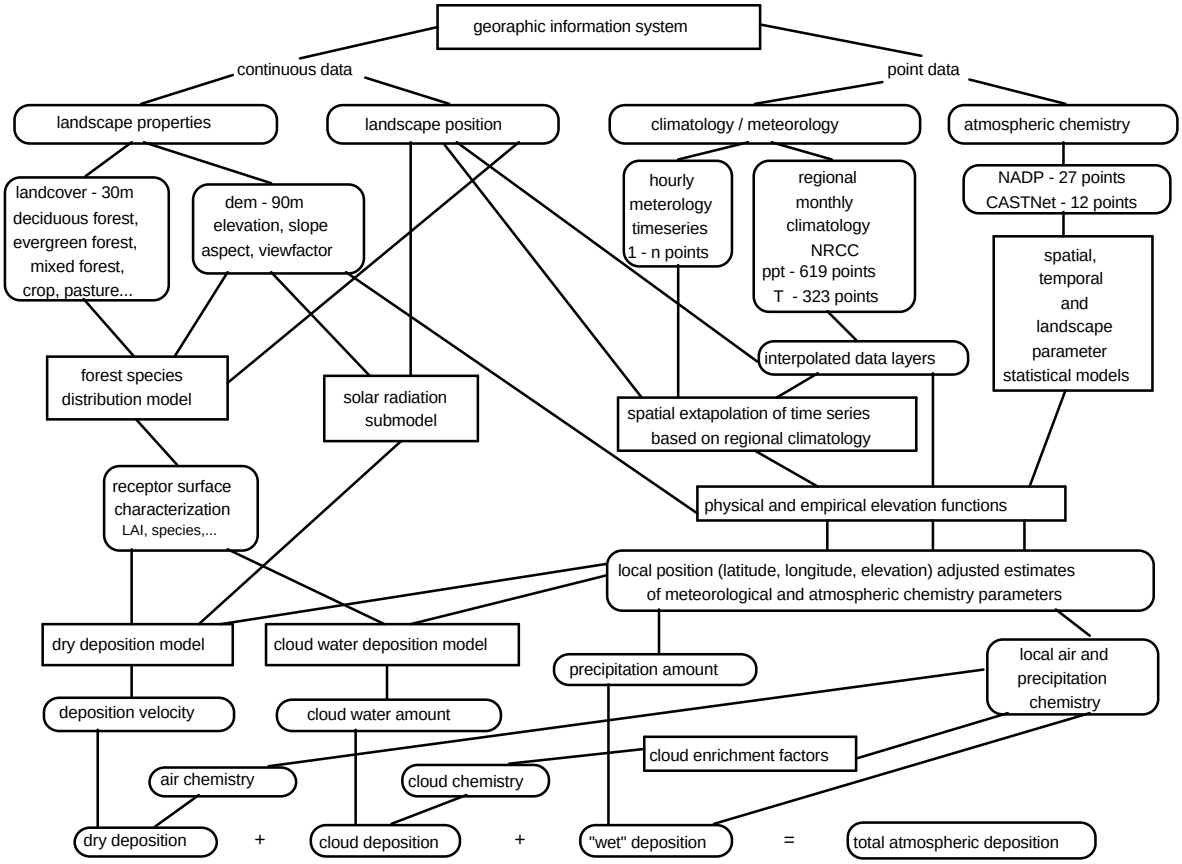

Figure 2. Relationships between model components and data layers in the high-resolution distributed modeling environment (HRDM).

Time Series

Regional Climatology is monthly, Meteorology (temperature, RH, wind speed, percent of possible solar radiation, cloud frequency) is hourly from multiple point records obtained as near as possible to the region of interest, extrapolated on the basis of terrain functions (for example see Miller et al. 1993b) and regional climatology fields. The model can also be driven with meteorology time series in the form of gridded output (any spatial resolution) from atmospheric models.

Precipitation Chemistry – monthly or seasonal – statistical models based on NADP observations at 27 sites are used to provide localized, terrain-corrected estimates (Miller, 2000).

Air Chemistry – monthly or seasonal – statistical models based on CASTNet observations (direct interpolation) or coupled CASTNet-NADP observations (scavenging ratio approach, Miller, 2000). Precipitation and Air Chemistry data can also be provided to the model in the form of gridded output from a regional transport model such as RADM (Chang et al. 1987)

Atmosphere-Surface Transfer Models

Dry Deposition Velocities for aerosol particles and gasses – big leaf model designed for complex terrain (Miller et al. 1993a,b). This model includes the appropriate physics to simulate deposition in a complex landscape. A big-leaf model is preferred over a multi-layer model for this application because of the limited information available to properly characterize the receptor surface at each 30-m pixel.

Cloud Water Deposition – due to both severe computational requirements and limitations of information on canopy structure, a multi-layer canopy model (Miller et al. 1993a,b) was parameterized with a representative canopy for the major surface types expected to receive cloud water deposition. Multiple sensitivity analyses were conducted with the multi-layer model in order characterized model response to a large set of possible canopy by meteorological condition interactions. We then statistically apportioned the multi-layer model response to key environmental parameters that can readily be obtained for each 30-m pixel.

"Wet" (rain and snow) Deposition – a statistical model of the effect of elevation on precipitation rate was derived using data from 619 observation stations for each season. Precipitation rate at each station was then corrected to sea level and regional precipitation fields were interpolated. Precipitation at each point in the model was then estimated from the regional sea level precipitation field and the statistical model of elevation effect on precipitation rate.

Submodels

Several submodels provide location-specific input to the atmosphere-landsurface transfer models.

Solar Radiation – simulates the effects of terrain on direct and diffuse solar radiation. An option is available to include local horizon blockage of direct beam radiation which is a significant factor in mountainous terrain.

Forest Species Distribution – estimates detailed biological character of receptor surface (tree species, LAI) as a function of landscape position using the NLCD as guidance on general surface type and data from the Eastwide FIA to characterize the probability of occurrence of different forest types at a given landscape position (for example see Iverson and Prasad 1998).

Meteorology – when gridded meteorological data are not used, this submodel is used to extrapolate observed point-location records of meteorological time series to the full model domain. Extrapolation methods include both empirical and physically-based representations of the effect of landscape position on monthly climatology (see Miller et al. 1993a, Miller and Friedland 1999).

Example Model Output

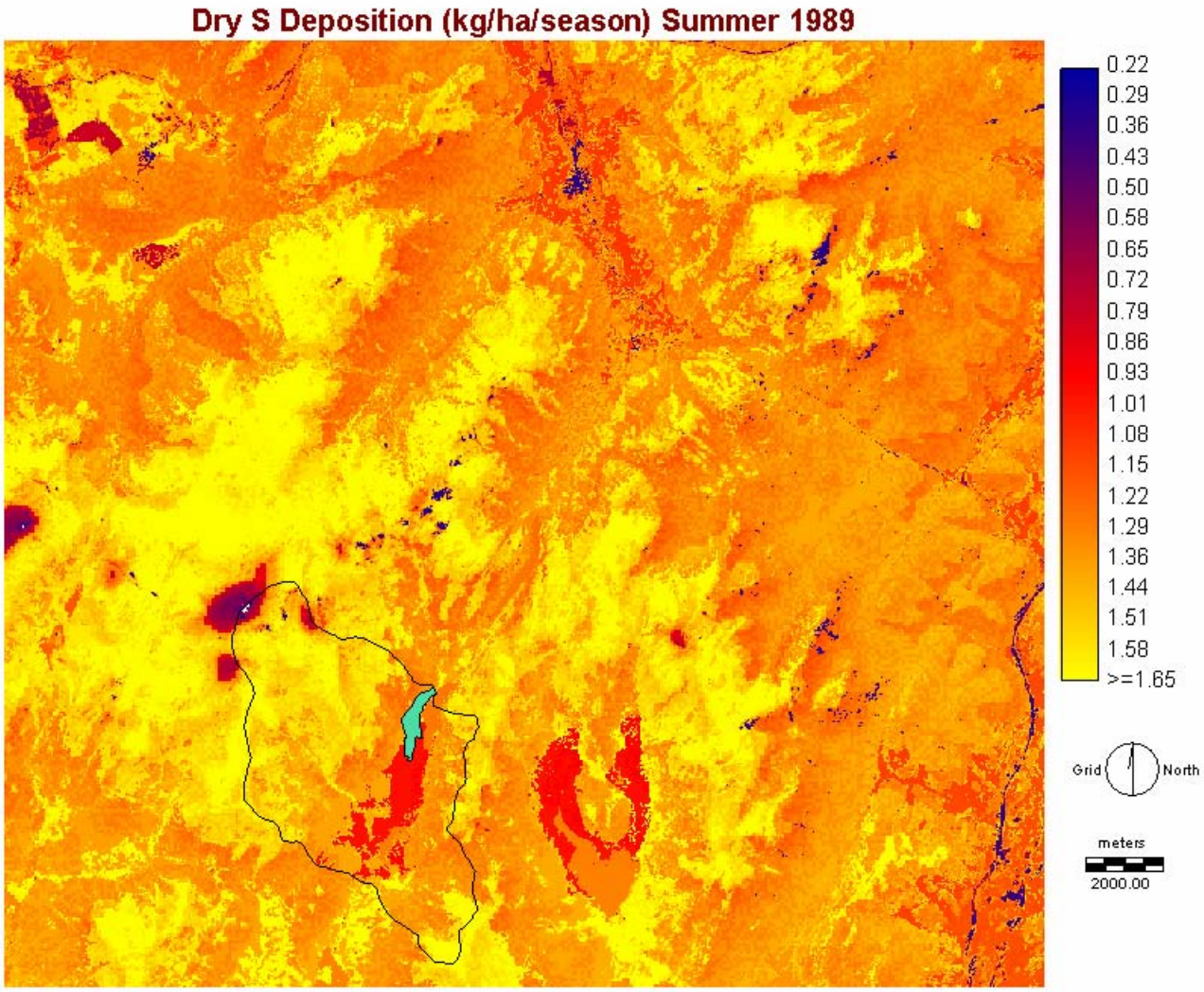

Figure 3. High-Resolution Deposition Model (HDRM) estimated summer dry sulfur deposition (SO_2 plus particle SO_4) for a portion of the High-Peaks region of the Adirondack Mountains, NY, USA. Mount Marcy is on the left side of the image. Keene Valley is near the top center of the image. The black line delineates the watershed of the Upper Ausable Lake (shown in light blue). The image represents an approximately 27x28 km ground area. Dry deposition to this region would be represented by a single value when using dry/wet ratios and the 40-km resolution NatChem or NADP wet deposition grid as a basis for the estimate.

A Brief Discussion of How the HRDM Differs from Previous Approaches to Spatially Distributed Estimates of Atmospheric Deposition

The high-resolution deposition model (HRDM) described in this document was developed to address the need for spatially explicit and spatially distributed estimates of atmospheric deposition in the complex mountainous landscape of the northeastern US. Many ecological applications of atmospheric deposition estimates in the northeastern US require appropriate representation at spatial scales of less than 100 meters. High spatial resolution simulations are necessary because it is recognized that tremendous variation in meteorological conditions such as temperature, wind speed and cloud immersion may occur within 1 km due to the topography of the region. The biophysical characteristics of receptor surfaces also vary substantially at scales less than 1 km, in part due the influence of the climate variation discussed above on vegetation distribution. Such small-scale variation in meteorology and surface type can result in very large (4-5X) and ecologically significant variations in atmospheric deposition rates over the same distances (see Figures 4 and 5 in Miller et al. 1993b). If atmospheric deposition estimates are required for small watersheds (1–20 km^2) or for identification of acid or nitrogen sensitive ecoregions, then sub-kilometer resolution approaches will be required to adequately represent what is currently understood about atmospheric deposition regimes in the Northeast.

Examples of Several Approaches to Spatially Distributed Estimates of Atmospheric Deposition

Chang et al. 1987 – (RADM) Reactive transport model for acid deposition

- Wet and dry deposition
- Meteorological data provided by a mesoscale model
- Very low horizontal spatial resolution (80 km) masks important topographic and landcover related variance
- Simplistic formulation of dry deposition and surface type due to coarse spatial scale
- Statistical aggregation of model scenarios representative of observed climatology to produce seasonal and annual totals

Ollinger et al. 1993 – Hybrid statistical – GIS-aided interpolation of NADP and NDDN observations

- Wet and dry deposition
- Published estimates represent average deposition over a variable 4 to 11-y time period in the 1980s and early 1990s
- Weak interpolations of dry air concentrations due to sparse observational network
- One surface type and one constant dry deposition velocity applied to the whole region

Brook et al. 1999 – (RDM) Hybrid mesoscale meteorology coupled to a dry deposition velocity model

- Dry deposition velocities only, but could be coupled with other sources of wet deposition and air concentrations to produce deposition estimates
- Meteorology averaged at 35 km horizontal resolution masks important topographic related variance
- Land cover input to deposition velocity model at 1 km resolution grossly simplifies biological characteristics of receptor surface. For example, forest surface types are simplified to broadleaf and needleleaf, evergreen and deciduous.
- While this model provides estimates of dry deposition velocities at 1 km resolution the 35 km resolution of input meteorological data suggests that the deposition velocities would be more appropriately interpreted at a much coarser scale in complex terrain.
- Unfortunately this model is not coupled in any way to landscape estimates of the air concentration field. At this point in time the authors intend for the model deposition velocities to be used with the sparse point observations of the CAPMoN, NAPS and CASTNet dry deposition networks.

Miller 2000 – (HRDM) Hybrid statistical – GIS – mixed resolution physical process model

- Combines the strengths of the Ollinger et al. 1993 and Brook et al. 1999 approaches with significant further improvements.
- Wet, dry and cloud-water deposition. Only true "total deposition" regional model for mountainous landscapes.
- Allows either point observational records or gridded meteorological model output to be spatially interpolated to 30-m resolution, corrected for local topographic and landscape positional effects based on monthly regional climatology.
- Receptor surface is represented at 30-m resolution. The biophysical characteristics of the receptor surface are estimated in terms of the proportion of leaf area expected to be attributable to specific plant species. Species proportions are estimated by the forest species distribution submodel with guidance from the USGS/EPA MRLC data set.
- Deposition estimates are generated on a seasonal basis using sub-season time steps including representations of diurnal fluctuations employed in the deposition process models
- Deposition can be calculated for each year of the period 1980 to the present

References

Brook, J.R., et al. 1999. Description and evaluation of a model of deposition velocities for routine estimates of air pollutant dry deposition over North America. Part I: model development. *Atm. Environ.* 33:5037-5051.

Chang, J.S., et al. 1987. A three-dimensional Eulerian acid deposition model: Physical Concepts and Formulation. *J. Geophys. Res.* 92: 681-14.

Iverson, L.R. and A.M. Prasad. 1998. Predicting potential future abundance of 80 tree species following climate change in the eastern United States. Ecol. Monographs 68:465-485.

Miller, E.K. et al. 1993a. Atmospheric deposition to a high-elevation forest at Whiteface Mountain, NY, USA. Tellus 45B:209-227.

Miller, E.K. et al. 1993b. Atmospheric deposition to forests along an elevational gradient at Whiteface Mountain, NY USA. Atmos. Environ. 27A:2121-2136.

Miller, E.K. and A.J. Friedland. 1999. Local climate influences on precipitation, cloud water, and dry deposition to an Adirondack subalpine forest: insights from observations 1986-1996. Journal of Environmental Quality **28**:270-277.

Miller, E.K. 2000. Atmospheric Deposition to Complex Landscapes: HRDM – a strategy for coupling deposition models to a high-resolution GIS. page 74 in R. Arts, editor. NADP 2000: Ten years after the Clean Air Act Amendments: Adirondacks in the Balance. Proceedings of the NADP Technical Meeting, October 17-20, 2000. Illinois State Water Survey, Champaign, IL.

Ollinger, S.V. et al. 1993. A spatial model of atmospheric deposition for the northeastern US. Ecol. Appl. 3:459-472.

Contact Information

Dr. Eric K. Miller
Ecosystems Research Group, Ltd.
Aldrich House Suite 11
16 Beaver Meadow Road
PO Box 1227
Norwich, VT 05055

email: ekmiller@ecosystems-research.com voice: 802-291-0831 fax: 802-649-5551